



A COMPUTATIONAL TOOL FOR EOS PARAMETER ESTIMATION:  
EVALUATION OF NEW METHODOLOGIES AND APPLICATION IN A  
NATURAL GAS PROCESSING SIMULATION

Samir Silva Abunahman

Dissertação de Mestrado apresentada ao Programa de Pós-graduação em Engenharia Química, COPPE, da Universidade Federal do Rio de Janeiro, como parte dos requisitos necessários à obtenção do título de Mestre em Engenharia Química.

Orientadores: Frederico Wanderley Tavares  
Leticia Cotia dos Santos

Rio de Janeiro  
Setembro de 2018

A COMPUTATIONAL TOOL FOR EOS PARAMETER ESTIMATION:  
EVALUATION OF NEW METHODOLOGIES AND APPLICATION IN A  
NATURAL GAS PROCESSING SIMULATION

Samir Silva Abunahman

DISSERTAÇÃO SUBMETIDA AO CORPO DOCENTE DO INSTITUTO ALBERTO LUIZ COIMBRA DE PÓS-GRADUAÇÃO E PESQUISA DE ENGENHARIA (COPPE) DA UNIVERSIDADE FEDERAL DO RIO DE JANEIRO COMO PARTE DOS REQUISITOS NECESSÁRIOS PARA A OBTENÇÃO DO GRAU DE MESTRE EM CIÊNCIAS EM ENGENHARIA QUÍMICA.

Examinada por:

---

Prof. Frederico Wanderley Tavares, D.Sc.

---

Eng. Letícia Cotia dos Santos, D.Sc.

---

Prof. Argimiro Resende Secchi, D.Sc.

---

Prof. Rogério Oliveira Espósito, D.Sc.

---

Prof. Victor Rolando Ruiz Ahón, D.Sc.

RIO DE JANEIRO, RJ – BRASIL  
SETEMBRO DE 2018

Abunahman, Samir Silva

A Computational Tool for EoS Parameter Estimation: Evaluation of New Methodologies and Application in a Natural Gas Processing Simulation/Samir Silva Abunahman. – Rio de Janeiro: UFRJ/COPPE, 2018.

XXIII, 134 p.: il.; 29,7cm.

Orientadores: Frederico Wanderley Tavares

Letícia Cotia dos Santos

Dissertação (mestrado) – UFRJ/COPPE/Programa de Engenharia Química, 2018.

Bibliografia: p. 124 – 132.

1. Equations of State. 2. Parameter Estimation. 3. Natural Gas Production. I. Tavares, Frederico Wanderley *et al.* II. Universidade Federal do Rio de Janeiro, COPPE, Programa de Engenharia Química. III. Título.

*To my family and my wife, for  
all the love and support.*

# Acknowledgements

I would like to thank my advisors Fred Tavares and Letícia Cotia for all the productive discussions we had during the research period. I would not have matured neither learnt so much if it were not for you.

I would like to thank Petrobras for allowing me to do this work, along with the other day-to-day work. Specifically, I would like to thank my managers Joyce Ayres, Luiz Antônio Zucco and Teo Veras for trusting me that this study will yield positive results to the Company.

I would like to thank prof. Kontogeorgis and the rest of his team at the DTU for providing me the .dll file containing the internal CPA calculations, which made possible most of the analyses performed in this work.

I would also like to thank my colleagues at Petrobras who help me along these years: Renato Barbosa and Cláudio Alcino, for all the support regarding Petrox<sup>®</sup>'s issues; Christiano Guerra, who helped me with the MEG model using the commercial simulators; Rodrigo Galvão, for the great help in inserting me into the L<sup>A</sup>T<sub>E</sub>X world, which considerably accelerated the writing of this work; Victor Virgens, for the accurate bug reports in the *ThermOptimizer*; And a second mention to Letícia Cotia for the great help she gave me. Once again, thank you very much.

There are also many honorable mentions which contributed to the attainment of this work and must not be forgotten: Lara Teixeira, Jacques Niederberger, Victor Ahón, Vinicius Menez, José Ataíde da Silva, Anna Eliza Zóboli, Flávio Francisco, Ellen Paixão, Anderson Soares and Leilane Correa.

I would also like to thank my best friends Thiago Ribeiro, Jasmille Guimarães, Marina Bastos and Júlia Ximenes. They do not need a reason.

I owe my deepest gratitude to my family for all the love and support. My parents Jorge and Anadeje for giving the educational basis to reach this point; my sisters Natalia and Mariana for everything we have been through; and special thanks to my beloved wife Vitória Barroso for so much love and help to keep me focused on this work.

Resumo da Dissertação apresentada à COPPE/UFRJ como parte dos requisitos necessários para a obtenção do grau de Mestre em Ciências (M.Sc.)

UMA FERRAMENTA COMPUTACIONAL PARA ESTIMAÇÃO DE  
PARÂMETROS DE EDES: AVALIAÇÃO DE NOVAS METODOLOGIAS E  
APLICAÇÃO EM UMA SIMULAÇÃO DE PROCESSAMENTO DE GÁS  
NATURAL

Samir Silva Abunahman

Setembro/2018

Orientadores: Frederico Wanderley Tavares

Letícia Cotia dos Santos

Programa: Engenharia Química

Nos reservatórios brasileiros do pré-sal são produzidas grandes quantidades de óleo leve contendo altos teores de  $\text{CO}_2$  em altas pressões, caracterizando um desafio na sua modelagem termodinâmica a partir de equações de estado (EdEs) convencionais. Para realizar predições mais acuradas nessa região, há uma necessidade frequente de se efetuar o procedimento de estimação de parâmetros. Portanto, neste trabalho foi desenvolvida uma ferramenta computacional que executa, de forma confiável, essa estimação de parâmetros, com interface interativa e amigável ao usuário, permitindo a criação de gráficos de avaliação paramétrica e da função objetivo em cada ponto da otimização. Foram sistematizadas novas metodologias para a estimação de parâmetros utilizando esta ferramenta: uma utilizando simultaneamente dados de equilíbrio líquido-vapor e líquido-líquido e outra utilizando dados de teor de água no ponto de orvalho. Utilizando a EdE *Cubic-Plus-Association* (CPA), essas metodologias foram devidamente validadas com dados de literatura. Foram obtidos novos parâmetros da CPA para a água, que levam em conta o valor experimental da energia de ligações de hidrogênio, e para a sua mistura binária com  $\text{CO}_2$ , cujo desvio médio absoluto relativo ao teor de água a pressões acima de 200 bar baixou de 27.3% para 3.3% em comparação com publicações anteriores. Por fim, esse estudo foi aplicado em uma unidade de processamento de gás natural, modelada com os parâmetros encontrados neste trabalho.

Abstract of Dissertation presented to COPPE/UFRJ as a partial fulfillment of the requirements for the degree of Master of Science (M.Sc.)

A COMPUTATIONAL TOOL FOR EOS PARAMETER ESTIMATION:  
EVALUATION OF NEW METHODOLOGIES AND APPLICATION IN A  
NATURAL GAS PROCESSING SIMULATION

Samir Silva Abunahman

September/2018

Advisors: Frederico Wanderley Tavares

Letícia Cotia dos Santos

Department: Chemical Engineering

Brazilian pre-salt reservoirs represent the discovery of large amounts of light oil, but at high pressures and containing high levels of CO<sub>2</sub>, being a challenge in its thermodynamic modelling by conventional equations of state (EoS). In order to perform more accurate predictions, it is necessary to execute the procedure of parameter estimation. Therefore, in this work a computational tool was developed that reliably carries out this parameter estimation with interactive and user-friendly interface, allowing the creation of charts containing parametric and objective function evaluations in each point of the optimization. New methodologies for parameter estimation were systematized utilizing this tool: the first one by applying simultaneously vapour-liquid and liquid-liquid equilibria and the other handling water content in dew point condition. Utilizing the EoS *Cubic-Plus-Association* (CPA), these methodologies were properly validated with literature data. New CPA parameters for water, which take into account the experimental value of its hydrogen bonds energy, and for its mixture with CO<sub>2</sub> were obtained, whose average absolute deviation in the water content at pressures higher than 200 bar fell from 23.7% to 3.3% compared to previous publications. Finally, this study has been applied into a natural gas process unit, modelled with the parameters found here.

# Contents

<b>List of Figures</b>	<b>xi</b>
<b>List of Tables</b>	<b>xix</b>
<b>1 Introduction</b>	<b>1</b>
1.1 Motivation . . . . .	1
1.2 Objectives . . . . .	4
1.3 Organization of the Text . . . . .	4
<b>2 Bibliographic Review</b>	<b>6</b>
2.1 Natural Gas Processing . . . . .	6
2.1.1 Absorption Process in Dehydration . . . . .	7
2.1.2 BTEX Issues in Dehydration . . . . .	8
2.2 Equations of State . . . . .	9
2.2.1 Overview . . . . .	9
2.2.2 The Soave-Redlich-Kwong (SRK) EoS . . . . .	11
2.2.3 The Peng-Robinson (PR) EoS . . . . .	12
2.2.4 Modifications for Polar Components . . . . .	12
2.2.5 Association Theories . . . . .	13
2.2.6 The Cubic-Plus-Association (CPA) EoS . . . . .	15
2.3 Parameter Estimation . . . . .	18
<b>3 Mathematical Modelling</b>	<b>20</b>
3.1 Thermodynamic Equilibrium Calculations . . . . .	20
3.1.1 Saturation, Bubble and Dew Pressures . . . . .	21
3.1.2 Liquid-liquid Equilibrium (LLE) . . . . .	22
3.1.3 Water Content of a Specified Gas . . . . .	24
3.2 Methods and Strategies of Optimization . . . . .	29
3.2.1 Stochastic Method . . . . .	30
3.2.2 Deterministic Method . . . . .	32
3.2.3 Hybridization . . . . .	35
3.3 Parameter Estimation . . . . .	37



3.3.1	Pure Components . . . . .	37
3.3.2	Binary Mixtures by Liquid-liquid Equilibrium Calculation . .	39
3.3.3	Validating Pure Component Parameters with LLE Data . . .	41
3.3.4	Binary Mixtures by Bubble or Dew Pressure Calculation . . .	42
3.3.5	Multicomponent Mixtures by Water Content Calculation . . .	43
3.4	Procedure to Parameter Estimation from Pure to Mixtures . . . . .	44
<b>4</b>	<b>Computational Aspects</b>	<b>46</b>
4.1	Software Basis . . . . .	46
4.2	Input Features . . . . .	47
4.2.1	Pure Component Tab . . . . .	47
4.2.2	Binary Mixture Tab . . . . .	51
4.2.3	Multicomponent Mixture Tab . . . . .	55
4.3	Output Features . . . . .	57
4.3.1	Output Results . . . . .	57
4.3.2	Plots and Reports . . . . .	59
4.3.3	Tables . . . . .	65
4.4	General Features . . . . .	66
4.4.1	Diagnostics Region . . . . .	66
4.4.2	Miscellaneous Region . . . . .	66
<b>5</b>	<b>Results and Discussion</b>	<b>75</b>
5.1	PSO Performance Analysis . . . . .	75
5.2	Pure Parameter Estimation . . . . .	77
5.2.1	Penalization Analysis for Water (SRK EoS + Kabadi-Danner $\alpha$ Function) . . . . .	77
5.2.2	Parameter Estimation for Polar Components Without Penalization (CPA EoS) . . . . .	82
5.3	VLE + LLE Methodology for CPA EoS Parameter Estimation . . . .	86
5.3.1	Glycols . . . . .	88
5.3.2	Water . . . . .	99
5.4	CPA Binary Parameter Estimation Using Water Dew Point . . . . .	103
5.4.1	Analysis of the Binary Mixture H <sub>2</sub> O + CO <sub>2</sub> . . . . .	104
5.4.2	Validation through Multicomponent Dew Point Calculations .	110
5.5	Application to an Industrial Dehydration Unit . . . . .	112
5.5.1	Generating New Parameters for Binary Mixtures With Water	112
5.5.2	The MEG Dehydration Unit . . . . .	113
5.5.3	Comparison with Commercial Process Simulators . . . . .	114
5.5.4	Discussion of the Results . . . . .	115

<b>6 Conclusions</b>	<b>120</b>
<b>Bibliography</b>	<b>124</b>
<b>A The MEG Dehydration Unit</b>	<b>133</b>

# List of Figures

1.1	An example of a clogged line due to the hydrate formation. Image taken from TECPETRO. . . . .	2
2.1	A simplified flowchart of a TEG dehydration plant, adapted from BRASIL <i>et al.</i> (2011) . . . . .	8
3.1	Random cluster formation for Simplex method. . . . .	33
3.2	Algorithm to evaluate objective function of pure component case. 'PSAT' and 'DPDVC' are internal functions, dependent to the temperature (T), thermodynamic model (EoS), component critical properties (Comp) and manipulated variables. . . . .	38
3.3	Algorithm of the objective function calculation of the binary mixture case in LLE. 'PBUB' calculates bubble pressure of the system and 'PSAT' calculates the saturation pressure of a pure component. . . .	40
3.4	Algorithm of the objective function calculation of the binary mixture case from the bubble or dew pressure of the system (Section 3.1.1). 'Comps' contains the components' critical properties and EoS parameters. . . . .	42
3.5	Algorithm of objective function calculation of multicomponent mixture case using gas humidity data. 'XH2O' is an internal function of the program, described in the Section 3.1.3. 'Comps' is an object containing the components' specifications, such as critical variables and EoS parameters. . . . .	44
4.1	Main features of Pure Component tab. 1) Input and experimental data. 2) Thermodynamic model used in this execution. 3) Parameters to be estimated. 4) Button to calculate objective function of a specific set of parameters, without optimizing. 5) Objective function to be minimized. 6) Diagnostics box, progress bar and 'abort' button (General Features). 7) Miscellaneous functions (General Features). . . .	47
4.2	Interfaces of each Equation of State implemented in <i>ThermOpt</i> . . . .	49
4.3	All $\alpha$ functions currently implemented into <i>ThermOpt</i> . . . . .	49

4.4	Interface shown when the option 'Fix a0 / b Parameters' is checked. . . . .	49
4.5	Combinations of parameters to be estimated. 1) SRK or PR + original $\alpha$ function; 2) SRK or PR + water-specific $\alpha$ functions, or CPA without self-association; 3) SRK or PR + Mathias-Copeman $\alpha$ function; 4) CPA with self-association; 5) SRK or PR + Mathias-Copeman AND $a_0$ and $b$ fixed; 6) SRK or PR + water-specific $\alpha$ functions AND $a_0$ and $b$ fixed. . . . .	50
4.6	Interface appearances of Density and Critical Region Penalization terms when turned off. . . . .	51
4.7	Interface appearance when the user clicks on 'Experimental Point' option in 'Variances' box, from the 'Fixed' option. . . . .	51
4.8	Main features of Binary Mixture tab. 1) Input, experimental data and phase equilibrium selector. 2) Thermodynamic model used in this execution, focused on mixture and combination rules. 3) Parameters to be estimated - depend on the EoS, combination rule and bounds given by the user. 4) Button to calculate objective function of a specific set of parameters, without optimizing. 5) Objective function to be minimized. 6) Diagnostics box, progress bar and 'abort' button (General Features). 7) Miscellaneous functions (General Features). . . . .	52
4.9	Possible combinations of parameters to be estimated in the Binary Mixture tab. 1) CPA EoS + Modified CR-1 option; 2) CPA EoS + Solvation Effect option; 3) CPA EoS + ECR/CR-1 option or PR/SRK EoS; 4) Same as (3), but with both limits of variable $k_{ij,1}$ equal to zero, forcing $k_{ij}$ to be constant. . . . .	54
4.10	Objective function interface for VLE case in Binary Mixture tab. The user can select the type of pressure calculation - bubble or dew. . . . .	54
4.11	Objective function interface for LLE case in Binary Mixture tab. . . . .	54
4.12	Main features of Multicomponent Mixture tab. 1) Input data for each component. 2) Experimental data needed. 3) Thermodynamic model used in this execution. 4) Button that adds manually a new component to the system. 5) Select parameters and check the objective function of a specific set of parameters, without optimizing. 6) Objective function to be minimized. 7) Diagnostics box, progress bar and 'abort' button (General Features). 8) Miscellaneous functions (General Features). . . . .	55

4.13	Interface formed when pressing the button 'Binary Parameters...' in the Multicomponent Mixture tab. It is important to notice that, although the parameters of all pairs are editable, only the ones containing water can be selected to manipulate in the optimization. Also, the user can check the objective function, the deviations and the graphs formed by the parameters to be input in this screen. . . .	56
4.14	Result's grid of a pure component estimation of water using CPA equation of state without penalization, showing parameters, objective function, average deviation of each variable and number of iterations of each method. The first line contains results for bank component parameters, if present. As there is no 'Water' component in the bank, it contains the original parameters instead, calculated by critical properties and acentric factor (no association). The second line contains PSO calculated parameters and the third line contains Simplex calculated parameters. . . . .	57
4.15	Result's grid of a pure component estimation of water using SRK equation of state + Kabadi-Danner $\alpha$ function. In this case, there is no 'Water0' component in the bank, so the first line is also calculated using original parameters. The First and Second Penalization Term columns refer to Equation (3.32) before multiplying them to the weights. . . . .	57
4.16	Result's grid of a binary parameter estimation of pair CO <sub>2</sub> -Water by pressure using CPA equation of state. In this case there are only the PSO and Simplex results' lines. It is important to notice that the column with values in bold means that this parameter was not estimated, but calculated by a combining rule. . . . .	58
4.17	Result's grid of a binary parameter estimation of the pair n-Hexane-Water by liquid-liquid compositions metric using the CPA equation of state. . . . .	58
4.18	Result's grid of a binary parameter estimation of a gas composed by water, CO <sub>2</sub> , H <sub>2</sub> S and methane by the water content metric using the CPA equation of state. This consists of a Simplex optimization procedure from a predefined initial guess. . . . .	58
4.19	Example of scatter plot. Parameter $a_0$ versus objective function evaluations calculated for water using CPA equation of state. All graphics can be zoomed freely to analyse local minima region. The maximum objective function value can be fixed, manipulating the heat color map to make the visualization easier. . . . .	59

4.20	Example of parameter analysis. Parameter $a_0$ versus $b$ , calculated for water using CPA equation of state. This plot shows clearly that possible solutions for the parameter $b$ lie on a narrow range, being in agreement with KONTAGEORGIS <i>et al.</i> (2006a). . . . .	60
4.21	Examples of statistical reports generated by <i>ThermOpt</i> regarding a parameter estimation of water using the SRK EoS with the Kabadi-Danner $\alpha$ function. (a) Chi-square test with confidence interval equal to 95%. (b) Maximum error analysis with $Err_{max,P} = Err_{max,\rho} = 1.0\%$ . . . . .	61
4.22	Parameter $a_0$ values versus the objective function, calculated for water using CPA EoS, in a Simplex method executed just after the PSO from figures 4.19 and 4.20. . . . .	62
4.23	Pressure (a) and density (b) deviations [%] for water calculated by CPA equation of state. Experimental data from DIPPr (DIADEM, 2004). . . . .	62
4.24	Experimental versus calculated values of pressure (a) and density (b) calculated for water using CPA equation of state. Experimental data from DIPPr (DIADEM, 2004). . . . .	63
4.25	Saturation curve – reduced temperature versus pressure – calculated for water using CPA equation of state. Experimental data from DIPPr (DIADEM, 2004). . . . .	63
4.26	Chart reporting liquid-liquid equilibria compositions versus temperature of the binary mixture n-Hexane-Water, calculated by CPA equation of state with $k_{ij} = 0$ and water parameters from KONTAGEORGIS <i>et al.</i> (1999), comparing to experimental data (TSONOPOULOS and WILSON, 1983). . . . .	64
4.27	Chart reporting dew pressures versus water content of the mixture CO <sub>2</sub> -Water, calculated by CPA equation of state using $k_{ij} = 0$ and $\beta^{A_i B_j} = \beta_{water} = 0.0692$ , with water parameters from KONTAGEORGIS <i>et al.</i> (1999) and $T = 348.15K$ . Experimental data are from VALTZ <i>et al.</i> (2004). . . . .	64
4.28	Variables table for the PSO results case mentioned on Section 4.3.2. Number of 'Total Function Evaluations' stands for the number of converged objective function evaluations. . . . .	65
4.29	Variables table for the Simplex results case mentioned on Section 4.3.2. Again, number of 'Total Function Evaluations' stands for the number of converged objective function evaluations. . . . .	65
4.30	Variables table for general results (phase equilibrium variables) case described in the Section 4.3.2. . . . .	66

4.31	Example of input .txt file of a pure component. Note that experimental values can be copied directly from an Excel sheet, and any text written after the character '%' will not be read, being used to comment the data. . . . .	67
4.32	Input .txt file to a binary pair CO <sub>2</sub> - water with VLE data. Note that any text written after the character '%' will not be read, being used to comment the data. . . . .	68
4.33	Input .txt file to a binary pair water - n-hexane with LLE data. Also, as pressure is not an obligatory variable, it is acceptable to have gaps in this field. . . . .	69
4.34	Input .txt file for a multicomponent mixture of water, CO <sub>2</sub> , H <sub>2</sub> S and methane. . . . .	70
4.35	Solvers in the 'Options' interface of <i>ThermOpt</i> . (a) PSO method solver options. (b) Simplex method solver options. (c) General options, such as thermodynamic tolerances. . . . .	71
4.36	Estimable parameter bounds inside the <i>ThermOpt</i> options. . . . .	72
4.37	Example of histogram generated, analysing the parameter $a_0$ of water calculated by SRK equation of state and Kabadi-Danner $\alpha$ function. The optimal solution in this case lies on $a_0 \approx 4.587 \text{ bar}\cdot\text{L}^2/\text{mol}^2$ . . . . .	73
4.38	Option to save results into the data bank. . . . .	73
4.39	.txt file to the data bank, named 'Water_CPA.txt'. . . . .	74
5.1	Diagnostics text-box showing a result for a parameter estimation procedure by the PSO method. . . . .	75
5.2	PSO options used for performance analysis for a case with 100 max iterations and 1 particle per iteration. The minimum number of iteration in optimum permanence must be the same as the maximum number of iterations in order to make the solver ignore the tolerances. . . . .	76
5.3	Input interface in the case studied in the Section 5.2.1. . . . .	78
5.4	Thermodynamic options for the case studied in the Section 5.2.1. . . . .	78
5.5	PSO options for the case studied in the Section 5.2.1. . . . .	79
5.6	Simplex options for the case studied in the Section 5.2.1. . . . .	79
5.7	Pressure deviations for two of the cases listed in Table 5.5. Left: $w_1 = w_2 = 0$ ( $AAP = 0.2281\%$ ). Right: $w_1 = w_2 = 0.001$ ( $AAP = 0.8547\%$ ). Experimental data: DIPPr correlations (DIADDEM, 2004). Critical temperature used for water = 647.13 K. Images taken directly from <i>ThermOpt</i> . . . . .	81
5.8	PSO options used in the parameter estimation procedures executed in the Section 5.2.2. . . . .	83

5.9	Simplex options used in the parameter estimation procedures executed in the Section 5.2.2. . . . .	83
5.10	Thermodynamic options used in the parameter estimation procedures executed in the Section 5.2.2. . . . .	84
5.11	Simplex options used in the parameter estimation procedures executed in the Section 5.3. . . . .	87
5.12	Pareto analysis containing both objective function terms of Equation (3.35) for MEG, as seen throughout the studied region, showing the 'Set 01', with $w = 0$ (red circle). Literature Set of parameters was taken from DERAWI <i>et al.</i> (2003). . . . .	89
5.13	Pareto analysis containing both objective function terms of Equation (3.35) for MEG, focusing on the region where the 'Set 02' was selected (diamond), comparing to the actual location of the Literature Set (DERAWI <i>et al.</i> , 2003), marked as a square. . . . .	89
5.14	Pareto analysis containing both objective function terms of Equation (3.35) for DEG, as seen throughout the studied region, showing the 'Set 01', with $w = 0$ (red circle). Literature Set of parameters was taken from DERAWI <i>et al.</i> (2003) . . . . .	92
5.15	Pareto analysis containing both objective function terms of Equation (3.35) for DEG, focusing on the region where the 'Set 02' was selected (diamond), comparing to the location of the set of parameters from the literature (DERAWI <i>et al.</i> , 2003), marked as a square. . . . .	92
5.16	Pareto analysis containing both objective function terms of Equation (3.35) for TEG, as seen throughout the studied region, showing the 'Set 01', with $w = 0$ (red circle). Literature Set of parameters was taken from DERAWI <i>et al.</i> (2003) . . . . .	94
5.17	Pareto analysis containing both objective function terms of Equation (3.35) for TEG, focusing on the region where the 'Set 02' was selected (diamond), comparing to the location of the set of parameters from the literature (DERAWI <i>et al.</i> , 2003), marked as a square. . . . .	94
5.18	Pareto analysis containing both objective function terms of Equation (3.35) for PG, as seen throughout the studied region, showing the 'Set 01', with $w = 0$ (red circle). Literature Set of parameters was taken from DERAWI <i>et al.</i> (2003) . . . . .	96



5.19	Pareto analysis containing both objective function terms of Equation (3.35) for PG, focusing on the region where the 'Set 02' was selected (diamond), comparing to the location of the literature set (DERAWI <i>et al.</i> , 2003), marked as a square. . . . .	97
5.20	Chart containing the values of association energy for water versus $S_{LLE}$ , comparing with the literature values and the chosen 'Set 03' in this work. Ref. A: KONTOGEORGIS <i>et al.</i> (1999). Ref B: KOH <i>et al.</i> (1993). . . . .	100
5.21	Pareto analysis containing both objective function terms of Equation (3.35) for water, showing the 'Set 01', with $w = 0$ (red circle). Literature Set was taken from KONTOGEORGIS <i>et al.</i> (1999).	101
5.22	Chart containing values of pressure versus water content in dew point for the mixture Water + CO <sub>2</sub> in an isotherm at $T = 298.15$ K. Experimental data: WIEBE and GADDY (1941). Literature parameters: KONTOGEORGIS <i>et al.</i> (1999) (pure water) and TSIVINTZELIS <i>et al.</i> (2011) (binary parameters). Optimized parameters: this work ('Set 03' for pure water). . . . .	106
5.23	Chart containing values of pressure versus water content in dew point for the mixture Water + CO <sub>2</sub> in an isotherm at $T = 304.15$ K. Experimental data: WIEBE and GADDY (1941). Literature parameters: KONTOGEORGIS <i>et al.</i> (1999) (pure water) and TSIVINTZELIS <i>et al.</i> (2011) (binary parameters). Optimized parameters: this work ('Set 03' for pure water). . . . .	107
5.24	Chart containing values of pressure versus water content in dew point for the mixture Water + CO <sub>2</sub> in an isotherm at $T = 323.15$ K. Experimental data: WIEBE and GADDY (1941). Literature parameters: KONTOGEORGIS <i>et al.</i> (1999) (pure water) and TSIVINTZELIS <i>et al.</i> (2011) (binary parameters). Optimized parameters: this work ('Set 03' for pure water). . . . .	107
5.25	Chart containing values of pressure versus water content in dew point for the mixture Water + CO <sub>2</sub> in an isotherm at $T = 348.15$ K. Experimental data: WIEBE and GADDY (1941). Literature parameters: KONTOGEORGIS <i>et al.</i> (1999) (pure water) and TSIVINTZELIS <i>et al.</i> (2011) (binary parameters). Optimized parameters: this work ('Set 03' for pure water). . . . .	108
5.26	Scatter plot of parameter $k_{ij}$ versus objective function evaluations calculated for the mixture water ('Set 03') + CO <sub>2</sub> using all $\sigma_{y,i} = 1$ in Equation (3.38). Image taken directly from <i>ThermOpt</i> . . . . .	109

5.27	Scatter plot of parameter $\beta_{ij}^{cross}$ versus objective function evaluations calculated for the mixture water ('Set 03') + CO <sub>2</sub> using all $\sigma_{y,i} = 1$ in Equation (3.38). Image taken directly from <i>ThermOpt</i> . . . . .	110
5.28	Abstract scheme of the dehydration unit studied in the Section 5.5.2. The inhibitor agent used is ethylene glycol (MEG). . . . .	114

# List of Tables

3.1	Numerical example for a pure water saturation pressure calculation ( $T_c = 647.13$ K, $P_c = 220.55$ bar, $w = 0.3449$ ), at $T = 350$ K and using the CPA equation of state parameters published by KONTOGEORGIS <i>et al.</i> (1999). Convergence tolerance = $10^{-4}$ .	22
3.2	Numerical example for a LLE calculation for the mixture water + n-hexane, at $T = 333.15$ K and CPA equation of state parameters modelled in the literature for water (KONTOGEORGIS <i>et al.</i> , 1999) and n-hexane (TSIVINTZELIS <i>et al.</i> , 2011), with $k_{ij} = 0$ . Convergence tolerance = $10^{-4}$ . The initial guesses to the compositions are related to the respective experimental data informed in the program interface.	24
3.3	Numerical example for a water content calculation for the mixture water + CO <sub>2</sub> , at $T = 298.15$ K, $P = 50.66$ bar and CPA equation of state parameters modelled in the literature for water (KONTOGEORGIS <i>et al.</i> , 1999) and CO <sub>2</sub> (TSIVINTZELIS <i>et al.</i> , 2010), with the binary parameters $k_{ij} = 0$ and $\beta_{ij}^{cross} = \beta_{water} = 0.0692$ , considering the solvation effect between these components (LI and FIROOZABADI, 2009). Convergence tolerance = $10^{-6}$ . The $y_{max}^{H_2O}$ value was set at 0.5% ( $n_1 \approx 0.00502$ ). 'BS' and 'SS' mean Bisection Step and Secant Step, respectively, as previously described.	29
5.1	PSO performance analysis results. Each objective function (ObjF) evaluation contains 100 saturation pressure (PSAT) calculations due to the number of experimental data inserted.	77
5.2	Parameter bounds for the case studied in the Section 5.2.1. These values were obtained by trial and error in order to select bounds that contain all of the possible solutions achieved in this Section.	79
5.3	Input summary for the case studied in the Section 5.2.1.	80
5.4	Minimum and maximum weights' values used in the Section 5.2.1, as well as their variation between each execution ( $\Delta w$ ).	80

5.5	Penalization analysis' results obtained from different values of weights. SRK-KD original parameters: calculated from critical properties and $c_1$ proposed by KABADI and DANNER (1985). . . . .	80
5.6	Summary of the general data used for the parameter estimation procedure of MEG, DEG, TEG, PG and water (CPA EoS). . . . .	82
5.7	Parameters' bounds used for MEG parameter estimation (CPA EoS), obtained by a previous trial and error method. . . . .	84
5.8	Comparison between the literature parameters for MEG (DERAWI <i>et al.</i> , 2003) and the calculated ones from <i>ThermOpt</i> . The difference between 'Set 01' and 'Set 02' lies on the $T_R$ range of the experimental data used in each case. . . . .	85
5.9	Bounds for the parameters to be estimated for DEG, TEG, PG and water, as well as their temperature range for the experimental data (DIADEM, 2004). . . . .	85
5.10	Parameters estimated by <i>ThermOpt</i> , using saturation pressure and liquid density, for DEG, TEG, PG and water. . . . .	86
5.11	Parameter bounds for the case studied in the Section 5.3. . . . .	87
5.12	Maximum errors in DIPPr correlations (DIADEM, 2004) for each studied component in the Section 5.3.1. . . . .	88
5.13	Parameters chosen using the VLE + LLE Methodology for MEG ( $S_{max,pure} = 1.0e - 3$ ), comparing to the parameters from the literature (DERAWI <i>et al.</i> , 2003). $w$ consists of the weight inserted on Equation (3.35). . . . .	90
5.14	Results for the binary mixture MEG + n-heptane (DERAWI <i>et al.</i> , 2002). $AAX_{MEG,HC}$ and $AAX_{HC,MEG}$ are calculated from Equations (5.4) and (5.5). . . . .	91
5.15	Results for the binary mixture MEG + n-hexane (DERAWI <i>et al.</i> , 2002). $AAX_{MEG,HC}$ and $AAX_{HC,MEG}$ are calculated from Equations (5.4) and (5.5). . . . .	91
5.16	Results for the binary mixture MEG + benzene (FOLAS <i>et al.</i> , 2006b). $AAX_{MEG,HC}$ and $AAX_{HC,MEG}$ are calculated from Equations (5.4) and (5.5). . . . .	91
5.17	Results for the binary mixture MEG + toluene (FOLAS <i>et al.</i> , 2006b). $AAX_{MEG,HC}$ and $AAX_{HC,MEG}$ are calculated from Equations (5.4) and (5.5). . . . .	91
5.18	Parameter sets chosen using the VLE + LLE Methodology for DEG ( $S_{max,pure} = 1.09e - 2$ ), comparing to the parameters from literature (DERAWI <i>et al.</i> , 2003). $w$ consists of the weight inserted on Equation (3.35). . . . .	93

5.19	Results for the binary mixture DEG + n-heptane (DERAWI <i>et al.</i> , 2002). $AAX_{DEG,HC}$ and $AAX_{HC,DEG}$ are calculated from Equations (5.4) and (5.5). . . . .	93
5.20	Parameter sets chosen using the VLE + LLE Methodology for TEG ( $S_{max,pure} = 1.09e - 2$ ), comparing to the parameters from literature (DERAWI <i>et al.</i> , 2003). The weight $w$ is taken from Equation (3.35). . . . .	95
5.21	Results for the binary mixture TEG + n-heptane (DERAWI <i>et al.</i> , 2002). $AAX_{TEG,HC}$ and $AAX_{HC,TEG}$ are calculated from Equations (5.4) and (5.5). . . . .	95
5.22	Results for the binary mixture TEG + benzene (FOLAS <i>et al.</i> , 2006b). $AAX_{TEG,HC}$ and $AAX_{HC,TEG}$ are calculated from Equations (5.4) and (5.5). . . . .	95
5.23	Results for the binary mixture TEG + toluene (FOLAS <i>et al.</i> , 2006b). $AAX_{TEG,HC}$ and $AAX_{HC,TEG}$ are calculated from Equations (5.4) and (5.5). . . . .	96
5.24	Parameters chosen using the VLE + LLE Methodology for PG ( $S_{max,pure} = 3.40 \times 10^{-3}$ ), comparing to the parameters from literature (DERAWI <i>et al.</i> , 2003). The weight $w$ is taken from Equation (3.35). . . . .	97
5.25	Results for the binary mixture PG + n-heptane (DERAWI <i>et al.</i> , 2002). $AAX_{PG,HC}$ and $AAX_{HC,PG}$ are calculated from Equations (5.4) and (5.5). . . . .	98
5.26	Maximum errors in DIPPr correlations (DIADEM, 2004) for water. . . . .	99
5.27	Parameter sets chosen using the VLE + LLE Methodology for water, comparing to the parameters from literature (KONTOGEOORGIS <i>et al.</i> , 1999). $w$ consists of the weight inserted on Equation (3.35). . . . .	101
5.28	Results for the binary mixture water + n-hexane (TSONOPOULOS and WILSON, 1983). $AAX_{W,HC}$ and $AAX_{HC,W}$ are calculated from Equations (5.4) and (5.5). . . . .	102
5.29	Results for the binary mixture water + n-octane (HEIDMAN and TSONOPOULOS, 1985). $AAX_{W,HC}$ and $AAX_{HC,W}$ are calculated from Equations (5.4) and (5.5). . . . .	102
5.30	Results for the binary mixture water + benzene (ANDERSON and PRAUSNITZ, 1986). $AAX_{W,HC}$ and $AAX_{HC,W}$ are calculated from Equations (5.4) and (5.5). . . . .	102
5.31	Results for the binary mixture water + toluene (ANDERSON and PRAUSNITZ, 1986). $AAX_{W,HC}$ and $AAX_{HC,W}$ are calculated from Equations (5.4) and (5.5). . . . .	102

5.32	Pure component parameters used in the Section 5.4.1. . . . .	104
5.33	Summary of the data of the mixture studied in this Section. . . . .	105
5.34	Bounds for the water + CO <sub>2</sub> parameter estimation in this Section. These values were obtained by trial and error. . . . .	105
5.35	Estimation results for water (KONTOGEOGRIS <i>et al.</i> , 1999) + CO <sub>2</sub> mixture studied in this Section. . . . .	105
5.36	Estimation results for water (Set 03) + CO <sub>2</sub> mixture studied in this Section. . . . .	105
5.37	Estimation results for water + CO <sub>2</sub> mixture studied in this Section for $P > 200$ bar. . . . .	108
5.38	Estimation results for water (Set 03) + CO <sub>2</sub> mixture studied in this Section with $S'_y$ defined by Equation (3.38) with all variances equal to 1. . . . .	109
5.39	Estimation results for each aqueous binary mixture studied in this work. All interaction parameters presented within the literature sets were taken from SANTOS <i>et al.</i> (2015b), and the 'Set 03' for water was used in the optimized sets from this work. 'mCR-1' means that $\varepsilon_{ij}^{cross}$ was calculated according to Equation (2.31). . . . .	111
5.40	Mean absolute deviations for water content ( $AAY$ [%]) calculated for each of the mixtures studied in this Section. Literature parameters were taken from SANTOS <i>et al.</i> (2015b). . . . .	111
5.41	All binary CPA EoS parameters obtained for the 'Set 03' parameters of water ('component i') with the components present in the simulation of the MEG unit. All calculations were performed in <i>ThermOpt</i> . . . . .	113
5.42	Dehydrated gas ('HC02') results for the MEG unit. Simulated at: Hysys <sup>®</sup> , Petro-SIM <sup>®</sup> , ProMax <sup>®</sup> and Petrox <sup>®</sup> . . . . .	115
5.43	Regenerator top outlet conditions ('VENT') results for the MEG unit. Simulated at: Hysys <sup>®</sup> , Petro-SIM <sup>®</sup> , ProMax <sup>®</sup> and Petrox <sup>®</sup> . . . . .	115
5.44	General results for the the MEG unit equipments. Simulated at: Hysys <sup>®</sup> , Petro-SIM <sup>®</sup> , ProMax <sup>®</sup> and Petrox <sup>®</sup> . . . . .	116
5.45	Dehydrated gas ('HC02') results for the MEG unit. Executed by the Petrox <sup>®</sup> process simulator. . . . .	116
5.46	Regenerator top outlet conditions ('VENT') results for the MEG unit. Executed by the Petrox <sup>®</sup> process simulator. . . . .	116
5.47	General results for the the MEG unit equipments. Executed by the Petrox <sup>®</sup> process simulator. . . . .	117
5.48	Binary parameters obtained (1,2-propylene glycol: component i). All calculations were performed in <i>ThermOpt</i> . . . . .	118

5.49 Dehydrated gas ('HC02') results for the MEG unit. Executed by the Petrox <sup>®</sup> process simulator using MEG and PG as solvents, respectively. All pure components' parameters were taken from the literature (SANTOS <i>et al.</i> , 2015b). . . . .	119
A.1 Condition of the fictitious feed stream of the MEG unit, labelled as 'HC01'. . . . .	133
A.2 Conditions of the vessels in the MEG unit simulated in this work. . .	134
A.3 Conditions of the Regenerator in the MEG unit simulated in this work.	134
A.4 Conditions of the glycol injection points in the MEG unit simulated in this work. . . . .	134
A.5 Conditions of the heat exchangers in the MEG unit simulated in this work. . . . .	134

# Chapter 1

## Introduction

### 1.1 Motivation

Petroleum is one of the most abundant natural resource in the world. Its refinery products can fuel factories, industries, vehicles, as well as be raw material to develop polymers such as plastic and rubber. It can also provide electric energy from the coal burning.

For this reason, the discovery of large amounts of petroleum under a thick salt layer in ultra-deep waters around Santos Basin, Brazil, is among the most important in the world over the last decade. These so called pre-salt reservoirs contain high quality light oil (over 25° API), with high commercial value.

However, it also involves a high gas-oil rate, high CO<sub>2</sub> content, high pressure (up to 1000 bar) and low temperature conditions (BELTRÃO *et al.*, 2009). Therefore, it is necessary to develop specific technologies adapted to this challenging scenario in order to make this exploration feasible (SANTOS, 2015).

Firstly, a common issue in oil and gas exploring is the possibility of hydrate formation, capable to clog entire oil lines. Figure 1.1 shows an example of its potential damage. In order to prevent that, a typical course of action is to add thermodynamic inhibitors (e.g. methanol) directly to the reservoir fluid. However, it is an expensive procedure due to the solvent loss, and used only as a last resource (LUNDSTRØM, 2005). These inhibitors change the chemical potential of the phases, causing an increase of the hydrate formation pressure (or decreasing its temperature).





Figure 1.1: An example of a clogged line due to the hydrate formation. Image taken from TECPETRO.

An alternative to methanol are glycols such as ethylene glycol (MEG). They have the upside of being less volatile, avoiding inhibitor losses with its recovery. However, when recovering the glycol aqueous solution, there is the possibility of BTEX compounds (benzene, toluene, ethyl-benzene and xylenes) to be dragged along the water removed. These components are extremely dangerous to health, and most legislations around the world fix a tight limit for their emissions, in the order of 1 ppm in water. Thus, it is essential to thermodynamically model precisely the hydrate equilibria in the presence of inhibitors and the phase equilibria with water to design or optimize the transport means, processing and production of natural gas (HAGHIGHI, 2009).

When designing or simulating equipments it is important to calculate correctly the thermodynamic properties of the fluids and solids involved. However, experimental data are not always available, so it is desirable to hold a model that has a high degree of data prediction or extrapolation. Some of the preferably used models in the oil and gas industry are the cubic equations of state, such as Soave-Redlich-Kwong - SRK (SOAVE, 1972) and Peng-Robinson - PR (PENG and ROBINSON, 1976), both based on the van der Waals' equation (VAN DER WAALS, 1873). They are relatively simple models, and the parameters for a vast quantity of compounds have been already determined in the literature.

However, these equations generate better predictions for non-polar substances. In the natural gas processing, some of the most central compounds are either highly polar (water, alcohols, glycols) or have the possibility to form induced hydrogen bonds ( $H_2S$ ,  $CO_2$ , aromatic compounds). In this scenario, an improved model may

be necessary to perform proper calculations.

Thermodynamic properties of these substances are determined by intermolecular forces (PRAUSNITZ *et al.*, 1999), particularly the hydrogen bonds. Numerous equations of state (EoS) have been proposed along the years, in order to predict these effects. Most of them belong to one of these theories: chemical, lattice or perturbation. One of the most important EoS proposed is derived from the Statistical Association Fluid Theory - SAFT (CHAPMAN *et al.*, 1988). Several variants of this EoS were proposed later.

From one of these variants, the Cubic Plus Association - CPA (KONTOGEORGIS *et al.*, 1996) was modelled, simpler but as efficient as the former for aqueous systems. It can be considered as an alternative to predict the behaviour of polar mixtures and uncomplicated enough to be implemented for modelling complex industrial systems.

One particularity of these equations is that they must have their parameters estimated from experimental data. However, KONTOGEORGIS *et al.* (2006a) stated that, due to the complexity of non-cubic EoS, there are known issues in this procedure such as multiple solution sets or correlations between the manipulated parameters. Therefore, this procedure tends to be complicated and time-consuming.

Because of that, this work proposes the development and validation of a computational tool to perform this procedure. The main idea is to offer a user-friendly interface, a wide variety of options and analyses, with the possibility to export the results to another application such as Excel. Besides, it will be possible to generate charts such as:

- The behaviour of each manipulated parameter versus the respective objective function in the search space of a stochastic method;
- The correlation effect between each pair of parameters in this same search space;
- General phase equilibria results (deviations, equilibrium diagrams etc).

Because this is a visual, fast and applicable tool, it was included the cubic EoS (SRK and PR) together with the CPA. Besides, it allows the user to flexibilize the cubic EoS parameters instead of using the ones calculated by critical properties and acentric factor, potentially improving their results. In the Oil and Gas industry, the simplest approach is always the best, as long as it is effective.

## 1.2 Objectives

In view of what has been exposed, the general objective of this dissertation is to develop, validate and provide a thermodynamic parameter estimation tool, with a user-friendly interface, and apply it to a natural gas processing plant simulation.

As for specific objectives, the following stand out:

- To develop a computational program for parameter estimation from experimental data;
- To study metrics, numerical methods and optimization strategies for each parameter estimation case;
- To re-estimate pure components' parameters using the CPA equation of state (KONTOGEOGRIS *et al.*, 1996) using systematic and fast procedures, after validating the program outputs with experimental data available in the literature for pure components and mixtures;
- To perform a parameter estimation of binary systems using data from mixtures containing water and light gases. Validation is to be performed from temperature, pressure and humidity of published data on multicomponent acid gases;
- To simulate an industrial natural gas processing unit applying all previous optimized parameters, comparing to commercial process simulators outputs.

## 1.3 Organization of the Text

In order to achieve the aforementioned objectives, this text is divided by chapters referent to each relevant stage of the development of this dissertation.

In Chapter 2 a natural gas dehydration process unit with glycols is presented, pointing out the importance of the right thermodynamic modelling. Besides, in this chapter a bibliographic review of the main equations of state is presented, from cubic equations to association models, arriving to the CPA equation of state. Thereon, the main parameter estimation procedures published in the literature are stated.

In Chapter 3 the mathematical modelling behind the parameter estimation applied to thermodynamics is detailed, along with the algorithms used in the program. It starts from the thermodynamic functions, then describes the optimization methods used in the calculations and finally presents the parameter estimation metrics and procedures.

Chapter 4 summarizes most of the main functions of the program proposed in this work, the *ThermOptimizer*. It details not only each interface component that is already designed, but also the features it offers.

In Chapter 5 some of the possible results achieved with the *ThermOptimizer* are presented. Among them, there is a performance analysis of the program; a penalization analysis related to the critical point behaviour of water using the SRK EoS; pure parameter estimation for polar components with the CPA EoS, validating the results with liquid-liquid equilibria data; a CPA EoS binary parameter estimation using the metrics described in Chapter 3; and a dehydration plant analysis, comparing the optimized results with commercial simulators.

Finally, in Chapter 6 the relevant conclusions are presented, as well as suggestions to future works.

# Chapter 2

## Bibliographic Review

### 2.1 Natural Gas Processing

In the natural gas processing, it is necessary to adequate the product to commercial specifications, removing some compounds that would otherwise decrease its sale value, or damage downstream equipments and lines. For example, these impurities can be water, liquid heavy hydrocarbon fractions (C<sub>6+</sub>) or acid gases (LUNDSTRØM, 2005).

The following is a set of specific compounds and what damage they would cause if not removed from the natural gas (SANTOS, 2015):

- Hydrogen sulphate – toxic and corrosive;
- Carbon dioxide – corrosive and can crystallize in low temperature processes;
- Water – hydrate formation and corrosion;
- Heavy hydrocarbons – can condensate or form solids in transport lines.

Besides, the environmental legislation about atmospheric emissions are increasingly tighter around the world, especially for benzene, toluene, ethyl-benzene and xylenes (BTEX compounds). The health risk of exposure to these substances in the downstream is extensively described and evaluated by authors such as EDOKPOLO *et al.* (2015). Therefore, they must be extracted from the stream.

As there are several processes to purify the natural gas, this work will focus on the dehydration processes. There are different approaches for them (BRASIL *et al.*, 2011):

- Absorption by a liquid solvent such as glycols;
- Adsorption by a solid such as silica gel, alumina or a molecular sieve;

- Permeation by polymeric membranes.

For instance, in Brazilian platforms the most common process is the glycol absorption.

### 2.1.1 Absorption Process in Dehydration

This process consists of inserting a substance capable to selectively solubilize water from the gas stream (BRASIL *et al.*, 2011). The choice of this solvent is usually for economic reasons, such as:

- Ease of regeneration, normally related to the non-volatility of the solvent;
- Potential loss to evaporation;
- Solvent cost.

Although alcohols like methanol and ethanol have high affinity with water, compounds of the glycol family (e.g. MEG – mono-ethylene glycol – or TEG – tri-ethylene glycol) are used more often because their vapour pressure is lower, facilitating the regeneration and avoiding evaporation losses.

Figure 2.1 shows an outline of this process. The main equipment is the absorption tower. The gas (already without heavy hydrocarbons) flows in counter-current with the regenerated TEG (or 'poor TEG'). The TEG solution, when it flows out of the bottom of the tower, changes into a 'rich TEG' solution, is heated and flows into a three-phase separator to remove any hydrocarbons from the gas that may have been solubilized. The TEG solution feeds the regenerator, being vaporized at a temperature close to its degradation temperature. Consequently, the water content of this solution is reduced when cooled back, becoming the 'poor TEG' in the bottom of the regenerator. After that it is further cooled and returns to the absorption tower.

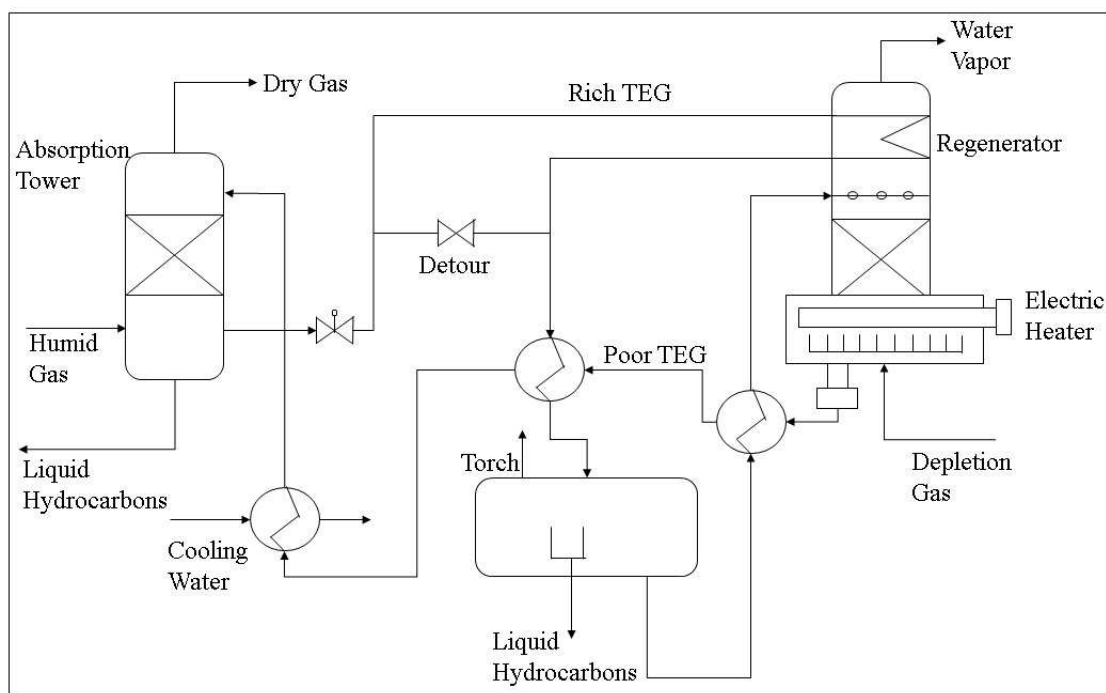


Figure 2.1: A simplified flowchart of a TEG dehydration plant, adapted from BRASIL *et al.* (2011)

### 2.1.2 BTEX Issues in Dehydration

In the separation stage just before the regeneration, utmost care must be taken because the BTEX compounds are some of the possible liquid hydrocarbons to be separated. If this stage is not done properly, some of these poisonous substances may leave the regenerator dragged with the water vapour. Thus, the solubility of aromatic components in solutions with water and glycols are of great academic and industrial interest (FOLAS *et al.*, 2006a).

Even though there is only partial solubility of BTEX compounds in aqueous glycol solutions, most legislations specify roughly 1 ppm as the maximum limit of these components in water, lower than the solubility in the conditions of the regenerator. Therefore, the thermodynamic modelling of these complex mixtures must be robust enough to predict how to avoid this limit. These phenomena are often better modelled by equations of state, which will be described in the Section 2.2.

However, it is important to mention that different commercial process simulators diverge greatly (often by orders of magnitude) when simulating streams containing benzene. Therefore, one of the focus of this work, which will be detailed later, is to perform a solid evaluation of these compounds and utilize an advanced thermodynamic model that can take into account the association effects between benzene and water and between benzene and glycols.

## 2.2 Equations of State

### 2.2.1 Overview

In the Oil and Gas industry, thermodynamic models based on equations of state are widely used, especially those of cubic format on the molar volume, for the following reasons (KONTOGEOGRIS and FOLAS, 2010):

- Suitable to be used in a wide range of pressure and temperature;
- Simple models with fast calculation and easy convergence;
- Can predict liquid and vapour properties;
- Most of cases there is no necessity to use more than one binary interaction parameter ( $k_{ij}$ );
- Good VLE prediction for multicomponent mixtures containing hydrocarbons and non-polar compounds;
- Extensive data bank and correlations available for the  $k_{ij}$  values.

Thus, cubic equations present a middle ground between applicability and simplicity, being the simplest equations capable to represent the vapour-liquid equilibrium behaviour (SMITH *et al.*, 2005).

The first famous cubic equation of state was proposed by VAN DER WAALS (1873), as can be seen in Equation (2.1):

$$P = \frac{RT}{V - b} - \frac{a}{V^2} \quad (2.1)$$

$P$  is the pressure of the system,  $T$  its temperature,  $V$  the molar volume and  $R \cong 0.0831446 \text{ bar.L/mol.K}$  the universal gas constant. This equation has two parameters:  $a$ , related to the attraction energy between the molecules, and  $b$ , which is the co-volume of the component. After his contribution, countless cubic equations of state were published, usually by the format described by Equation (2.2):

$$P = \frac{RT}{V - b} - \frac{a(T)}{(V + \epsilon b)(V + \sigma b)} \quad (2.2)$$

where the parameters  $\epsilon$  and  $\sigma$  depend on the equation, and  $a$  and  $b$  can be evaluated by an adjustment in the critical region. It is based on the fact that the critical isotherm shows a horizontal inflection, resulting on the condition dictated by Equation (2.3):

$$\left(\frac{\partial P}{\partial V}\right)_{T|_{crit}} = \left(\frac{\partial^2 P}{\partial V^2}\right)_{T|_{crit}} = 0 \quad (2.3)$$



Solving Equations (2.2) and (2.3) for  $a$  and  $b$  in the critical point, Equations (2.4) and (2.5) are formed:

$$a(T_c) = \psi \frac{R^2 T_c^2}{P_c} \equiv \psi \frac{\alpha(T_R, \omega) R^2 T_c^2}{P_c} \quad (2.4)$$

$$b = \Omega \frac{RT_c}{P_c} \quad (2.5)$$

The parameters  $\psi$  and  $\Omega$  also depend on the equation.  $T_c$  is the critical temperature of the component,  $P_c$  its critical pressure,  $\alpha(T_R, \omega)$  an auxiliary function which must be equal to 1 in the critical point, with  $T_R = T/T_c$  being the reduced temperature and  $\omega$  the Pitzer acentric factor (PITZER, 1995), defined by Equation (2.6):

$$\omega = -1.0 - \log(P_R^{sat})_{T_R=0.7} \quad (2.6)$$

$P_R^{sat} = P^{sat}/P_c$  is the reduced saturation pressure of the component. These equations of state are implicit to volume, which means that they must be solved either analytically or numerically. Let  $q$  and  $B$  be defined by Equations (2.7) and (2.8):

$$q = \frac{a}{bRT} \quad (2.7)$$

$$B = \frac{bP}{RT} \quad (2.8)$$

Rearranging Equation (2.2), Equations (2.9) and (2.10) are formed:

$$F(Z) = Z^3 + [(\epsilon + \sigma - 1)B - 1]Z^2 + [qB - (\epsilon + \sigma - \epsilon\sigma)B^2 - (\epsilon + \sigma)B]Z - \epsilon\sigma B^2(B + 1) - qB^2 = 0 \quad (2.9)$$

$$Z = \frac{PV}{RT} \quad (2.10)$$

The compressibility factor  $Z$  is then calculated by solving Equation (2.9). Note that there can be found three different roots of  $Z$ : the lowest is a liquid phase type root; the highest is a vapour phase type root; and the intermediary does not have any physical meaning.

For mixtures, the most common approach is the classic mixing rules (VAN DER WAALS, 1873). In a compound with  $n$  components, it is possible to evaluate parameters  $a$  and  $b$  of mixture, according to Equations (2.11) and (2.12):

$$a = \sum_{i=1}^n \sum_{j=1}^n x_i x_j (a_i a_j)^{0.5} (1 - k_{ij}) \quad (2.11)$$

$$b = \sum_{i=1}^n x_i b_i \quad (2.12)$$

$x_i$  is the composition of the component  $i$  in the mixture, and the parameter  $k_{ij}$  is called the binary interaction parameter, and it is calculated usually by estimation from experimental data. Besides, it is common to introduce a temperature dependent expression for this parameter (Equation (2.13)):

$$k_{ij} = k_{ij,0} + k_{ij,1}T \quad (2.13)$$

In order to improve the accuracy of these EoS when modelling polar mixtures, it is also possible to apply more advanced mixing rules, based on activity coefficient expressions such as Wilson, UNIQUAC or NRTL (PRAUSNITZ *et al.*, 1999). However, in this project the classical mixing rules will be focused. Therefore, a suggestion for future works will be to insert one or more of these advanced rules into the parameter estimation procedures, analysing their effectiveness.

Finally, as stated earlier, the parameters  $\epsilon$ ,  $\sigma$ ,  $\psi$  and  $\Omega$  change to each equation of state, with two of the most notable being the Soave-Redlich-Kwong (SOAVE, 1972) and the Peng-Robinson (PENG and ROBINSON, 1976) equations of state.

## 2.2.2 The Soave-Redlich-Kwong (SRK) EoS

The SRK equation of state is defined when  $\epsilon = 0$  and  $\sigma = 1$ , forming Equation (2.14):

$$P = \frac{RT}{V - b} - \frac{a(T)}{V(V + b)} \quad (2.14)$$

The parameter  $a$  is a function of  $T$ , given by Equations (2.15) and (2.16):

$$a(T) = a_0 \alpha(T_R, \omega) = a_0 [1 + m(1 - T_R^{0.5})]^2 \quad (2.15)$$

$$m = 0.480 + 1.57\omega - 0.176\omega^2 \quad (2.16)$$

$a_0$  and  $b$  can then be defined by Equations (2.4) and (2.5), using  $\psi \cong 0.42748$  and  $\Omega \cong 0.08664$ .

### 2.2.3 The Peng-Robinson (PR) EoS

For the PR equation of state,  $\epsilon = 1 - \sqrt{2}$  and  $\sigma = 1 + \sqrt{2}$ , forming Equation (2.17):

$$P = \frac{RT}{V - b} - \frac{a(T)}{V(V + b) + b(V - b)} \quad (2.17)$$

The parameter  $a$  is calculated by the same Equation (2.15) as SRK, but with a different expression for  $m$ , described in Equation (2.18):

$$m = 0.37464 + 1.54226\omega - 0.26992\omega^2 \quad (2.18)$$

$a_0$  and  $b$  can also be defined by Equations (2.4) and (2.5), but using  $\psi \cong 0.45724$  and  $\Omega \cong 0.07780$ .

### 2.2.4 Modifications for Polar Components

Despite all aforementioned advantages of cubic equations of state, they still have some downsides, especially when modelling polar compounds, such as water.

Therefore, various authors have proposed modifications for them, attempting to improve the results on modelling mixtures with polar compounds, principally in the  $\alpha$  function of their attractive term (VALDERRAMA, 2003). Some notable functions studied are:

#### Mathias-Copeman Modification (MATHIAS and COPEMAN, 1983)

These authors expanded the original  $\alpha$  function, adding two more terms in it, forming Equation (2.19):

$$\alpha(T_R, \underline{c}) = [1 + c_1(1 - T_R^{0.5}) + c_2(1 - T_R^{0.5})^2 + c_3(1 - T_R^{0.5})^3]^2 \quad (2.19)$$

The parameters  $c_1$ ,  $c_2$  and  $c_3$  are specific for each component. One disadvantage of this function is that, although the results indeed improved for polar compounds, the insertion of two more empirical parameters causes a super-parametrization of the model: it needs more experimental data to become reliable.

#### Kabadi-Danner Modification (KABADI and DANNER, 1985)

This modification is exclusively applied to water in the SRK equation of state, and it is defined by Equation (2.20):

$$\alpha(T_R, c_1) = [1 + c_1(1 - T_R^{0.8})]^2 \quad (2.20)$$

The value of  $c_1 = 0.662$  is originally used for water. For all other substances, Equation (2.15) applies.

### Peng Modification (PENG *et al.*, 1985)

This modification is also exclusively applied to water, but used only in the PR equation of state, according to Equation (2.21):

$$\alpha(T_R, c_1) = \begin{cases} [1.0085677 + c_1(1 - T_R^{0.5})]^2, & T_R^{0.5} < 0.85 \\ [1 + m(1 - T_R^{0.5})]^2 & , T_R^{0.5} \geq 0.85 \end{cases} \quad (2.21)$$

The value of  $c_1 = 0.8215$  is used for water, only when  $T_R^{0.5} < 0.85$ . For all other substances, the second expression of Equation (2.21) applies, with  $m$  calculated by Equation (2.18).

### Extension to Parameter Estimation

For parameter estimation purposes, detailed in Chapter 3, it is preferable to flexibilize all EoS specific parameters, when applicable:  $a_0$ ,  $b$ ,  $c_1$ ,  $c_2$  and  $c_3$ .

Therefore, Equations (2.4), (2.5), (2.16) and (2.18), as well as the definitions of  $c_1$  in this Section, will be suppressed in these procedures. However, in order to compare the optimized results with the literature parameters, these equations were also implemented. Hereafter, when the parameters are defined by these equations they will be called the original parameters of each equation of state or  $\alpha$  function.

In the specific case of the Peng Modification to the  $\alpha$  function, there is a discontinuity when  $T_R^{0.5} = 0.85$ . In order to prevent that in the parameter estimation procedure, the parameter  $c_1$  is recalculated through the temperature range according to Equation (2.22):

$$c'_1 = c_1 + \frac{1.0085677 - 1}{1 - 0.85} \quad (2.22)$$

where  $c'_1$  is the parameter  $c_1$  value calculated when  $T_R^{0.5} \geq 0.85$ . No publication in the literature with such implementation was found.

## 2.2.5 Association Theories

Standard cubic equations do not have a term that takes into account explicitly chemical association and, because of that, their efficacy when modelling complex mixtures is limited (AVLUND *et al.*, 2011). In this context, it can be necessary to modify them more deeply, from theoretic expressions rather than empirical. With this background, the association theories became extensively studied.

Association theories can be assigned to three great subjects (SANTOS, 2015):

- Chemical theories, based on the formation of new species. The extension of association is defined by the number of oligomers formed;
- Lattice (quasi-chemical) theories, based on the formation of connections between segments of different molecules that occupy adjacent sites of the lattice. In this case, the extension of association is defined by the number of connections;
- Perturbation theories, based on statistical mechanics. The extension of the association is defined by the number of sites bonded per molecule.

When these theories are described in an equation of state, for instance, new terms appear in the compressibility factor as contributions. Usually, in chemical and lattice theories, these contributions are not completely separable (SANTOS, 2010), but, in perturbation theories, these terms are explicit and additive. Models that follow these theories are called Association Models: with them, it is possible to predict phase equilibrium of mixtures containing polar compounds or any other capable to form hydrogen bonds.

Compounds that form complex mixtures to be studied in this work, such as water and glycols, are called self-associating components because they are capable to form hydrogen bonds. The formation of these bonds between two of the same molecule is called self-association, such as pure water, while between two different molecules this bond is called cross-association, such as water-ethanol mixture (SANTOS, 2015).

Although these theories have different origins, it is worth mentioning that various authors (ECONOMOU and DONOHUE, 1991; HENDRIKS *et al.*, 1997; MICHELSEN and HENDRIKS, 2001) concluded independently that there are mathematical similarities between them for the contribution of hydrogen bonds.

One of the most popular model based on association theories is the SAFT equation of state (Statistical Associating Fluid Theory). This model was first idealized by WERTHEIM (1984a,b, 1986a,b) when he presented a perturbation theory that took explicitly into account hydrogen bonds. Then, CHAPMAN *et al.* (1989, 1990) presented this theory in the form of an equation of state, named SAFT. Its main feature is the consideration of the effects as additive terms of free energy.

Thus, these models based on perturbation theory are usually written as a summation of terms of the Helmholtz function ( $A$ ), as shown in Equation (2.23):

$$F \equiv \frac{A}{RT} = F_{id} + F_{segm} + F_{chain} + F_{assoc} \quad (2.23)$$

The total dimensionless free energy  $F$  is then obtained from the contributions of the reference fluid (ideal gas,  $F_{id}$ ), attraction forces ( $F_{segm}$ ), chain formation ( $F_{chain}$ ) and association ( $F_{assoc}$ ) free energies.

The SAFT equation of state is referred by numerous authors as the Original SAFT, because there have been countless modifications to this model throughout the years. They differed basically in the reference fluid, the radial distribution function and the dispersion term used. The chain formation and association contributions are all similar to the Original SAFT (AVLUND, 2011).

## 2.2.6 The Cubic-Plus-Association (CPA) EoS

The downside of the SAFT family equations is their complexity and difficulty to converge reliably. Thus, it is convenient to develop an equation that could be simple enough to be applied to engineering processes.

Based on these concepts, KONTOGEORGIS *et al.* (1996) proposed the Cubic-Plus-Association (CPA) equation of state. According to the authors, it was developed to model complex mixtures with a mathematically simpler approach. They wrote the Helmholtz function as a summation of two contributions (Equation (2.24)):

$$F \equiv \frac{A}{RT} = F_{phys} + F_{assoc} \quad (2.24)$$

In this expression, the term  $F_{phys}$  is the contribution made by a cubic equation of state, and  $F_{assoc}$  is a SAFT related association term. These authors chose the SRK equation of state to represent the physical contribution. Applying this to Equation (2.24) and deriving it, Equation (2.25) is formed (KONTOGEORGIS *et al.*, 1996):

$$P = \frac{RT}{V-b} - \frac{a(T)}{V(V+b)} - \frac{1}{2} \frac{RT}{V} \left( 1 + \rho \frac{\partial \ln g}{\partial \rho} \right) \sum_i x_i \sum_{A_i} (1 - X_{A_i}) \quad (2.25)$$

with  $\rho = 1/V$  being the molar density of the mixture,  $X_{A_i}$  the molar fraction of type  $i$  molecules unbounded to type  $A$  sites and  $x_i$  the molar fraction of the component  $i$ .  $X_{A_i}$  can be calculated using Equation (2.26):

$$X_{A_i} = \frac{1}{1 + \rho \sum_j x_j \sum_{B_j} \Delta^{A_i B_j}} \quad (2.26)$$

where  $B$  represents a type of bonding site different to  $A$ , and  $j$  represents the index of a molecule that may or may not be different to the molecule  $i$ .  $\Delta^{A_i B_j}$  is the association strength between the type  $A$  site in molecule  $i$  and the type  $B$  site in molecule  $j$ , described by Equation (2.27):

$$\Delta^{A_i B_j} = g(V)^{ref} \left[ \exp \frac{\varepsilon^{A_i B_j}}{RT} - 1 \right] b_{ij} \beta^{A_i B_j} \quad (2.27)$$

$\varepsilon^{A_i B_j}$  and  $\beta^{A_i B_j}$  are called, respectively, the association energy and the association volume parameter;  $b_{ij} = (b_i + b_j)/2$  is the mean value of co-volumes of molecules  $i$  and  $j$ ; and  $g(V)^{ref} \equiv g$  is the radial distribution function, defined by the Equation (2.28) (KONTOGEORGIS *et al.*, 1999):

$$g = \frac{1}{1 - 1.9\eta}, \quad \eta = \frac{b\rho}{4} \quad (2.28)$$

It is important to mention that if  $\varepsilon^{A_i B_j} = \beta^{A_i B_j} = 0$  (i.e. there is no association effect in the compound) then the CPA EoS automatically reduces to the SRK EoS (KONTOGEORGIS and FOLAS, 2010).

The physical energy parameter  $a(T)$  is calculated similarly to Equation(2.15), adapted to Equation (2.29):

$$a(T) = a_0[1 + c_1(1 - T_R^{0.5})]^2 \quad (2.29)$$

On the other hand, other authors such as LI and FIROOZABADI (2009) have preferred to use the Peng-Robinson equation of state for the cubic term of the CPA, forming the Equation (2.30) instead of Equation (2.25):

$$P = \frac{RT}{V - b} - \frac{a(T)}{V(V + b) + b(V - b)} - \frac{1}{2} \frac{RT}{V} \left( 1 + \rho \frac{\partial \ln g}{\partial \rho} \right) \sum_i x_i \sum_{A_i} (1 - X_{A_i}) \quad (2.30)$$

In this work KONTOGEORGIS *et al.* (1996) model will be used for calculations because of the extensive literature available to validate the program (DERAWI *et al.*, 2003; FOLAS *et al.*, 2006a; SANTOS *et al.*, 2015a; YAKOUMIS *et al.*, 1998). Besides, KONTOGEORGIS *et al.* (2006a,b) made a throughout revision of the advances of the CPA (SRK based) equation of state in its ten first years of the original publication, contributing with even more data to this work. Therefore, the implementation of the Equation (2.30) is not in the scope of this dissertation. A suggestion for future works would be the implementation of this equation of state.

Therefore, when applied to parameter estimation procedures, there are five parameters to be manipulated in the CPA equation of state: three of them in the physical term ( $a_0$ ,  $b$  and  $c_1$ ) and two in the association term ( $\varepsilon^{A_i B_j}$  and  $\beta^{A_i B_j}$ ).

For binary mixtures, the classical mixing rules in Equations (2.11), (2.12) and (2.13) apply for the physical part of this EoS.

Besides, there can be a combination between two potential associating compounds (e.g. water and TEG), resulting on a cross-association mixture. Thus, the parameters  $\varepsilon^{A_i B_j}$  and  $\beta^{A_i B_j}$  from the association term need combining rules (CR) rather than mixing rules.

According to KONTOGEORGIS and FOLAS (2010), various CRs were

suggested over the years, but only two of them kept generating promising and satisfactory results: CR-1 rule (Equations (2.31) and (2.32)) and the Elliott's Combining Rule (ECR, Equation (2.33)):

$$\varepsilon^{A_i B_j} = \frac{\varepsilon^{A_i B_i} + \varepsilon^{A_j B_j}}{2} \quad (2.31)$$

$$\beta^{A_i B_j} = \sqrt{\beta^{A_i B_i} \beta^{A_j B_j}} \quad (2.32)$$

$$\Delta^{A_i B_j} = \sqrt{\Delta^{A_i B_i} \Delta^{A_j B_j}} \quad (2.33)$$

Besides, the CPA equation of state can also be used in mixtures with a self-associative component and an 'inert' component, but with the possibility of an induced cross-association between them. This is called solvating effect (SANTOS, 2015). In this case, a modified CR-1 rule is used, successfully applied to mixtures with water or glycols and aromatic or olefinic hydrocarbons (FOLAS *et al.*, 2006a). In this case,  $\beta^{A_i B_j}$  must be estimated from experimental data and  $\varepsilon^{A_i B_j}$  can still be calculated from Equation (2.31), considering  $\varepsilon^{A_j B_j} = 0$  (i.e. non self-associating component).

For parameter estimation purposes, another possibility is to further modify the CR-1 rule, estimating both the parameters  $\varepsilon^{A_i B_j}$  and  $\beta^{A_i B_j}$  from experimental data, as well as  $k_{ij,0}$  and  $k_{ij,1}$  from Equation (2.13), if convenient. Some results of this approach will be discussed in Chapter 5.

In this work, the cubic equations of state were fully programmed by this author. However, for the CPA it was decided to link the core of the program to a pre-programmed Dynamic Link Library (or 'dll', for short), developed by the Center for Energy Resources Engineering (CERE), from Denmark Technical University (DTU). The reason for this choice is that it is a well matured code, where all the main thermodynamic properties are available as output, including stability analysis for liquid-liquid equilibria, allowing this work to focus directly on its applications.

Moreover, this equation is more complex than pure cubic equations of state, demanding more computational effort, and MICHELSEN (MICHELSEN, 2006; MICHELSEN and HENDRIKS, 2001) proposed numerous modifications to its solution methods and to the radial distribution function  $g$  in order to make it faster to converge and thus applicable to engineering processes.

On the other side, outer thermodynamic calculations such as saturation pressure, liquid-liquid flash and water content in dew point conditions, as well as optimization methods, metric assembly and the interface objects, were also fully programmed by this author.



## 2.3 Parameter Estimation

In general, models are useful tools to describe physical processes. For practical purposes, a process designer will choose the model that can better predict the system over one that contemplates the most phenomena involved. Therefore, a simple model with well-estimated parameters can be superior to a sophisticated model with poorly estimated parameters (ALBERTON, 2010).

Thus, parameter estimation can be defined as an optimization procedure where a model is used as a reference and the parameters are modified until the values obtained by this model become as near as possible to the experimental data (SCHWAAB and PINTO, 2007). In order to assure the attainment of the best parameters, the objective function and optimization methods must be chosen carefully. As a minimization method, all estimation procedures must follow Equation (2.34):

$$\min S(\underline{X}), \text{ subject to } \underline{h}(\underline{X}) = 0 \quad (2.34)$$

The vector  $\underline{X}$  is composed of the parameters to be manipulated, the restrictions  $\underline{h}(\underline{X})$  in this work are defined by the thermodynamic model and the objective function  $S(\underline{X})$  is described in Equation (2.35):

$$S(\underline{X}) = (\underline{Y}^e - \underline{Y}^*)^T \underline{\underline{V}}^{-1} (\underline{Y}^e - \underline{Y}^*) \quad (2.35)$$

Considering that experimental measures of variable  $\underline{Y}$  are not correlated, the matrix  $\underline{\underline{V}}$  becomes diagonal (ALBERTON, 2010), and Equation (2.35) takes the form of Equation (2.36):

$$S(\underline{X}) = \sum_k^{n_v} \left[ \frac{1}{n_e} \sum_i^{n_e} \frac{(y_{k,i}^e - y_{k,i}^*)^2}{\sigma_{k,i}^2} \right] \quad (2.36)$$

$n_e$  is the number of experiments and  $n_v$  is the number of calculated variables; the superscript  $e$  means 'experimental' and  $*$  means 'calculated'; and  $\sigma_{i,k}$  is the variance of the experimental variable.

Experimental data can be scarce and often there is no replica to them, so variance values can be unavailable or unreliable; in these cases,  $\sigma_{i,k}$  is commonly equalled to the experimental point  $y_{i,k}^e$  itself for thermodynamic purposes (KONTOGEOORGIS *et al.*, 2006a; SANTOS, 2015). The main advantage of this practice is that the term becomes dimensionless. Also, when estimating pure components' parameters, it takes into account that measure errors are higher in regions of high pressure. This assumption agrees with reality, even if not with the same proportions. For instance, there are only a few equipments available to take precise measures at higher

pressures. On the other hand, it is possible to apply statistical analysis techniques to construct a critical evaluation to this approach and verify which simplifications derive from it, since the development of a fast computational tool can allow advances in this study that is non-usual in literature.

When applied to the CPA EoS pure parameter estimation, there are a wide variety of possible solutions. That is, different parameters sets resulted in similar deviations from experimental data (usually, saturation pressures and liquid densities). Nevertheless, KONTOGEORGIS *et al.* (2006a) stated that the usual variables alone are not enough to properly predict the thermodynamic properties. For instance, when applied to mixtures with liquid-liquid equilibrium (LLE), frequently the solution set of this optimization failed to predict the experimental data (DERAWI *et al.*, 2003). Therefore, in order to select the best parameters, they used LLE experimental data to 'guide' the optimal solution.

Originally, they did not recommend inserting LLE terms directly to the Equation (2.36), using the compositions of each phase as variables, but instead testing 'good' sets of parameters (i.e. with low deviations of pure saturation pressure and liquid density/volume) in some mixtures with LLE (for example, water + n-hexane, or MEG + n-heptane) until a general solution is found.

Besides, SANTOS *et al.* (2015c) suggested that a combination of objective functions of the VLE variables and LLE variables could be useful to facilitate this selection, weighted by a user defined variable. Chapter 3 explains in details a slight variation of this analysis applied to this work.

For binary parameters, they are usually estimated by bubble pressure or composition in LLE, as in FOLAS *et al.* (2006a). Also, in Chapter 3 all these procedures will be detailed.

# Chapter 3

## Mathematical Modelling

### 3.1 Thermodynamic Equilibrium Calculations

Equilibrium properties are essential in chemical process studies and designs, thus most commercial process simulators provide various thermodynamic models to be selected by the user.

In order to foresee thermodynamic properties, the phase equilibrium fundamental equation must be solved, which is the fugacity equality, described by Equation (3.1):

$$\widehat{f}_i^\alpha = \widehat{f}_i^\beta = \widehat{f}_i^\gamma = \dots, \quad i = 1, 2, \dots, n \quad (3.1)$$

where  $n$  is the number of components and  $\alpha, \beta, \gamma, \dots$ , are the phases in equilibrium.

Alternatively, fugacity can be written in the form of its coefficient, according to Equation (3.2):

$$\widehat{\phi}_i = \frac{\widehat{f}_i}{f_i^0} = \frac{\widehat{f}_i}{y_i P} \quad (3.2)$$

where  $f_i^0$  is a fugacity of a component  $i$  in the ideal gas mixture, equal to the partial pressure, where  $y_i$  is its molar fraction and  $P$  the system pressure.

Fugacity coefficients can be calculated from volumetric data or from an equation of state, which are often expressed as functions of  $P(T, V)$  (Equation (3.3)) or  $V(T, P)$  (Equation (3.4)) (PRAUSNITZ *et al.*, 1999).

$$RT \ln \widehat{\phi}_i = RT \ln \frac{\widehat{f}_i}{y_i P} = \int_V^\infty \left[ \left( \frac{\partial P}{\partial n_i} \right)_{T, V, n_j} - \frac{RT}{V} \right] dV - RT \ln Z \quad (3.3)$$

$$RT \ln \widehat{\phi}_i = RT \ln \frac{\widehat{f}_i}{y_i P} = \int_0^P \left( \overline{V}_i - \frac{RT}{P} \right) dP \quad (3.4)$$

$R$  is the universal gas constant,  $V$  the molar volume,  $\bar{V}_i$  the partial volume of the component  $i$  and  $Z$  is the compressibility factor, given by Equation (2.10).

Using the equations of state described in Chapter 2, it is possible to evaluate Equations (3.3) and (3.4), and consequently all other properties can be calculated.

In this work, the main thermodynamic properties evaluated were saturation pressure, compositions in liquid-liquid equilibrium (LLE) and water content in dew point conditions.

### 3.1.1 Saturation, Bubble and Dew Pressures

Saturation pressure is defined here as the pressure of the system in vapour-liquid equilibrium (VLE). When modelling mixtures, it may be called bubble pressure, when the main phase is liquid (vapour is incipient), or dew pressure, when the vapour phase prevails (liquid is incipient).

These calculations were implemented in a similar fashion as in Petrobras's Petrox<sup>®</sup> Process Simulator (NIEDERBERGER *et al.*, 2009), based on a secant method for converging composition and pressure simultaneously. The initial estimative  $P_0$  derives from Wilson's expression (Equation (3.5)):

$$P_0 = P_c \exp \left[ 5.373(\omega + 1) \left( 1 - \frac{T_c}{T} \right) \right] \quad (3.5)$$

where  $P_c$  is the critical pressure,  $T_c$  the critical temperature and  $\omega$  the acentric factor.

For pure components, this algorithm becomes slightly different, as there is no necessity of an inner loop for composition. Therefore, it can be solved by a successive substitution method, briefly described as follows:

#### 1. Initialization:

- (a) Read the component's properties and parameters, the EoS model, temperature  $T$ , maximum number of iterations  $i_{max}$  and the tolerance  $\epsilon$ .
- (b) IF  $P_0$  is not known THEN calculate it from Equation (3.5).
- (c) Make  $P = P_0$ ,  $iter = 0$ ,  $flag = 0$ .

#### 2. Loop:

- (a)  $iter = iter + 1$ .
- (b) Calculate  $\phi_L(T, P)$  and  $\phi_V(T, P)$  from Equation (3.4) applied to pure components.
- (c)  $K_{eq} = \phi_L/\phi_V$ ;  $err_P = |1 - K_{eq}|$ .

- (d)  $P_1 = P; P = K_{eq} \times P_1$ .
- (e) IF  $|err_P| > \epsilon$  and  $iter < i_{max}$  THEN return to **Step 2a**.
- (f) IF  $|err_P| \leq \epsilon$  THEN  $flag = 1$ . **Exit Loop**.
- (g) IF  $iter \geq i_{max}$  THEN  $flag = -1$ . **Exit Loop**.

### 3. Solution:

- (a) IF  $flag = 1$  (i.e. convergence achieved) THEN **RETURN**  $P$ .  
ELSE it did not converge. **RETURN**  $-1$ .

In order to illustrate this calculation, Table 3.1 presents a numerical example of a pure component saturation pressure calculation. It is important to note that the value of  $P_1$  in its first row was previously calculated from Equation (3.5).

Table 3.1: Numerical example for a pure water saturation pressure calculation ( $T_c = 647.13$  K,  $P_c = 220.55$  bar,  $w = 0.3449$ ), at  $T = 350$  K and using the CPA equation of state parameters published by KONTORGEOGIS *et al.* (1999). Convergence tolerance =  $10^{-4}$ .

$iter$	$K_{eq} \equiv \phi_L/\phi_V$	$err_P$	$P_1$ [bar]	$P$ [bar]
1	0.8658	1.342e-1	0.4929	0.4268
2	0.9971	2.884e-3	0.4268	0.4256
<b>3</b>	<b>0.9999</b>	<b>5.375e-5</b>	<b>0.4256</b>	<b>0.4255</b>

### 3.1.2 Liquid-liquid Equilibrium (LLE)

For this calculation, a liquid-liquid flash was solved using the Rachford-Rice Equation (PRAUSNITZ *et al.*, 1999). Firstly, it is important to check the necessary variables to calculate the compositions at each phase and the respective degree of freedom (Equation (3.6)).

$$F = C - P + 2 \tag{3.6}$$

In the LLE calculations performed in this work, there are two components ( $C = 2$ ) and two phases in equilibrium ( $P = 2$ ). Therefore, Equation (3.6) shows that only two specified variables are needed to solve the LLE calculations ( $F = 2$ ), for instance the temperature and pressure. That is, the compositions of each liquid phase are independent of the feed global composition, as shown in Equations (3.7) and (3.8):

$$x_{1(2)} = \frac{K_2 - 1}{K_2 - K_1} \tag{3.7}$$

$$x_{2(1)} = \frac{K_2(1 - K_1)}{K_2 - K_1} \quad (3.8)$$

where  $x_{i(j)}$  stands for the composition of  $i$  in phase rich in component  $j$ . In a mixture water (1) with n-hexane (2), for example,  $x_{1(2)}$  is the composition of water in organic phase. Besides,  $K_i \equiv \widehat{\phi}_{i(2)}/\widehat{\phi}_{i(1)}$  is the liquid-liquid equilibrium constant, function of  $T$ ,  $P$  and  $x_{i(j)}$ .

When calculating equilibrium in mixtures, it is important to avoid 'false solutions', in which  $K_i \approx 1.0 \forall$  components. They are called trivial solutions and they are a sign that the calculations did not converge. In all calculations containing mixtures implemented in this work, an absolute tolerance of 0.01 was defined to check if the system is in a trivial solution, summarized by Equation (3.9).

$$\text{IF } |K_i - 1.0| < 0.01 \forall i = 1, \dots, n_c \text{ THEN solution is trivial.} \quad (3.9)$$

Therefore, the algorithm implemented in this work can be summed up as follows:

### 1. Initialization:

- (a) Read the components' properties and parameters, the EoS model, the temperature  $T$ , pressure  $P$ , initial guesses for the compositions  $x_{i(j),0}$ , maximum number of iterations  $i_{max}$  and the tolerance  $\epsilon$ .
- (b) Initialize  $K_i = 1$ ,  $err_K = 1$ ,  $iter = 0$  and  $flag = 0$ .

### 2. Loop:

- (a)  $iter = iter + 1$ ,  $K_{i,old} = K_i$  for  $i = 1, 2$ .
- (b) Calculate  $x_{i(j)}$  from Equations (3.7) and (3.8).
- (c) Calculate  $\widehat{\phi}_{i(j)}(T, P, x_{i(j)})$  for  $i = 1, 2$  from Equation (3.4).
- (d)  $K_i = \widehat{\phi}_{i(2)}/\widehat{\phi}_{i(1)}$  for  $i = 1, 2$
- (e) IF  $iter > 1$  THEN make  $err_K = \sum_i^2 \frac{|K_{i,old} - K_i|}{K_i}$ .
- (f) IF  $err_K > \epsilon$  and  $iter < i_{max}$  THEN return to **Step 2a**.
- (g) IF  $|err_K| \leq \epsilon$  THEN  $flag = 1$ . **Exit Loop**.
- (h) IF  $iter \geq i_{max}$  THEN  $flag = -1$ . **Exit Loop**.

### 3. Solution:

- (a) Check for trivial solution (Equation (3.9)). IF trivial THEN make  $flag = -2$ . **RETURN empty array**.  
ELSE IF  $flag = 1$  (i.e. convergence achieved) THEN **RETURN the compositions**  $x_{i(j)}$ .  
ELSE it did not converge. **RETURN empty array**.

Table 3.2 presents a numerical example of a LLE calculation for the binary mixture water + n-hexane.

Table 3.2: Numerical example for a LLE calculation for the mixture water + n-hexane, at  $T = 333.15K$  and CPA equation of state parameters modelled in the literature for water (KONTOGEOORGIS *et al.*, 1999) and n-hexane (TSIVINTZELIS *et al.*, 2011), with  $k_{ij} = 0$ . Convergence tolerance =  $10^{-4}$ . The initial guesses to the compositions are related to the respective experimental data informed in the program interface.

<i>iter</i>	$K_1$	$K_2$	$K_{1,old}$	$K_{2,old}$	$x_{1(2)}$	$x_{2(1)}$	<i>err<sub>K</sub></i>
0	1.0000	1.0000	-	-	1.800e-3	4.500e-6	1.000e0
1	507.103	5.218e-6	1.0000	1.0000	1.972e-3	5.207e-6	1.916e5
2	503.951	5.218e-6	507.103	5.218e-6	1.984e-3	5.208e-6	6.255e-3
3	503.726	5.218e-6	503.951	5.218e-6	1.985e-3	5.208e-6	4.467e-4
4	<b>503.710</b>	<b>5.218e-6</b>	<b>503.726</b>	<b>5.218e-6</b>	<b>1.985e-3</b>	<b>5.208e-6</b>	<b>3.176e-5</b>

### 3.1.3 Water Content of a Specified Gas

This calculation returns the water content of a known gas in order to allow the system to be in the dew point at a specified temperature and pressure, based on SHIGUEMATSU (2014), calculated according to Equation (3.10):

$$y_{H_2O} = y_{H_2O} \left( T, P, \underline{y}_{DG}, param \right) \quad (3.10)$$

where  $T$  is the system temperature,  $P$  the system pressure and  $\underline{y}_{DG}$  stands for the dry gas composition. Also, *param* stands for all EoS parameters related to the system (from either pure components and each pair), including the manipulated variables in the optimization. These variables are fixed throughout the algorithm.

This is an implicit calculation, solved by a numerical method, originally being the bisection due to its sturdiness (SHIGUEMATSU, 2014). However, in this work, this method was improved to a combination of bisection and secant mathematical methods in order to accelerate it.

The function  $f_{dew}$ , the objective function of this method, is calculated from the vapour-liquid equilibrium of the system (Equation (3.11)).

$$f_{dew}(n_{H_2O}) = \sum_{i=1}^{n_c} x_i - 1 \quad (3.11)$$

where  $n_{H_2O}$  is the mole quantity of water in the gas in the current iteration (manipulated variable in the numerical method) and  $x_i$  the mole fraction of each of the  $n_c$  components in the liquid phase in equilibrium. Every time this function

is evaluated, two other variables are calculated in its output:  $err$ , defined by Equation (3.12), and a boolean  $trv$ , which informs whether the current system is or not in trivial solution (Equation (3.9)).

$$err = \sqrt{\sum_{i=1}^{n_c} (y_i - x_i)^2} \quad (3.12)$$

where  $y_i$  is the molar fraction of the vapour in equilibrium with the liquid with molar composition  $x_i$ .

The algorithm implemented for calculating  $f_{dew}$  is described as follows:

### 1. Initialization:

- (a) Read the components' properties and parameters, the EoS model,  $n_{H_2O}$ ,  $T$ ,  $P$ ,  $y_{DG}$ , as well as the maximum number of iterations  $i_{max}$  and the tolerance  $\epsilon$ .
- (b) For  $i = 1 \cdots n_c$ : IF  $i \neq i_{H_2O}$  THEN  $y_i = y_{DG,i}/(1 + n_{H_2O})$ .
- (c)  $y_{i_{H_2O}} = n_{H_2O}/(1 + n_{H_2O})$ .
- (d) Calculate  $K_i = P_i^{sat}/P$ , with  $P_i^{sat}$  by Equation (3.5).
- (e) Calculate  $x_i = y_i/K_i$  for  $i = 1 \cdots n_c$  and normalize  $x$ .
- (f) Make  $iter = 0$ ,  $S_{x1} = 1$ ,  $err_x = 1$ .

### 2. Loop:

- (a)  $iter = iter + 1$ ;  $S_x = 0$ .
- (b) Calculate  $\widehat{\phi}_{L,i}(T, P, x)$  and  $\widehat{\phi}_{V,i}(T, P, y)$  for  $i = 1 \cdots n_c$  from Equation (3.4).
- (c) Calculate  $K_i = \widehat{\phi}_{L,i}/\widehat{\phi}_{V,i}$  for  $i = 1 \cdots n_c$ .
- (d) Calculate  $x_i = y_i/K_i$ ,  $S_x = S_x + x_i$  for  $i = 1 \cdots n_c$ .
- (e)  $S_{x2} = S_{x1}$ ,  $S_{x1} = S_x$ ,  $err_x = |S_{x1} - S_{x2}|$ . Normalize  $x$ .
- (f) IF  $err_x > \epsilon$  and  $iter < i_{max}$  THEN return to **Step 2a**.
- (g) IF  $|err_x| \leq \epsilon$  THEN  $flag = 1$ . **Exit Loop**.
- (h) IF  $iter \geq i_{max}$  THEN  $flag = -1$ . **Exit Loop**.

### 3. Solution:

- (a) IF  $flag = -1$  THEN make  $err = 0$ ;  $F = 1$ ;  $trv = true$ .  
ELSE Check for trivial solution (Equation (3.9)). IF trivial then  $trv = true$  and make  $err = F = 0$ ;  
ELSE  $trv = false$ ,  $err = \sqrt{\sum_{i=1}^{n_c} (y_i - x_i)^2}$ ,  $F = S_{x1} - 1$ .



(b) **RETURN** [ $F$   $err$   $trv$ ].

Also, as in the work of SHIGUEMATSU (2014), it was decided to convert the variable  $n_{H_2O}$  to another basis, in order to keep its limits between 0 and 1, as presented in Equation (3.13).

$$\xi \equiv \exp(-n_{H_2O}) \quad (3.13)$$

This variable is originally limited in the interval  $[0, 1]$ . Nevertheless, trivial solutions in this calculation mean that the current water content is too low (that is, the respective value of  $\xi$  is too high). Therefore, whenever a trivial solution is achieved in a  $f_{dew}$  evaluation, the current value of  $\xi$  substitutes the upper limit of this variable,  $\xi_{max}$ , as in Equation (3.14):

$$\xi_{max} = \text{Min}(\xi_{trivial}, \xi_{max,old}) \quad (3.14)$$

As previously mentioned, in this work the numerical method related to this calculation was implemented as a hybridization of bisection and secant methods. These methods are described in the following algorithms:

- Bisection Step (B.S.), from known values of  $\xi_1$  and  $\xi_2$ :
  1. Make  $n_1 = -\ln(\xi_1)$  and evaluate  $[F_1, err_1, trv_1] = f_{dew}(n_1)$  if these variables were not already obtained in previous iterations.
  2. IF  $trv_1 = false$  THEN
    - (a) IF  $F_1 > 0$  and  $F_2 < 0$  or  $F_1 < 0$  and  $F_2 > 0$  THEN  $d\xi = \xi_2 - \xi_1$ .  
ELSE  $d\xi = \xi_1 - \xi_2$ .
    - (b)  $\xi_N = \xi_1 + 0.5d\xi$ .
    - ELSE  $\xi_1$  is already too high. Make  $\xi_N = 0.5\xi_1$ .
  3.  $n_N = -\ln(\xi_N)$ .
  4. Evaluate  $[F_N, err_N, trv_N] = f_{dew}(n_N)$ .
- Secant Step (S.S.), from known values of water mole quantity  $n_1$  and  $n_2$  and the respective values of  $F$ ,  $err$  and  $trv$  calculated by  $f_{dew}$  in prior iterations:
  1. IF  $trv_1 = true$  or  $trv_2 = true$  THEN  $\xi_N = \xi_1 - 0.1 F_1(\xi_2 - \xi_1)/(F_2 - F_1)$ .  
ELSE  $\xi_N = \xi_1 - F_1(\xi_2 - \xi_1)/(F_2 - F_1)$ .
  2. Protection to avoid reaching values out of bounds:
    - IF  $\xi_N \geq \xi_{max}$  THEN  $\xi_N = \xi_{max} - 0.5(\xi_{max} - \text{Max}(\xi_1, \xi_2))$
    - ELSE IF  $\xi_N \leq 0$  THEN  $\xi_N = 0.5\text{Min}(\xi_1, \xi_2)$

3.  $n_N = -\ln(\xi_N)$ .
4. Evaluate  $[F_N, err_N, trv_N] = f_{dew}(n_N)$ .

The main method is solved then as follows:

### 1. Initialization:

- (a) Read the components' parameters, EoS model, temperature  $T$ , pressure  $P$ , dry gas composition  $\underline{y}_{DG}$  and the maximum percent to the water content  $y_{max}^{H2O}$ , as well as the maximum number of iterations  $i_{max}$  and the tolerance  $\epsilon$ .
- (b) Calculate  $n_1 = y_{max}^{H2O} / (100\% - y_{max}^{H2O})$ .
- (c) Define the auxiliary variable:  $\xi_1 = \exp(-n_1)$ .
- (d) Make  $\xi_{max} = 1$ ,  $\xi_2 = 1$  and  $\xi_{10} = \xi_1$ .
- (e) Execute B.S., obtaining  $n_N$ ,  $\xi_N$ ,  $F_N$ ,  $err_N$  and  $trv_N$ .
- (f) Make  $\xi_2 = \xi_N$ ,  $F_2 = F_N$ ,  $err_2 = err_N$ ,  $trv_2 = trv_N$ .
- (g) Execute S.S., obtaining new values for  $n_N$ ,  $\xi_N$ ,  $F_N$ ,  $err_N$  and  $trv_N$ .
- (h) Initialize  $iter = 0$ ,  $flag = 0$ ,  $bis = false$  (checker for case 02)

### 2. Loop:

- (a) Make  $iter = iter + 1$ ,  $err_{old} = err_N$ .
- (b) Current solution lies on three possible cases:
  - Case 01: IF  $trv_N = true$  THEN reinitialize the method modifying the value of  $\xi_{10}$ :
    - i.  $\xi_{10} = 0.8 \xi_{10} + 0.2 \xi_{max}$ ,  $\xi_1 = \xi_{10}$ ,  $\xi_2 = 1$ .
    - ii. Execute B.S., obtaining  $n_N$ ,  $\xi_N$ ,  $F_N$ ,  $err_N$  and  $trv_N$ .
    - iii. Make  $\xi_2 = \xi_N$ ,  $F_2 = F_N$ ,  $err_2 = err_N$ ,  $trv_2 = trv_N$ .
    - iv. Execute S.S., obtaining new values for  $n_N$ ,  $\xi_N$ ,  $F_N$ ,  $err_N$  and  $trv_N$ .
  - Case 02: IF  $trv_N = false$  and  $bis = true$  THEN execute B.S. with current values of  $\xi_1$  and  $\xi_2$ , obtaining  $n_N$ ,  $\xi_N$ ,  $F_N$ ,  $err_N$  and  $trv_N$ .
  - Case 03: IF  $trv_N = false$  and  $bis = false$  THEN proceed with the secant method as usual:
    - i. Make  $\xi_1 = \xi_2$ ,  $F_1 = F_2$ ,  $err_1 = err_2$ ,  $\xi_2 = \xi_N$ ,  $F_2 = F_N$ ,  $err_2 = err_N$ .

- ii. Execute S.S., obtaining new values for  $n_N$ ,  $\xi_N$ ,  $F_N$ ,  $err_N$  and  $trv_N$ .
- (c) IF  $|err_{old} - err_N| < |err_{old}|$ , then  $bis = false$ .  
ELSE  $bis = true$ , enabling the B.S. in the next iteration (Case 02).
- (d) IF  $|F_N| < \epsilon$  and  $trv_N = false$  THEN  $flag = 1$ . **Exit Loop**.  
ELSE IF  $iter > i_{max}$  THEN  $flag = -1$ . **Exit loop**.  
ELSE return to **Step 2a**.

### 3. Solution:

- (a) Make  $y_{H_2O} = 100\% \times n_N / (1 + n_N)$ .
- (b) IF  $flag = 1$  THEN **RETURN**  $y_{H_2O}$ .  
ELSE the method did not converge. **RETURN 0**.

In the Case 02, the equilibrium variables in previous iteration are too different than in current iteration, even if it is not a trivial solution. It is a sign that a trivial solution may be nearby and another secant step could attain this undesirable result. This is the least common case, but it was still implemented in order to avoid resetting the calculations unnecessarily (Case 01).

Table 3.3 presents a numerical example of this method in a binary mixture water + CO<sub>2</sub> using the CPA equation of state. It is important to mention that  $iter = 0$  means that the variables in this column were obtained before the loop. Also, although the  $\xi_2$  value is always initialized with 1, this Table shows in this column its value calculated from the first bisection step, cited in the item **1f** of the algorithm.

In this example, the first two iterations resulted in trivial solutions. In both of them, the variable  $\xi_0$  was recalculated accordingly and the bisection and secant steps were performed. Consequently, the value of  $\xi_N$  reduced in each iteration and it eventually reached a value whose  $f_{dew}$  calculation did not end in a trivial solution. After that it was possible to perform successive secant steps until the convergence was attained. There were 12  $f_{dew}$  evaluations in this procedure.

Table 3.3: Numerical example for a water content calculation for the mixture water + CO<sub>2</sub>, at  $T = 298.15 \text{ K}$ ,  $P = 50.66 \text{ bar}$  and CPA equation of state parameters modelled in the literature for water (KONTOGEOGRIS *et al.*, 1999) and CO<sub>2</sub> (TSIVINTZELIS *et al.*, 2010), with the binary parameters  $k_{ij} = 0$  and  $\beta_{ij}^{cross} = \beta_{water} = 0.0692$ , considering the solvation effect between these components (LI and FIROOZABADI, 2009). Convergence tolerance =  $10^{-6}$ . The  $y_{max}^{H_2O}$  value was set at 0.5% ( $n_1 \approx 0.00502$ ). 'BS' and 'SS' mean Bisection Step and Secant Step, respectively, as previously described.

<i>iter</i>	0	1	2	3	4	5
Case	Initial: BS + SS	Case 01: BS + SS	Case 01: BS + SS	Case 03: SS only	Case 03: SS only	<b>Case 03: SS only</b>
$\xi_0$	0.99499	0.99599	0.99679	0.99679	0.99679	<b>0.99679</b>
$\xi_1$	0.99499	0.99599	0.99679	0.99840	0.99956	<b>0.99943</b>
$F_1$	4.15188	3.30829	2.60364	1.09350	-0.13408	<b>0.00796</b>
$\xi_2$	0.99749	0.99799	0.99840	0.99956	0.99943	<b>0.99944</b>
$F_2$	1.96181	1.48627	1.09350	-0.13408	0.00796	<b>3.08e-5</b>
$\xi_N$	0.99974	0.99963	0.99956	0.99943	0.99944	<b>0.99944</b>
$trv_N$	true	true	false	false	false	<b>false</b>
$err_N$	-	-	0.81592	0.89984	0.89619	<b>0.89618</b>
$F_N$	-	-	-0.13408	0.00796	3.08e-5	<b>-2.12e-8</b>
$N_N$	0.00026	0.00037	0.00044	0.00057	0.00056	<b>0.00056</b>
$y_{H_2O}$	0.0261%	0.0369%	0.0442%	0.0569%	0.0562%	<b>0.0562%</b>

## 3.2 Methods and Strategies of Optimization

Parameter estimation problem in Thermodynamics is a complex system, may be highly sensitive to initial guesses and consequently may contain several possible local minima. Hence, the optimization procedures executed in this work demanded multi-variable search methods: a stochastic method to evaluate different local minima and a deterministic method to refine the results.

The main advantage of using a stochastic method is that it does not need the computation of derivative properties. Also, it performs a global optimization by being possible to evaluate the objective function in any region of the search space within a probability (SCHWAAB *et al.*, 2008).

In this work, these methods were combined in two possible schemes, based on DAS *et al.* (2006): direct and parallel. As a consequence, there is the possibility of the optimization methods' hybridization.

### 3.2.1 Stochastic Method

The stochastic method implemented is the Particle Swarm Optimization - PSO (KENNEDY and EBERHART, 1995), conveniently adapted to the calculations performed in this work. It is based on the behaviour of a group of animals, such as a swarm of bees. It takes into account each individual solution (particle) and the global solution in each iteration. The particles move around the search region in an iteration  $k$  according to Equations (3.15) and (3.16):

$$v_{i,j}^{(k)} = wv_{i,j}^{(k-1)} + c_1rnd_1(p_{i,j} - u_{i,j}^{(k-1)}) + c_2rnd_2(p_{i,ipg} - u_{i,j}^{(k-1)}) \quad (3.15)$$

$$u_{i,j}^{(k)} = u_{i,j}^{(k-1)} + v_{i,j}^{(k)} \quad (3.16)$$

$rnd_1$  and  $rnd_2$  are random numbers with uniform distribution between 0 and 1, and  $v_{i,j}$  is the velocity of the particle  $u_{i,j}$ .  $i$  varies from 1 to the number of manipulated variables, and  $j$  goes from 1 to the number of particles in the system.  $p_{i,j}$  is the set of best particles updated each iteration and the subscript  $ipg$  is the position of its best point.  $w$ ,  $c_1$  and  $c_2$  are internal parameters of PSO:

- $w$  is called inertial weight, implemented by SHI and EBERHART (1998) in order to increase the odds of attaining the optimal solution during the search. It decreases linearly, from a given  $w_0$  to a given  $w_f$ , so that in the beginning there is an exploration phase and, in the end, an *exploitation* phase;
- $c_1$  is called cognition parameter, related to the individual movement, and  $c_2$  is called social parameter, related to the whole group movement.

In order to implement this method in this work, the following procedure was conducted:

#### 1. Initialization:

- (a) Read  $w_0$ ,  $w_f$ ,  $c_1$ ,  $c_2$ ,  $i_{max}$ ,  $\epsilon_A$ ,  $\epsilon_R$ ,  $N_{pt}$ ,  $N_{max}$ ,  $x_0$ ,  $L_0$ ,  $U_0$ .
- (b) Initialize  $k = 0$ ,  $S_{otim} = 10^{15}$ ,  $w = w_0$ ,  $N_V = 0$ .
- (c) For  $i = 1, \dots, N_x$  and  $j = 1, \dots, N_{pt}$  do:
  - i. Initialize the normalized position  $u_{i,j}^{(k)}$  to random values between 0 and 1.
  - ii. Initialize the velocities to 0.
  - iii. Initialize the vectors  $y_{i,j}^{(k)} = p_{i,j} = u_{i,j}^{(k)}$ .
  - iv. Evaluate the objective function  $f_j^{(k)} = F_{obj}(x^{(k)})$ , with  $x_i^{(k)} = L_{0i} + (U_{0i} - L_{0i})u_{i,j}^{(k)}$ .

- v. After an objective function evaluation, save internally the intermediary values:  $x^{(k)}, f_j^{(k)} \rightarrow x_{int}, S_{int}$ .
- vi. IF  $f_j^{(k)} < S_{otim}$  THEN make  $x^{(k)}, f_j^{(k)} \rightarrow x_{otim}, S_{otim}$  and  $ipg = j$ .
- vii. Make  $f_{pj} = f_j^{(k)}$ .

2. **Loop:**

- (a)  $opt_B = false, opt_N = false, k = k + 1$ .
- (b) For  $i = 1, \dots, N_x$  and  $j = 1, \dots, N_{pt}$  do:
  - i. Evaluate the new positions and velocities according to Equations (3.15) and (3.16).
  - ii. Evaluate the objective function, just as **Step 1(c)iv**.
  - iii. IF  $f_j^{(k)} < f_{pj}$  THEN  $f_{pj} = f_j^{(k)}$  and  $p_{i,j} = u_{i,j}^{(k)}$ . ELSE go to **Step 2(b)vii**.
  - iv. IF  $f_{pj} \leq S_{otim}$  THEN make  $opt_N = true$ . ELSE go to **Step 2(b)vii**.
  - v. IF  $(S_{otim} - f_{pj}) \geq (\epsilon_R S_{otim} + \epsilon_A)$  THEN make  $opt_B = true$  and  $N_V = 0$ .
  - vi. Make  $x^{(k)}, f_j^{(k)} \rightarrow x_{otim}, S_{otim}$  and  $ipg = j$ .
  - vii. Evaluate  $y_j$  according to Equations (3.17) and (3.18):

$$\widehat{f}_{pj} = \frac{f_{pj} - f_{pj,min}}{f_{pj,max} - f_{pj,min}} \quad (3.17)$$

$$y_j = [u_j | \widehat{f}_{pj}] \quad (3.18)$$

- (c) IF  $opt_N = false$  or ( $opt_N = true$  and  $opt_B = false$ ) (i.e. if no new best solution was found or new best solution found is closer to the previous one than the tolerance  $\epsilon$ ) THEN  $N_V = N_V + 1$ .
- (d) Update the inertial factor (Equation (3.19)):

$$w = w_0 + (w_f - w_0) \frac{N_V}{N_{max} + N_V} \quad (3.19)$$

- (e) Evaluate Equations (3.20) to (3.22), as recommended by MORAES *et al.* (2015).

$$\bar{y}_i = \sum_{j=1; j \neq ipg}^{N_{pt}} \omega_j y_{i,j} \quad (3.20)$$

$$\omega_j = \frac{\frac{1}{\|y_j - y_{ipg}\|}}{\sum_{k=1; k \neq ipg}^{N_{pt}} \frac{1}{\|y_k - y_{ipg}\|}} \quad (3.21)$$

$$\|y\| \equiv \left[ \frac{1}{n} \sum_{i=1}^n y_i^2 \right]^{\frac{1}{2}} \quad (3.22)$$

- (f) Evaluate the stop criterion:  $\|\bar{y} - \bar{y}_{old}\| < \epsilon_A$ . IF this expression is false or  $N_V < N_{max}$  THEN go to **Step 2a**. ELSE go to **Step 3**.

**3. Optimal point achieved. RETURN**  $x_{otim}$  and  $S_{otim}$ .

It is important to note that there were some adaptations included to the PSO in this work:

- In order to ensure the reached solution is the best one, it has been decided to modify the convergence test: the optimal solution has to be inside the tolerance for a number of consecutive times (defined by the user in the interface) in order to be checked for stop criterion. Because of the random feature of PSO, it is noted that sometimes when the method is going to a local minimum and suddenly a better minimum is found far from the previous value. It happened specially if  $c_1 \gg c_2$ .
- Whenever there is a computation of the objective function, its value is saved on an array  $S_{int}$ , and respective parameters on an array  $x_{int}$ . This practice is essential to generate scatter plots and parameter analysis charts detailed in Chapter 4.

### 3.2.2 Deterministic Method

The deterministic method implemented is the Flexible Polyhedra Method, also known as Simplex (NELDER and MEAD, 1965). It has been chosen mainly because it does not need computation of the derivatives of the objective function. Also, its implementation is relatively simple and it is efficient to find the optimal solution near the initial guess.

From a set of  $(n + 1)$  points forming a simplex in a  $n$ -dimensional plane, new simplexes would be formed by reflecting one of the points and/or expanding or contracting it according to the objective function value. Considering  $P_0, P_1, \dots, P_n$  sets of  $n$  variables each forming points of a known simplex, and  $y_0, y_1, \dots, y_n$  their respective objective functions, Equation (3.23) defines its centroid, discarding the highest value of  $y$ ,  $y_{high}$ :

$$Pc_i = \frac{1}{n} \sum_{j=1, j \neq high}^{n+1} P_{i,j}, \quad i = 1, \dots, n \quad (3.23)$$

There are then three possible movements in this method: reflection, contraction and expansion, defined, respectively, in Equations (3.24), (3.25) and (3.26):

$$P_{i,\alpha} = (1 + \alpha)Pc_i - \alpha P_{i,high} \quad (3.24)$$

$$P_{i,\beta} = \beta P_{i,high} + (1 - \beta)Pc_i \quad (3.25)$$

$$P_{i,\gamma} = \gamma P_{i,\alpha} + (1 - \gamma)Pc_i \quad (3.26)$$

$\alpha$  is the reflection parameter,  $\beta$  the contraction parameter (must be lower than 1) and  $\gamma$  the expansion parameter (must be greater than 1). All these movements were implemented as NELDER and MEAD (1965) described, thus the focus of this work is to point out the differences in how these points were initially obtained.

Firstly, these authors suggested to initialize the simplex from its vertices. However, as the EoS parameters are correlated with each other, not all sets of parameters result in convergence in the calculations. Therefore, it was decided in this work to generate a cluster around the initial guess, implemented according to Figure 3.1.

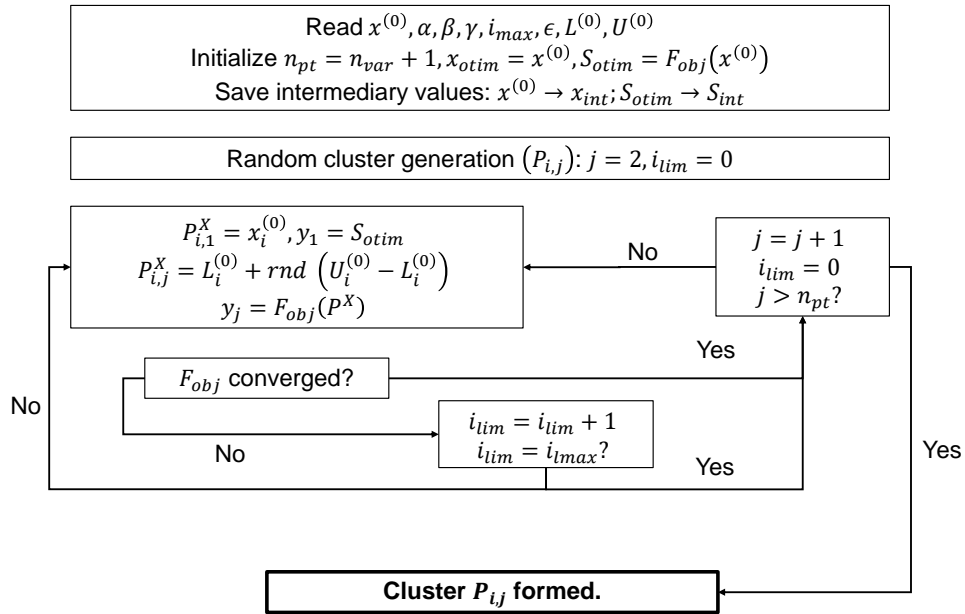


Figure 3.1: Random cluster formation for Simplex method.

Another adaptation implemented was due the fact that despite the simplex's



points originally have no bounds, thermodynamic variables must be bounded to avoid major convergence problems. NELDER and MEAD (1965) suggested in their work to apply logarithm to a non-negative variable. Based on this affirmation, Equation (3.27) and its inverse, Equation (3.28), are proposed and implemented in this work.

$$P_{i,j} = \tau \ln \left( \frac{x_{i,j} - L_i + \epsilon}{U_i - x_{i,j} + \epsilon} \right) \quad (3.27)$$

$$x_{i,j} = \frac{(L_i - \epsilon) + (U_i + \epsilon) \exp \left( \frac{P_{i,j}}{\tau} \right)}{1 + \exp \left( \frac{P_{i,j}}{\tau} \right)} \quad (3.28)$$

$\epsilon$  is a low value (order of  $10^{-9}$ ) inserted to avoid division by zero or logarithm of zero;  $\tau \equiv 1$  is a possible tuning factor to the expression; and  $L_i$  and  $U_i$  are the lower and upper bounds of  $x_{i,j}$ , respectively. Consequently,  $P_{i,j}$  is limitless while  $L_i < x_{i,j} < U_i$ .

Specifically in this stage, there is an option in the developed software to tighten the bounds of the manipulated variables in order to accelerate the cluster formation. It is called Initial Cluster Size and will be further described in Chapter 4. These new bounds substitute the variables  $L_i^{(0)}$  and  $U_i^{(0)}$  in Figure 3.1 to the variables  $L_i$  and  $U_i$ .

Once the cluster is formed, the algorithm is described as follows:

1. **Initialization:** Make  $iter = 0$ .
2. **Loop:**
  - (a)  $iter = iter + 1$ .
  - (b) Reflection, expansion and contraction tests implemented according to Equations (3.24), (3.26) and (3.25), respectively.
  - (c) Each time  $y = F_{obj}(x)$  is evaluated, save intermediary values:  $x \rightarrow x_{int}$ ;  $y \rightarrow S_{int}$ .
  - (d) Re-evaluate the new positions of the lowest value ( $y_{low}$ ) and highest value ( $y_{high}$ ) of  $y$ .
  - (e) Evaluate the convergence criterion, calculating  $Err = \|y - y_{mean}\|$  using the norm defined by Equation (3.22), and  $y_{mean}$  defined by Equation (3.29):

$$y_{mean} = \frac{1}{n_{pt}} \sum_{j=1}^{n_{pt}} y_j \quad (3.29)$$

- (f) Calculate  $Err_P = \sum_{j=1}^{n_{pt}} \|P_j - P_{low}\|$  using the norm defined by Equation (3.22).  $P_{low}$  stands for the point whose objective function results in  $y_{low}$ .
- (g) IF  $Err_P < Err$  THEN  $Err = Err_P$ .
- (h) IF  $y_{low} < 1$  THEN  $Err = Err/y_{low}$ .
- (i) IF  $y_{low} \geq S_{int,0}$  THEN  $Err = Err + \epsilon_A$ .
- (j) IF  $Err > \epsilon_A$  and  $iter < i_{max}$  THEN go to **Step 2a**.

### 3. Solution:

- (a)  $x_{otim}$  is calculated from Equation (3.28), with  $P_{i,j} = P_{i,low}$ , and  $S_{otim} = y_{low}$ .
- (b) **Optimal point achieved. RETURN**  $x_{otim}$  and  $S_{otim}$ .

As it can be seen in the algorithm, another modification implemented was related to the convergence criteria. Even though the variable  $Err$  is calculated as proposed by NELDER and MEAD (1965), some modifications were included in the implementation:

- If the lowest value of  $y$  is lower than 1, then  $Err$  was divided by  $y_{low}$ . This modification tightens the tolerance, ensuring the attainment of the best solution;
- If no new minimum value of  $y$  is found yet, than add the given tolerance to  $Err$ . This forces the optimizer to find a new solution at least once during the loop.
- $Err_P$  is a variable calculated analogously to  $Err$ , but with respect to the size of the simplex. If it is smaller than the variable  $Err$  at any iteration (i.e. after successive failed contractions) then  $Err_P$  becomes the new criterion.

### 3.2.3 Hybridization

It is commonly seen in the literature - e.g. SANTOS (2015) - a serial combination of a stochastic and a deterministic method in order to perform a global optimization of the desired system. The former method searches for all possible local minima in the region and the latter acts as a refinement of its result, as can be seen in the following scheme:

- Run PSO Method as previously described.

- Make  $x_{SIMPLEX}^{(0)} = x_{otim,PSO}$  and  $S_{SIMPLEX}^{(0)} = S_{otim,PSO}$ .
- Run Simplex with a random cluster around its initial guess.
- Optimal point of the Simplex execution is the final solution. **RETURN**  $x_{otim}$  and  $S_{otim}$ .

Nevertheless, DAS *et al.* (2006) proposed a combination between these methods inside the same loop in order to achieve the optimal solution most efficiently. Based on this approach, this work also proposes a combination between the implemented PSO and Simplex methods in parallel, further hybridizing them. The algorithm for this purpose is shown below.

1. **Initialization:** Initialize PSO method as previously described.
2. **Loop:**
  - (a) Execute one iteration of PSO.
  - (b) Make  $x_{simplex}^{(0)} = x_{otim,PSO}$  and  $S_{simplex}^{(0)} = S_{otim,PSO}$ . Generate a random cluster according to Figure 3.1 around this point.
  - (c) Run Simplex method.
  - (d)  $err_S = \epsilon_R S_{otim,simplex} + \epsilon_A$ . IF  $|S_{otim,PSO} - S_{otim,simplex}| \geq err_S$  THEN  $N_V = 0$ . ELSE  $N_V = N_V + 1$ .
  - (e) Update  $x_{otim,PSO} = x_{otim,simplex}$  and  $S_{otim,PSO} = S_{otim,simplex}$ .
  - (f) Replace the worst point of the swarm (i.e. the point whose objective function value is the highest) by the Simplex solution. Make *ipg* equal to its position.
  - (g) Update the inertial factor and evaluate the tolerance of PSO just as previously described.
  - (h) Evaluate the stop criterion:  $\|\bar{y} - \bar{y}_{old}\| < \epsilon_A$ . IF this expression is false or  $N_V < N_{max}$  THEN go to **Step 2a**. ELSE go to **Step 3**.
3. **Optimal point achieved.** **RETURN**  $x_{otim,PSO}$  and  $S_{otim,PSO}$ .

It is important to state that, although the implementation is based on the work of DAS *et al.* (2006), they are not equal. Their 'tandem' approach consists of creating several simplex clusters in each iteration, solving them simultaneously. In this work, after each iteration of PSO only one cluster is formed around the current PSO's best point (i.e. the point with the lowest value of objective function). Then it is solved by the Simplex method and its solution substitutes the former PSO's

worst point (i.e. the point with the highest value of objective function), making it the new best point of the stochastic method.

Despite the fact that the combination of the optimization methods in parallel allows to reach the optimal value faster than the usual linear 'PSO - Simplex' approach, both calculations were implemented in this work, and the user will be able to select them freely in the interface. The advantage of the serial approach is that it allows the generation of proper parametric and statistical analysis, as well as scatter points evaluations.

### 3.3 Parameter Estimation

For the purposes of this work there will be five different approaches to the objective function:

- Parameter estimation of a pure compound using vapour pressure and liquid density data.
- Binary parameter estimation using compositions in liquid-liquid equilibrium.
- Parameter estimation of a pure compound using simultaneously vapour pressure, liquid density and liquid-liquid equilibrium compositions (binary mixture between an associating and a non-associating compound).
- Binary parameter estimation using pressure calculation (for vapour-liquid equilibrium).
- Binary parameter estimation using water content calculation in a multicomponent mixture (containing obligatorily water and at least one more compound).

#### 3.3.1 Pure Components

In this case, the calculated variables studied are the saturation vapour pressure ( $P$ ) and the liquid density ( $\rho$ ) of a pure component. Thus, the objective function becomes (Equations (3.30) and (3.31)):

$$S(\underline{X}_P) = \frac{1}{n_e} \left[ \sum_{i=1}^{n_e} \frac{(P_i^e - P_i^*)^2}{\sigma_{P,i}^2} + \sum_{i=1}^{n_e} \frac{(\rho_i^e - \rho_i^*)^2}{\sigma_{\rho,i}^2} \right] + F_W(\underline{W}, \underline{X}_P) \quad (3.30)$$

$$\underline{X}_P = \begin{cases} [a_0 \ b \ c_1 \ c_2 \ c_3]^T & \text{IF not CPA} \\ [a_0 \ b \ c_1 \ \varepsilon/R \ \beta]^T & \text{IF CPA} \end{cases} \quad (3.31)$$

In addition to the original expression in Equation (2.35), in this work an extra restriction  $F_W(\underline{W}, \underline{X}_P)$ , related to the critical region behaviour of the system, are implemented, with  $\underline{W}$  being the weights defined by the user. Therefore, this restriction takes the form of a penalization function.

The original values of  $a_0$  and  $b$  of the cubic equations of state (Equations (2.4) and (2.5)) were calculated based on the restrictions dictated by Equation (2.3). However, when these parameters become freely manipulated, such restrictions are violated, so they were inserted in the objective function as can be seen in Equation (3.32), transforming them into dimensionless terms and squaring them to avoid negative values.

$$F_W(\underline{W}, \underline{X}_P) = w_1 \left[ \frac{V_c}{P_c} \left( \frac{\partial P}{\partial V} \right)_{T=T_c} \right]^2 + w_2 \left[ \frac{V_c^2}{P_c} \left( \frac{\partial^2 P}{\partial V^2} \right)_{T=T_c} \right]^2 \quad (3.32)$$

The weights  $\underline{W} = [w_1 \ w_2]^T$  are specified by the user. It is important to emphasize that no relevant publication has been found regarding this parameter estimation procedure as described in this work. Therefore, adding the critical region penalization effect term in the metric is a potential contribution of this work to the academic community.

The general algorithm can be seen on Figure 3.2.

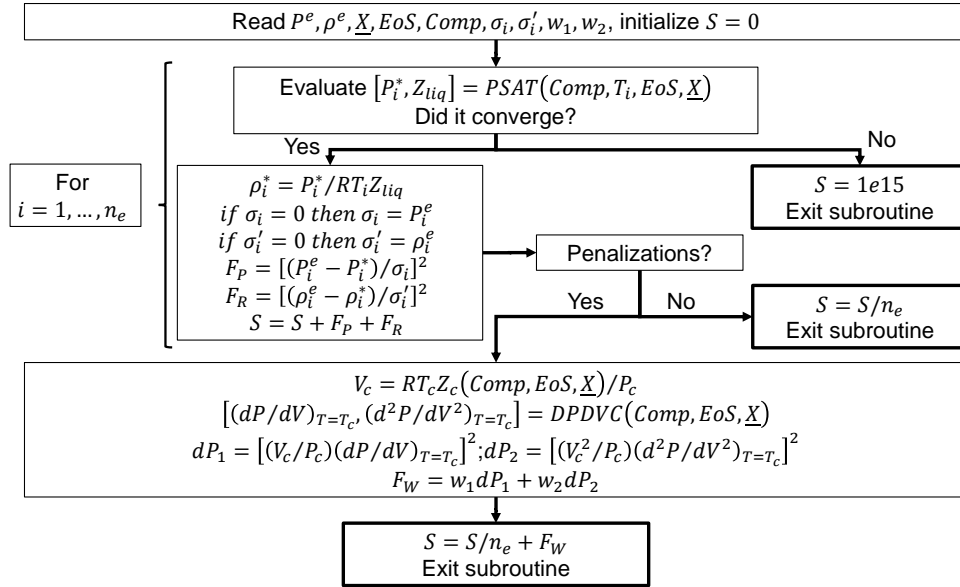


Figure 3.2: Algorithm to evaluate objective function of pure component case. 'PSAT' and 'DPDVC' are internal functions, dependent to the temperature (T), thermodynamic model (EoS), component critical properties (Comp) and manipulated variables.

This approach needs the following data to accomplish the parameter estimation:

- Critical properties ( $T_c$ ,  $P_c$  and  $\omega$ );

- Experimental temperature data ( $T$ );
- Experimental pressure data ( $P^e$ ) and their variances ( $\sigma_P$ ), if available;
- Experimental liquid density data ( $\rho^e$ ) and their variances ( $\sigma_\rho$ ), if available (optional).

If there is no liquid density data available, calculations may proceed using only pressure as calculated variable. Also, the penalization effect is optional and the user is able to add or remove it in the interface, as will be explained in details in Chapter 4.

The experimental variances are not obligatory data either. If the user does not wish to enter their values, there will be an option to allow that  $\sigma_{P,i} = P_i^e$  and  $\sigma_{\rho,i} = \rho_i^e$  (i.e. the respective experimental variables). This applies to all metrics described here.

Thus, with these data, the saturation pressure is calculated in order to satisfy Equation (3.1), where the phases  $\alpha$  and  $\beta$  are, respectively, liquid and vapour. Density can be calculated as the inverse of the molar volume.

Also, if the user activated the penalization effect, the program will then calculate the critical volume and the necessary derivative properties, according to Equation (3.32), adding them to the objective function.

If the pressure calculation does not converge, the program will automatically return a very high value to the objective function (currently it is equal to  $10^{15}$ ).

### 3.3.2 Binary Mixtures by Liquid-liquid Equilibrium Calculation

This case is similar to the previous metric, with the main difference being the calculated variables in the objective function, related to the liquid-liquid equilibrium (LLE) of the system, calculated by the algorithm described in the Section 3.1.2. Also, there is no penalization function, i.e.  $F_W(\underline{W}, \underline{X}_P) = 0$ . Therefore, the objection function is calculated by Equation (3.33) and, with the estimable variables indicated in Equation (3.34). Among the available EoS in the program, only the CPA can perform this calculation.

$$S(\underline{X}_P) = \frac{1}{n_e} \left[ \sum_{i=1}^{n_e} \frac{(x_{I-II,i}^e - x_{I-II,i}^*)^2}{\sigma_{x_{I-II,i}}^2} + \sum_{i=1}^{n_e} \frac{(x_{II-I,i}^e - x_{II-I,i}^*)^2}{\sigma_{x_{II-I,i}}^2} \right] \quad (3.33)$$

$$\underline{X}_P = [k_{12,0} \quad k_{12,1} \quad \varepsilon_{12}^{cross}/R \quad \beta_{12}^{cross}]^T \quad (3.34)$$

As stated in the Section 3.1.2, the LLE calculations do not depend on the global composition of the liquid. Then, with these data, the compositions of each liquid phase in equilibrium can be calculated according to Equations (3.7) and (3.8).

The algorithm is shown in Figure 3.3.

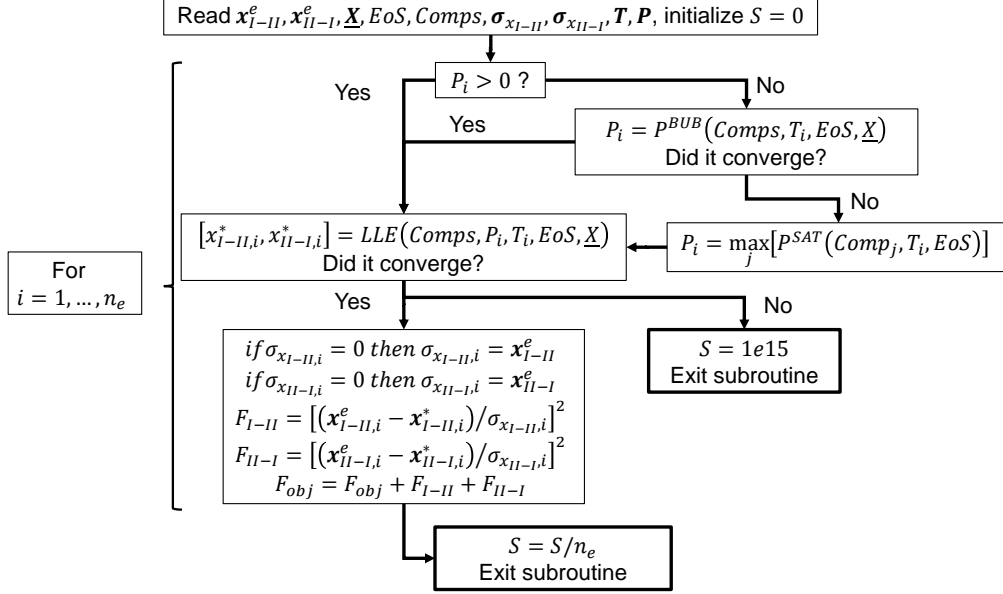


Figure 3.3: Algorithm of the objective function calculation of the binary mixture case in LLE. 'PBUB' calculates bubble pressure of the system and 'PSAT' calculates the saturation pressure of a pure component.

It is not uncommon that experimental data on LLE do not explicit the pressure of the system. In these cases, the program may calculate the bubble pressure of an equimolar mixture of the compounds. If this calculation does not converge either, then the highest pure component's saturation pressure will be applied in the calculation of the liquid compositions. Thus, the required data for this approach are:

- Components 1 and 2's pure parameters and critical data.
- Experimental temperatures ( $T$ ).
- Experimental pressures ( $P_i^e$ , optional).
- Experimental composition data of component 1 in phase rich in component 2 ( $x_{I-II}^e$ ) and vice-versa ( $x_{II-I}^e$ ), as well as their variances ( $\sigma_{x_{I-II}}$  and  $\sigma_{x_{II-I}}$ , respectively), if available.

### 3.3.3 Validating Pure Component Parameters with LLE Data

As described in the Section 2.3, several authors recommended to use LLE calculations with specific compounds to select the best parameters for pure components. This work proposes an improvement to this analysis, in order to automate it. It consists in unifying both previous objective functions into Equation (3.35).

$$S(\underline{X}_P) = S_{pure}(\underline{X}_{P1}) + \omega S_{LLE}(\underline{X}_{P2}) \quad (3.35)$$

$S_{pure}$  is the objective function defined by Equation (3.30),  $S_{LLE}$  is the objective function defined by Equation (3.33) and  $\omega$  is a user-defined weight. All pure ( $\underline{X}_{P1}$ ) and binary ( $\underline{X}_{P2}$ ) parameters can be manipulated at once in this approach, i.e.  $\underline{X}_P = [\underline{X}_{P1} \ \underline{X}_{P2}]$ . The methodology proposed is as follows:

1. Select the range of temperatures of the experimental points to calculate  $S_{pure}$ .
2. Generate a set of pure parameters using the approach in the Section 3.3.1. Both optimization methods PSO and Simplex are required.
3. Choose a second component to calculate  $S_{LLE}$ . Usually aliphatic hydrocarbons are chosen (e.g. n-hexane or n-heptane), provided there are available experimental data.
4. Generate a set of binary parameters using the approach in the Section 3.1.2, with the parameters obtained in **Step 2**. Both optimization methods PSO and Simplex are required.
5. Select the initial weight  $\omega_0$  (it is recommended to be  $\ll 1$ ), the final weight  $\omega_F$  and the number of calculations  $n$ .
6. Make  $\Delta\omega \equiv (\omega_F - \omega_0)/n$ .
7. Generate a new set of parameters using Equation (3.35) for  $\omega = \omega_0$ , using only the method Simplex with the parameters found in **Steps 2** and **4** as an initial guess.
8. Make  $\omega = \omega_0 + \Delta\omega$
9. Generate a new set of parameters using Equation (3.35) for  $\omega$ , using only the method Simplex. Use the set of parameters obtained in the previous step as an initial guess to this step.
10. Return to **Step 8** until  $\omega = \omega_F$ .



From this method, it is possible to analyse the behaviour of  $S_{pure}$  and  $S_{LLE}$  for various values of weight, enabling the generation of Pareto analyses. Also, once there is an initial guess relatively close to the solution, the Simplex method can be used without a previous global search, greatly accelerating the calculations. Thus, this can be considered a major contribution of this work to the academic community. In Chapter 5 the VLE-LLE Methodology will be properly validated and results for some components will be shown and discussed.

### 3.3.4 Binary Mixtures by Bubble or Dew Pressure Calculation

As for the case with the LLE metric,  $F_W(W, \underline{X}_P) = 0$ . Also, there is only one calculated variable, which is the pressure of the system, as can be seen on Equations (3.36) and (3.37):

$$S(\underline{X}_P) = \frac{1}{n_e} \sum_{i=1}^{n_e} \frac{(P_i^e - P_i^*)^2}{\sigma_{P,i}^2} \quad (3.36)$$

$$\underline{X}_P = \begin{cases} [k_{12,0} \ k_{12,1}]^T & \text{IF not CPA} \\ [k_{12,0} \ k_{12,1} \ \varepsilon_{12}^{cross}/R \ \beta_{12}^{cross}]^T & \text{IF CPA} \end{cases} \quad (3.37)$$

The pressure can be calculated as bubble or dew, depending on the available composition data, whether they are from liquid phase or vapour phase. If both are available, the user can choose the type of calculation in the interface. The algorithm is similar to the pure component case, as shown in Figure 3.4.

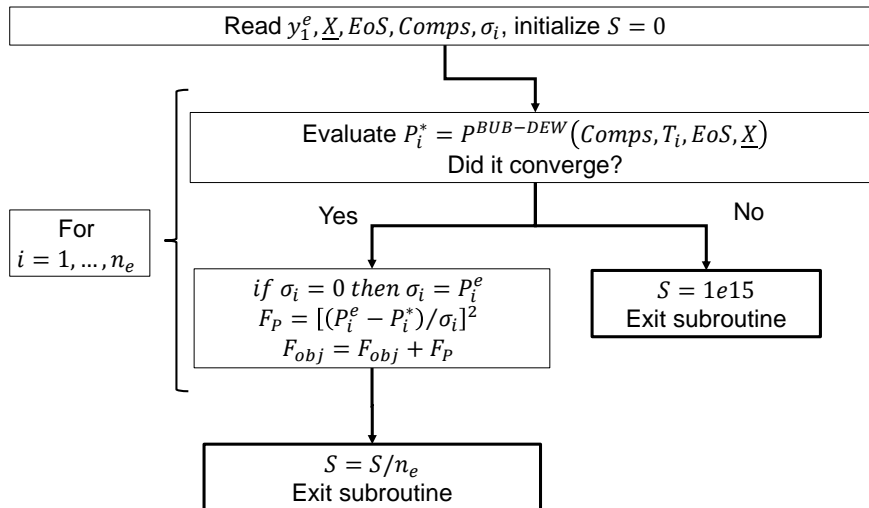


Figure 3.4: Algorithm of the objective function calculation of the binary mixture case from the bubble or dew pressure of the system (Section 3.1.1). 'Comps' contains the components' critical properties and EoS parameters.

Therefore, the data required in this approach are:

- Components 1 and 2's pure parameters and critical data;
- Experimental temperature data ( $T$ );
- Experimental pressure data ( $P_i^e$ ) and their variances ( $\sigma_P$ ), if available;
- Experimental composition data of component 1 (if  $x_1$ , bubble calculations are performed; if  $y_1$ , dew calculations are performed; if both, the user decides the type of pressure calculation).

With these data, bubble or dew pressures are also calculated in order to satisfy Equation (3.1), where the phases  $\alpha$  and  $\beta$  are, respectively, liquid and vapour.

### 3.3.5 Multicomponent Mixtures by Water Content Calculation

In this case there is also only one calculated variable, which is water content in dew point, as previously described in the Section 3.1.3. As in the binary calculations, the penalization function  $F_W(\underline{W}, \underline{X}_P) = 0$ .

Hence, the objective function is given by Equation (3.38), with the estimable variables by Equation (3.39).

$$S(\underline{X}_P) = \frac{1}{n_e} \sum_{i=1}^{n_e} \frac{(y_{H_2O}^e - y_{H_2O}^*)^2}{\sigma_{y,i}^2} \quad (3.38)$$

$$\underline{X}_P = \begin{cases} [k_{i-water,0} \ k_{i-water,1}]^T & \text{IF not CPA} \\ [k_{i-water,0} \ k_{i-water,1} \ \varepsilon_{i-water}^{cross}/R \ \beta_{i-water}^{cross}]^T & \text{IF CPA} \end{cases} \quad (3.39)$$

The user is allowed to choose which pair(s) whose parameters are desired to be estimated, as long as one of the components of the pair is water. Figure 3.5 shows how this objective function is implemented.

The input data required in this approach are:

- All components' pure parameters and critical data.
- All non-estimated binary parameters.
- Binary parameters to be estimated.
- Experimental temperature data ( $T$ ).
- Experimental pressure data ( $P$ ).

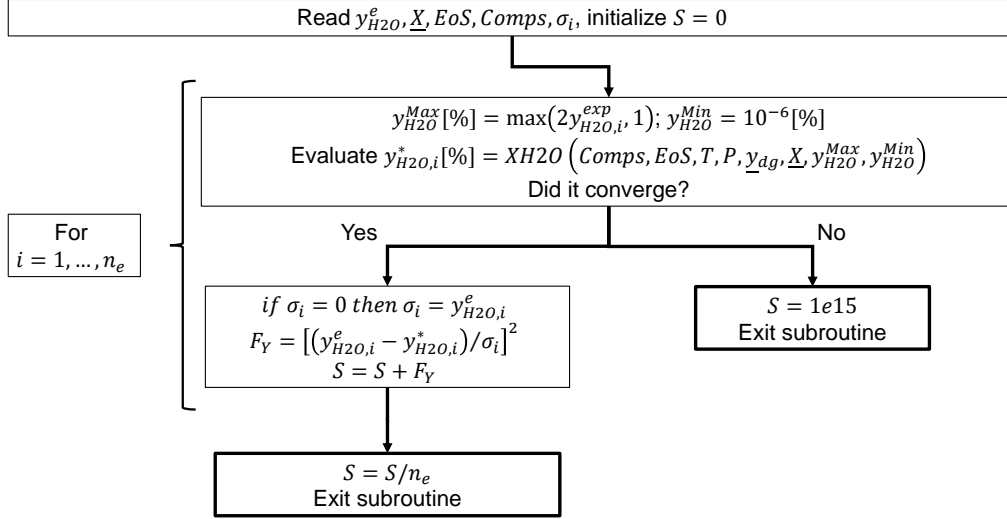


Figure 3.5: Algorithm of objective function calculation of multicomponent mixture case using gas humidity data. 'XH2O' is an internal function of the program, described in the Section 3.1.3. 'Comps' is an object containing the components' specifications, such as critical variables and EoS parameters.

- Composition of the dry gas in each point ( $\underline{y}_{DG}$ ).
- Experimental water content data ( $y_{H2O}$ ) and their variances ( $\sigma_{y,i}$ ), if available.

All binary parameters not filled by the user will be considered equal to zero. Also, as only the Simplex method is executed with this metric, an initial guess is necessary. That is why the binary parameters values to be estimated are required to this calculation. Section 3.4 presents an example of how to initialize these parameters.

### 3.4 Procedure to Parameter Estimation from Pure to Mixtures

When modelling water saturation points of natural gas streams containing high levels of CO<sub>2</sub> (60%) and H<sub>2</sub>S at high pressures, a proposed procedure (providing that experimental data is available in all cases) is:

- If the pure component parameters are not available, estimate them by Section 3.3.1, solving by PSO and Simplex, or by Section 3.3.3;
- Estimate the binary parameters of each pair by Section 3.3.2 or Section 3.3.4, depending on the availability of the experimental data, solving by PSO and Simplex;

- From an initial guess composed of the previous results, re-estimate the binary parameters of pairs containing water using Section 3.3.5, solving by only Simplex.

# Chapter 4

## Computational Aspects

This Chapter will address the details of the program written to perform the necessary calculations to this work, showing its features, interfaces and advantages of modelling and calculating thermodynamic properties.

### 4.1 Software Basis

The program developed in this work is called *ThermOptimizer*, or *ThermOpt* for short. It has been written in two computational languages: C# and Fortran, both using the Visual Studio environment.

Firstly, C# is an object-oriented language, most commonly used to create forms and interface items in general. Its advantages are:

- It shows all possible methods and properties of a variable while writing it on a code;
- Excellent error feedback, being able to track errors at real time;
- Automatic garbage memory handler, avoiding memory leakage;
- Open libraries available for free on the Internet (e.g. matrix calculations);
- Can establish connections with many other languages by .dll files, such as Fortran.

Therefore, it was chosen to be the main interface language. The thermodynamic calculations, however, have been written in a sturdier language such as Fortran. Its main benefit is the management of arrays, which is faster than C#'s.

Currently, *ThermOpt*'s interface is divided in three tabs: Pure Component, Binary Mixture and Multicomponent Mixture, inside two major tabs: Input and Output. All tabs have their own features, implemented in user-friendly interfaces.

Besides, there are some components present in all tabs, henceforth called the General Features of *ThermOpt*. In the next topics, these features will be detailed.

## 4.2 Input Features

### 4.2.1 Pure Component Tab

Figure 4.1 shows the interface of this tab. It contains the following traits: Input Data, Thermodynamic Model, Parameters to be Estimated and Objective Function. Each feature will be detailed further in this Section.

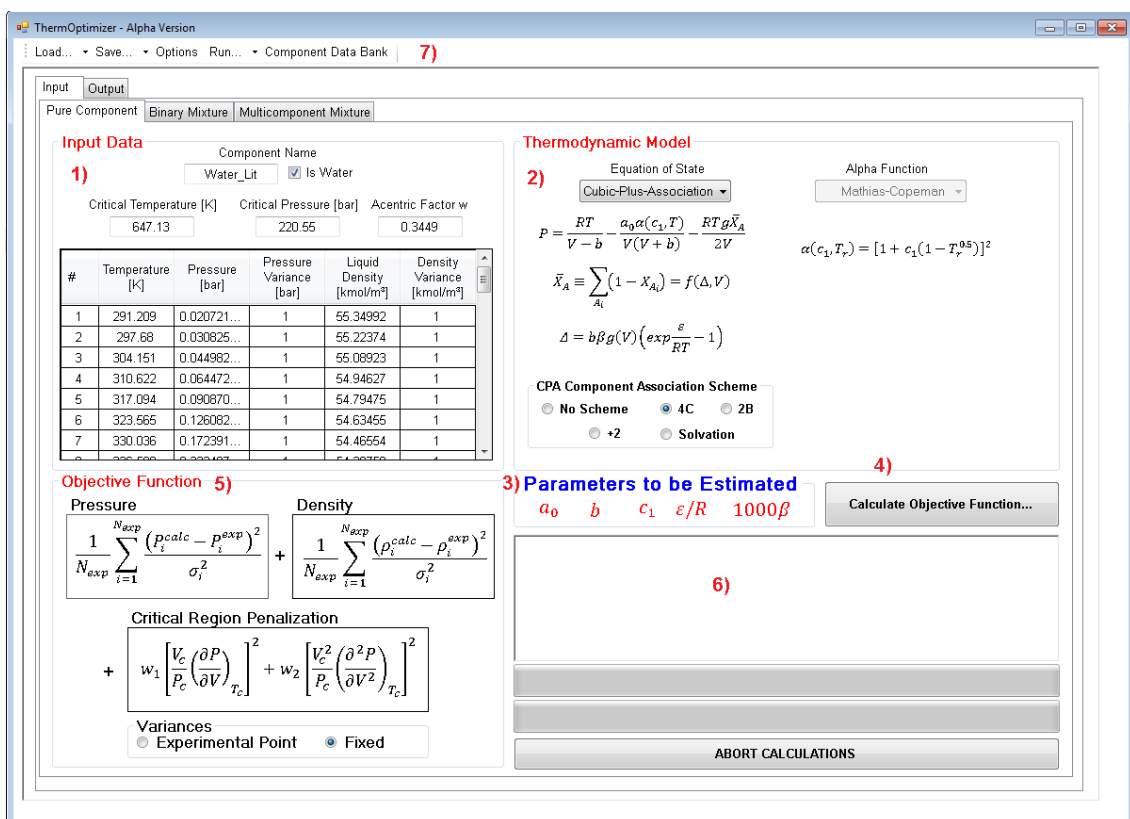


Figure 4.1: Main features of Pure Component tab. 1) Input and experimental data. 2) Thermodynamic model used in this execution. 3) Parameters to be estimated. 4) Button to calculate objective function of a specific set of parameters, without optimizing. 5) Objective function to be minimized. 6) Diagnostics box, progress bar and 'abort' button (General Features). 7) Miscellaneous functions (General Features).

### Input Data

In this field the user must insert the following information:

- Name of component. It does not have to be the real name of component.

It acts as a means to differentiate from other components when calculating mixtures.

- 'Is Water' check-box. If checked, *ThermOpt* will consider that this component is water, regardless of what the user named it. Some internal calculations are specific to water, for instance some  $\alpha$  functions described in Chapter 2.
- Critical temperature, critical pressure and acentric factor. It is important to mind the units of measure in each field: temperatures are always shown in Kelvin, pressures in bar and densities in kmol/m<sup>3</sup>.
- Experimental Data: list of experimental temperatures, pressures, densities and their variances. Depending on the objective function details, some columns will be hidden making it easy to the user visualize which inserted data is actually used on each execution of the program.

### Thermodynamic Model

In this region the user will select the thermodynamic model (equation of state +  $\alpha$  function, when applicable) which will suit the parameter estimation procedure.

Currently there are three equations of state inserted: SRK (Equation (2.14)), PR (Equation (2.17)) and CPA (Equation (2.25)). For each cubic equation, the available  $\alpha$  functions are: original (Equation (2.15)), Mathias-Copeman (Equation (2.19)) and modifications specially made for water (SRK: Equation (2.20); PR: Equation (2.21)). As for the CPA EoS, the only option available is a modified Mathias-Copeman equation with  $c_2 = c_3 = 0$ .

Each time the user changes the equation of state or the  $\alpha$  function, the interface will change dynamically in order to help the visualization of the system. Figures 4.2 and 4.3 show these interfaces.

Another option available only for cubic equations is to fix the parameters  $a_0$  and  $b$  to their original values, calculated by critical properties. This option does not appear for CPA because it does not have 'original parameters', they have to be estimated instead. When this option is checked, Figure 4.4 is shown.

<p>Equation of State</p> <p><b>Peng-Robinson</b> ▼</p> $P = \frac{RT}{V-b} - \frac{a_0 \alpha(c_1, T_r)}{V(V+b) + b(V-b)}$	<p>Equation of State</p> <p><b>Soave-Redlich-Kwong</b> ▼</p> $P = \frac{RT}{V-b} - \frac{a_0 \alpha(c_1, T_r)}{V(V+b)}$
<p>Equation of State</p> <p><b>Cubic-Plus-Association</b> ▼</p> $P = \frac{RT}{V-b} - \frac{a_0 \alpha(c_1, T_r)}{V(V+b)} - \frac{RTg\bar{X}_A}{2V}$ $\bar{X}_A \equiv \sum_{A_i} (1 - X_{A_i}) = f(\Delta, V)$ $\Delta = b\beta g(V) \left( \exp \frac{\varepsilon}{RT} - 1 \right)$	

Figure 4.2: Interfaces of each Equation of State implemented in *ThermOpt*.

<p>Alpha Function</p> <p><b>Original</b> ▼</p> $\alpha(c_1, T_r) = [1 + c_1(1 - T_r^{0.5})]^2$ $c_1 = 0.37464 + 1.54226w - 0.26992w^2$ <p>Peng-Robinson Equation of State Only</p>	<p>Alpha Function</p> <p><b>Peng et al Modification</b> ▼</p> <p>If Water:  <math>T_r^{0.5} &lt; 0.85</math>:  <math>\alpha(c_1, T_r) = [1.0085677 + c_1(1 - T_r^{0.5})]^2</math>  <math>T_r^{0.5} \geq 0.85</math>:  <math>\alpha(c_1, T_r) = [1 + c'_1(1 - T_r^{0.5})]^2</math>  <math>c'_1 = c_1 + \frac{(1.0085677 - 1)}{1 - 0.85}</math></p> <p>Else: <math>\alpha(c_1, T_r) = [1 + c_1(1 - T_r^{0.5})]^2</math></p>
<p>Alpha Function</p> <p><b>Original</b> ▼</p> $\alpha(c_1, T_r) = [1 + c_1(1 - T_r^{0.5})]^2$ $c_1 = 0.480 + 1.57w - 0.176w^2$ <p>Soave-Redlich-Kwong Equation of State Only</p>	<p>Alpha Function</p> <p><b>Kabadi-Danner</b> ▼</p> <p>If Water: <math>\alpha(c_1, T_r) = [1 + c_1(1 - T_r^{0.8})]^2</math></p> <p>Else: <math>\alpha(c_1, T_r) = [1 + c_1(1 - T_r^{0.5})]^2</math></p>
<p>Alpha Function</p> <p><b>Mathias-Copeman</b> ▼</p> $\alpha(\underline{c}, T_r) = [1 + c_1(1 - T_r^{0.5}) + c_2(1 - T_r^{0.5})^2 + c_3(1 - T_r^{0.5})^3]^2$ <p>All Equations of State</p>	

Figure 4.3: All  $\alpha$  functions currently implemented into *ThermOpt*.

Fix a0 / b Parameters

$$a_0 = \frac{\Omega_a R^2 T_c^2}{P_c}, \quad b = \frac{\Omega_b RT_c}{P_c}$$

Figure 4.4: Interface shown when the option 'Fix a0 / b Parameters' is checked.



## Parameters to be Estimated

This field is extremely important to a user-friendly interface, because it changes dynamically as the thermodynamic model is modified. Figure 4.5 shows some possible combinations.

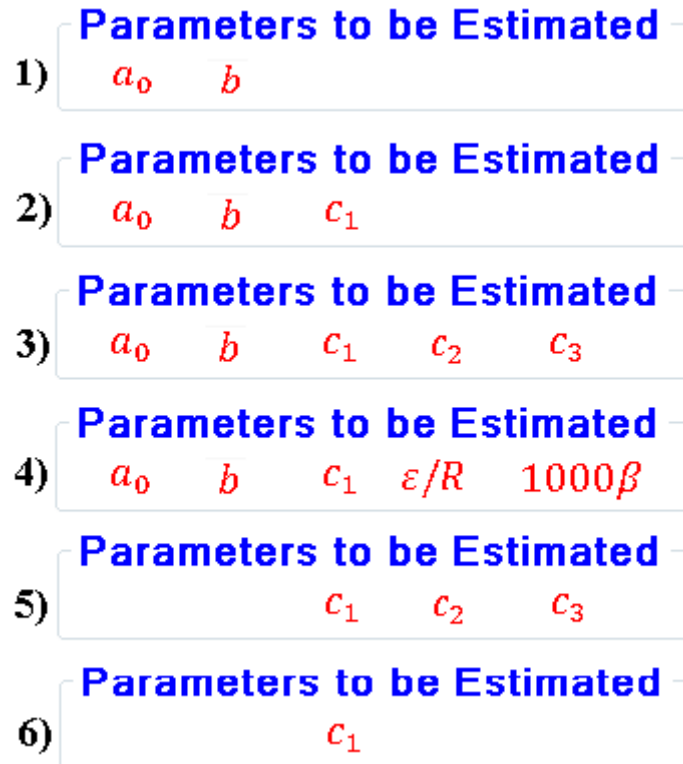


Figure 4.5: Combinations of parameters to be estimated. 1) SRK or PR + original  $\alpha$  function; 2) SRK or PR + water-specific  $\alpha$  functions, or CPA without self-association; 3) SRK or PR + Mathias-Copeman  $\alpha$  function; 4) CPA with self-association; 5) SRK or PR + Mathias-Copeman AND  $a_0$  and  $b$  fixed; 6) SRK or PR + water-specific  $\alpha$  functions AND  $a_0$  and  $b$  fixed.

Besides, if the user specifies the upper and lower bounds of a variable to the same value, it will also disappear from this interface, because this variable will become specified instead of manipulated.

## Objective Function

For the Pure Component tab, this region consists of three dynamic images, each one referring to a term of the objective function defined on Equations (3.30) and (3.32). The Density and Critical Region Penalization options can be turned on or off just by clicking on them, as shown on Figure 4.6.

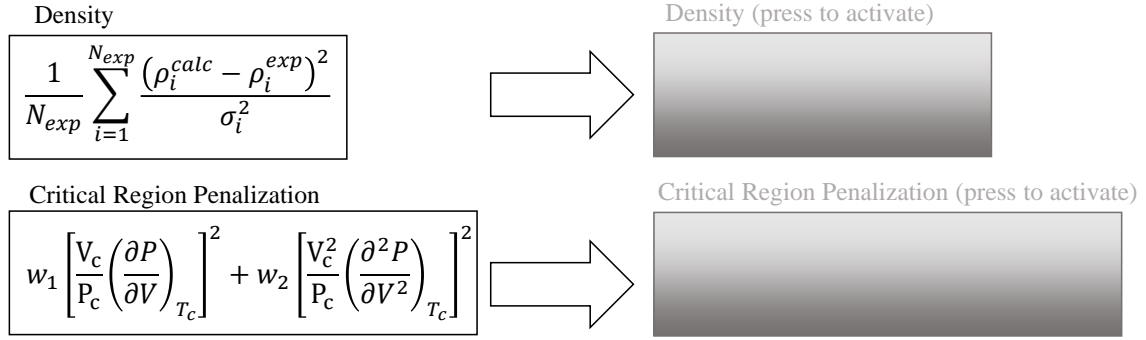


Figure 4.6: Interface appearances of Density and Critical Region Penalization terms when turned off.

In addition to that, as detailed in Chapter 3, it is not common to have experimental variances available on the literature, so there is the possibility to use the own experimental points as denominators of the objective function. To perform that, the user should click the option correspondent inside the box labelled 'Variances': either fixed values or the experimental variables. Figure 4.7 shows how these selections will appear in the interface.

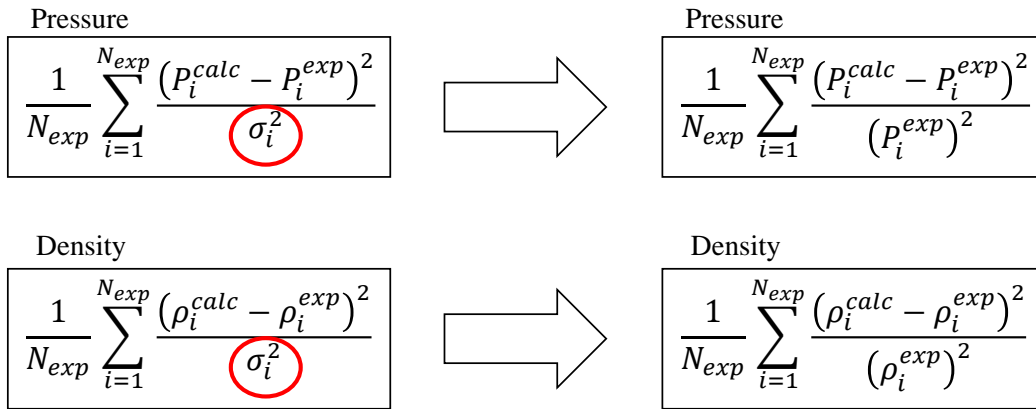


Figure 4.7: Interface appearance when the user clicks on 'Experimental Point' option in 'Variances' box, from the 'Fixed' option.

## 4.2.2 Binary Mixture Tab

Figure 4.8 shows the interface to this tab. It also contains the features Input Data, Thermodynamic Model, Parameters to be Estimated and Objective Function. Each of them will be detailed further in this Section.

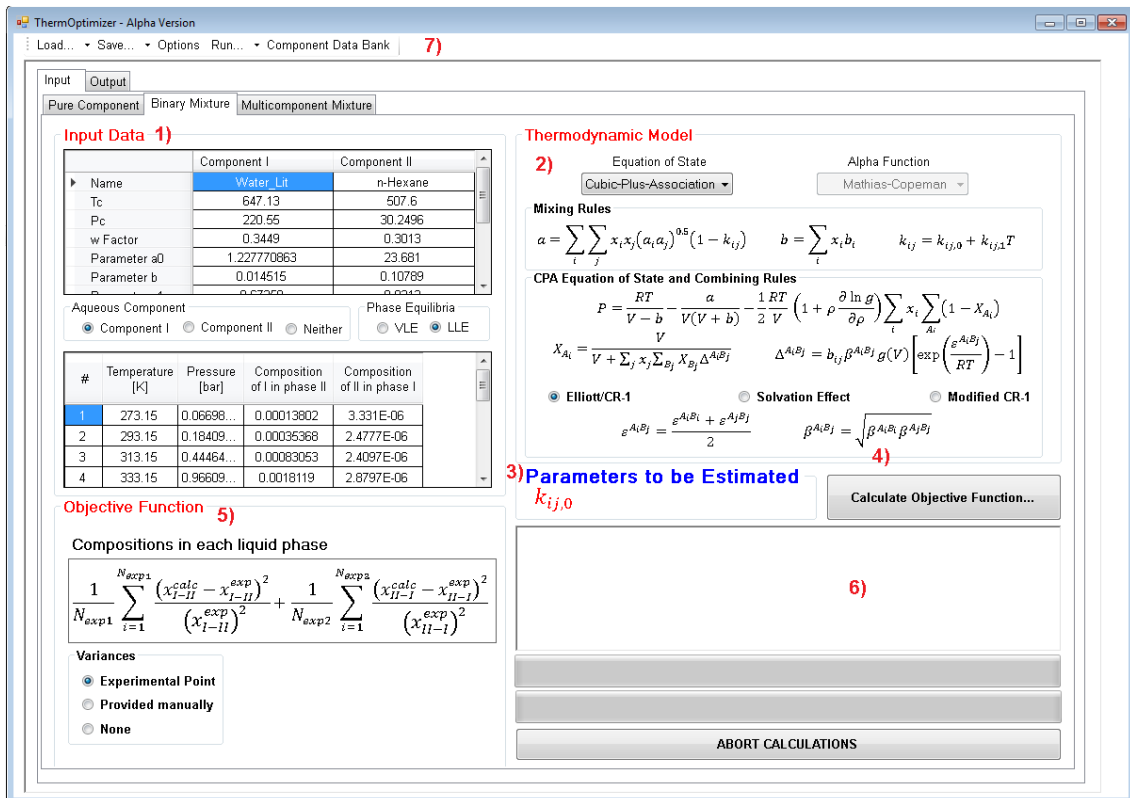


Figure 4.8: Main features of Binary Mixture tab. 1) Input, experimental data and phase equilibrium selector. 2) Thermodynamic model used in this execution, focused on mixture and combination rules. 3) Parameters to be estimated - depend on the EoS, combination rule and bounds given by the user. 4) Button to calculate objective function of a specific set of parameters, without optimizing. 5) Objective function to be minimized. 6) Diagnostics box, progress bar and 'abort' button (General Features). 7) Miscellaneous functions (General Features).

## Input Data

In this field, the user must input the following data:

- Name and specifications of both components. If these components are available in the Component Data Bank, then just entering their names is enough to fill the remaining fields of this table (critical properties, EoS parameters, ...).
- Aqueous component. Select which component is water (regardless of its name): Component I, Component II or neither.
- Phase equilibria. Select whether VLE or LLE calculations are to be conducted. Note that LLE calculations are available only for CPA EoS.
- Experimental data. List of the experimental temperature, pressure, compositions data and their variances, if needed. Analogously to the Pure

Component Tab, some columns will be hidden depending on the format of the objective function. The intention is to facilitate the visualization which inserted data is actually used on each execution of the program.

## Thermodynamic Model

In this region, the user can select the EoS and the  $\alpha$  function which will suit the parameter estimation procedure, in the same way as in the Pure Component Tab. The difference lies on the combining rules for CPA model, where the user can select depending on the mixture to be studied:

- Elliott/CR-1. Uses the CR-1 Combination Rule (Equations (2.31) and (2.32)). Used on mixtures of two self-associating components where this rule can be used without great deviations, or on mixtures where at least one of the components is non-associating at all (e.g. water + ethanol, or water + n-hexane). The Elliott Combining Rule (ECR, Equation (2.33)) is an implementation for future versions of *ThermOpt*.
- Solvating Effect. Makes use of Equation (2.31) and manipulates the parameter  $\beta^{A_i B_j}$ . Used on mixtures with a self-associating and a non self-associating compound that performs cross association in this mixture (e.g. water + benzene).
- Modified CR-1. Manipulates both cross association parameters  $\varepsilon^{A_i B_j}$  and  $\beta^{A_i B_j}$ . Used on mixtures of two self-associating components or mixtures described on Solvating Effect item, in order to improve predictions by adding parameters to the optimization.

Each time the user changes the EoS or the combining rule, the interface will also be modified dynamically in order to facilitate the visualization.

## Parameters to be Estimated

As in the Section 4.2.1, this field changes dynamically as the thermodynamic model's options are adjusted. Figure 4.9 shows some possible combinations.

- 1) **Parameters to be Estimated**  
 $k_{ij,0}$   $k_{ij,1}$   $\beta^{A_i B_j}$   $\varepsilon^{A_i B_j} / R$
- 2) **Parameters to be Estimated**  
 $k_{ij,0}$   $k_{ij,1}$   $\beta^{A_i B_j}$
- 3) **Parameters to be Estimated**  
 $k_{ij,0}$   $k_{ij,1}$
- 4) **Parameters to be Estimated**  
 $k_{ij,0}$

Figure 4.9: Possible combinations of parameters to be estimated in the Binary Mixture tab. 1) CPA EoS + Modified CR-1 option; 2) CPA EoS + Solvation Effect option; 3) CPA EoS + ECR/CR-1 option or PR/SRK EoS; 4) Same as (3), but with both limits of variable  $k_{ij,1}$  equal to zero, forcing  $k_{ij}$  to be constant.

### Objective Function

For the Binary Mixture tab, it consists on one dynamic image for VLE option or another dynamic image for LLE option (see Figures 4.10 and 4.11).

Pressure - calculation mode: Bubble Pressure ▾

$$\frac{1}{N_{exp}} \sum_{i=1}^{N_{exp}} \frac{(p_i^{calc} - p_i^{exp})^2}{(p_i^{exp})^2}$$

Dew Pressure  
Bubble Pressure

Figure 4.10: Objective function interface for VLE case in Binary Mixture tab. The user can select the type of pressure calculation - bubble or dew.

**Compositions in each liquid phase**

$$\frac{1}{N_{exp1}} \sum_{i=1}^{N_{exp1}} \frac{(x_{I-II}^{calc} - x_{I-II}^{exp})^2}{(x_{I-II}^{exp})^2} + \frac{1}{N_{exp2}} \sum_{i=1}^{N_{exp2}} \frac{(x_{II-I}^{calc} - x_{II-I}^{exp})^2}{(x_{II-I}^{exp})^2}$$

Figure 4.11: Objective function interface for LLE case in Binary Mixture tab.

As for the variances, there are three options available:

- Experimental Point. The objective function is normalized by own experimental points.

- Provided manually. The user will insert the variances.
- None. All variances will be equal to 1.

### 4.2.3 Multicomponent Mixture Tab

Figure 4.12 shows the interface to this tab. Analogously to the previous tabs, it contains Input Data, Thermodynamic Model and Objective Function, but the parameters to be estimated are shown in a separate interface, inside the 'Binary Parameters...' button. Each feature will be detailed further in this Section.

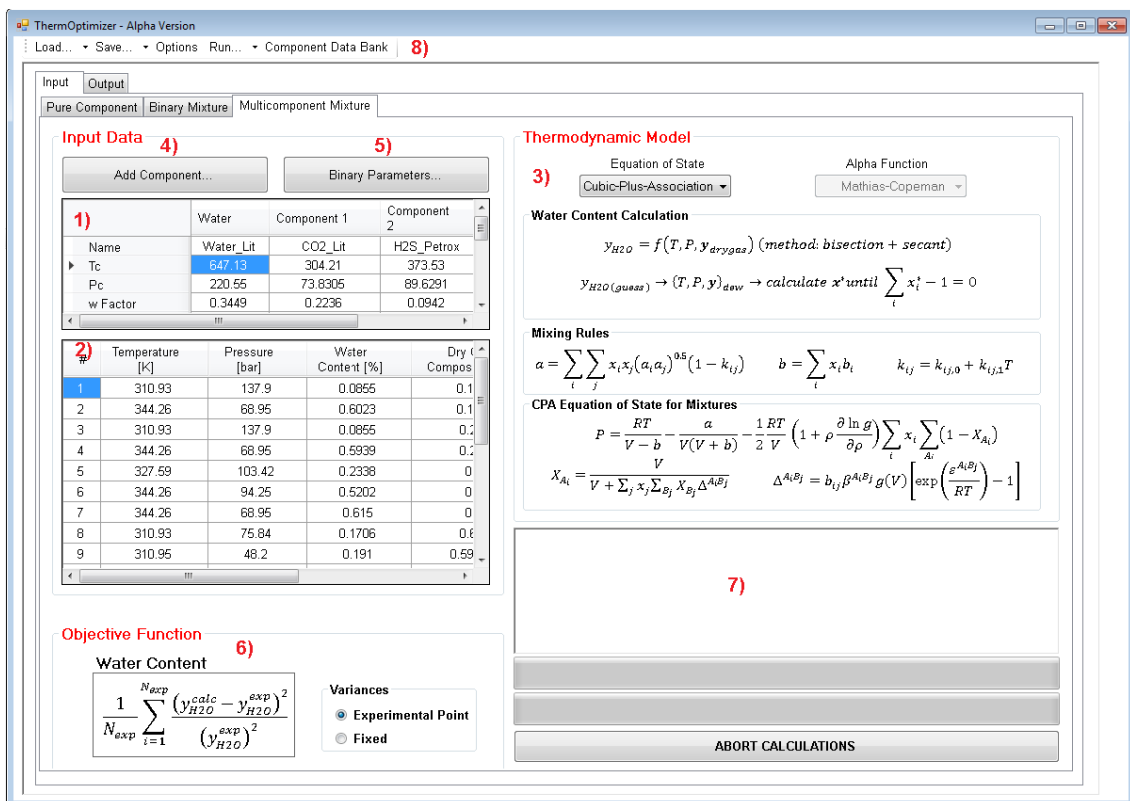


Figure 4.12: Main features of Multicomponent Mixture tab. 1) Input data for each component. 2) Experimental data needed. 3) Thermodynamic model used in this execution. 4) Button that adds manually a new component to the system. 5) Select parameters and check the objective function of a specific set of parameters, without optimizing. 6) Objective function to be minimized. 7) Diagnostics box, progress bar and 'abort' button (General Features). 8) Miscellaneous functions (General Features).

#### Input Data & Thermodynamic Model

In this field, the user must input the following data:

- Name and parameters of all components in the mixture, with the first one obligatorily being the water. As in the Binary Mixture tab, if these components

are available in the Component Data Bank, then just entering their names is enough to fill the remaining fields of this table. The 'Add Component...' button can be used to add as many components as the user needs.

- All available experimental temperatures, pressures, water content and dry gas compositions. As already stated, the variance of the water content is an optional variable;
- The binary parameters matrix and combination rule of each pair, accessed when pressing the 'Binary Parameters...' button. Figure 4.13 shows an example of this interface.

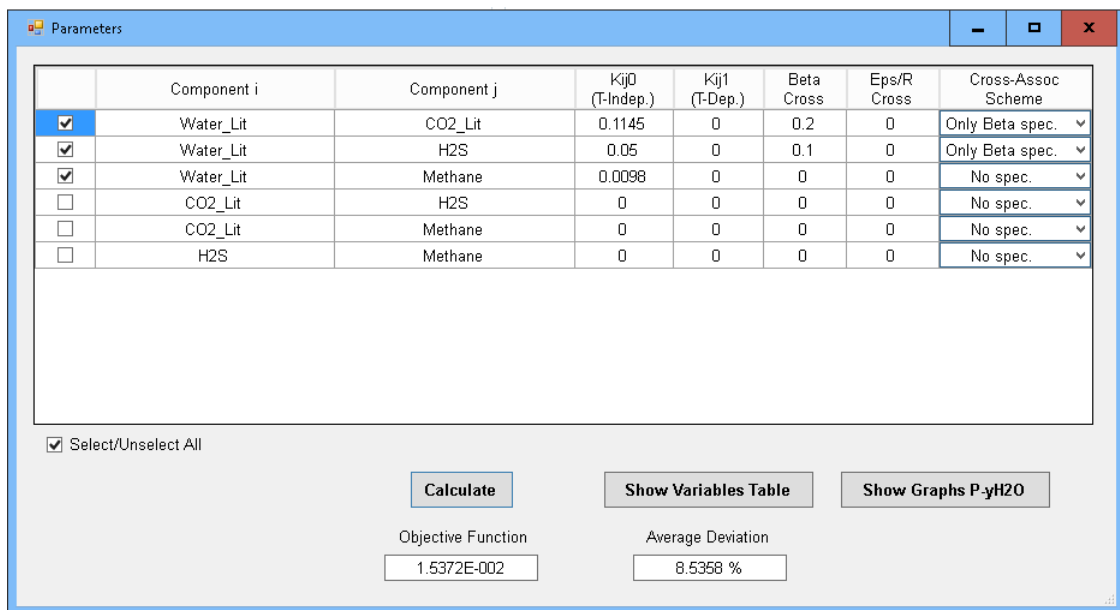


Figure 4.13: Interface formed when pressing the button 'Binary Parameters...' in the Multicomponent Mixture tab. It is important to notice that, although the parameters of all pairs are editable, only the ones containing water can be selected to manipulate in the optimization. Also, the user can check the objective function, the deviations and the graphs formed by the parameters to be input in this screen.

Finally, the thermodynamic model region in this tab has the sole purpose of showing the EoS to the user, depending on the model chosen. The combining rules are selected in the 'Binary Parameters...' screen, as stated previously. Besides, the details of the water content calculations are not shown in the interface due to its complexity, as described in Section 3.1.3.

## Objective Function

In this tab, the objective function has the most simple interface, consisting of only one dynamic image, related to the Equation (3.38).

Analogously to the previous tabs, the variances can be inserted manually in the input data or they can be equal to the respective experimental value of  $y_{H_2O}$ .

## 4.3 Output Features

These features are divided in three main groups: output results, plots and tables.

### 4.3.1 Output Results

These results consist of grids containing the main results of an estimation. Depending on the case, there are some possible combinations, as shown in Figures 4.14 to 4.18.

**Optimization Results - Pure Component Parameters: Water**

	a (bar.L <sup>2</sup> /mol <sup>2</sup> )	b (L/mol)	c1	eps/R [K]	1000*beta	Obj Function	AAP%	AAD%	# Iterations
Original Parameters (No Bank Data Available)	5.61125966936884	0.021136...	1.001936...	0	0	8.5753E-002	7.0422 %	27.2695 %	-
Calculated Parameters - PSO	1.3059308296679	0.014716...	0.949697...	1825.127...	88.65164...	9.3527E-005	0.2648 %	0.7869 %	119
Refined Parameters - SIMPLEX	1.28568572186595	0.014729...	1.036010...	1787.020...	95.63728...	9.1491E-005	0.2252 %	0.7863 %	306

Figure 4.14: Result's grid of a pure component estimation of water using CPA equation of state without penalization, showing parameters, objective function, average deviation of each variable and number of iterations of each method. The first line contains results for bank component parameters, if present. As there is no 'Water' component in the bank, it contains the original parameters instead, calculated by critical properties and acentric factor (no association). The second line contains PSO calculated parameters and the third line contains Simplex calculated parameters.

**Optimization Results - Pure Component Parameters: Water0. Penalization weights: w1 = 0.001; w2 = 0.001**

	a (bar.L <sup>2</sup> /mol <sup>2</sup> )	b (L/mol)	c1	Obj Function	AAP%	# Iterations	1st Penalization Term	2nd Penalization Term
Original Parameters (No Bank Data Available)	5.61125966936884	0.021136...	0.662	2.5318E-004	1.3409 %	-	9.3616E-021	1.2452E-009
Calculated Parameters - PSO	5.73642139462017	0.021757...	0.664246...	4.2152E-005	0.5263 %	170	1.3588E-003	1.7087E-002
Refined Parameters - SIMPLEX	5.66056720772115	0.021343...	0.658247...	4.5397E-005	0.5556 %	67	2.8871E-005	1.9822E-004

Figure 4.15: Result's grid of a pure component estimation of water using SRK equation of state + Kabadi-Danner  $\alpha$  function. In this case, there is no 'Water0' component in the bank, so the first line is also calculated using original parameters. The First and Second Penalization Term columns refer to Equation (3.32) before multiplying them to the weights.



**Optimization Results - Binary Parameter - CO<sub>2</sub>\_Lit + Water\_Lit**

	Kij0	beta (Cross)	eps/R (Cross)	Obj Function	AAP [%]	# Iterations
▶ Calculated Parameters - PSO	-0.201867311416005	0.05772866016452...	<b>1001.625</b>	8.8033E-002	24.1235 %	200
Refined Parameters - SIMPLEX	-0.178209989686273	0.06856474979194...	<b>1001.625</b>	5.4461E-002	19.3608 %	58

Figure 4.16: Result's grid of a binary parameter estimation of pair CO<sub>2</sub>-Water by pressure using CPA equation of state. In this case there are only the PSO and Simplex results' lines. It is important to notice that the column with values in bold means that this parameter was not estimated, but calculated by a combining rule.

**Optimization Results - Binary Parameter - Water\_Lit + n-Hexane**

	Kij0	Obj Function	AAxII [%]	AAxIH [%]	# Iterations
▶ Calculated Parameters - PSO	0.03927812233887...	2.5100E-001	19.5462 %	36.1081 %	31
Refined Parameters - SIMPLEX	0.03927800846072...	2.5100E-001	19.5462 %	36.1082 %	11

Figure 4.17: Result's grid of a binary parameter estimation of the pair n-Hexane-Water by liquid-liquid compositions metric using the CPA equation of state.

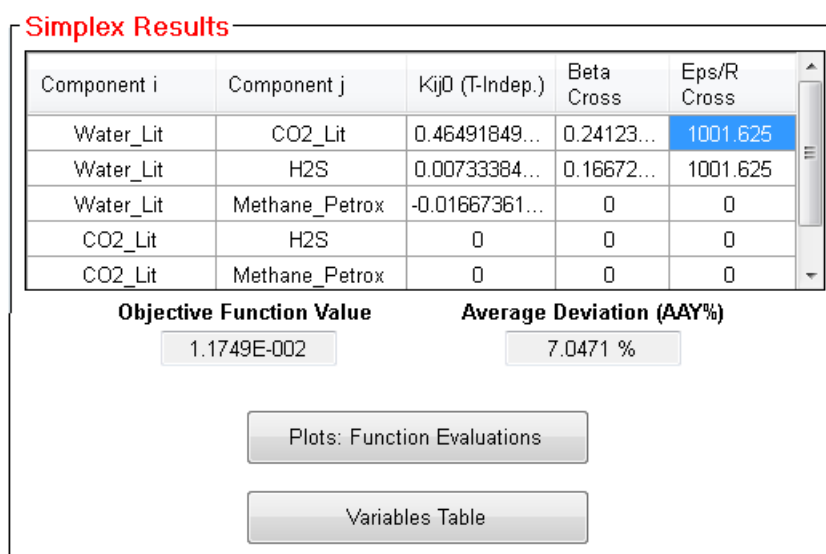


Figure 4.18: Result's grid of a binary parameter estimation of a gas composed by water, CO<sub>2</sub>, H<sub>2</sub>S and methane by the water content metric using the CPA equation of state. This consists of a Simplex optimization procedure from a predefined initial guess.

It is important to mention that the results presented in Figures 4.14 to 4.18 are merely explicative. The recommended procedure is detailed in Section 3.4. The binary parameters' initial guesses are the results of estimation using the respective binary mixtures, calculated by pressure, if their values are not available in the literature.

## 4.3.2 Plots and Reports

*ThermOpt* contains various graphic analyses to help the user visualize the results. Although many of the following examples have been taken from pure component cases, most of them can also be applied to mixtures.

### PSO Results

In Chapter 3 it was shown that all of the intermediary values of the objective function are saved in arrays  $x_{int}$  and  $S_{int}$ . These values allow *ThermOpt* to generate scatter plots of each manipulated parameter, such as in Figure 4.19. Thus, the user can check if there are multiple local minima and adjust the bounds to execute a more efficient optimization. Also, these plots are coloured by a heat map, varying from red (highest objective function values) to blue and then black (lowest objective function values).

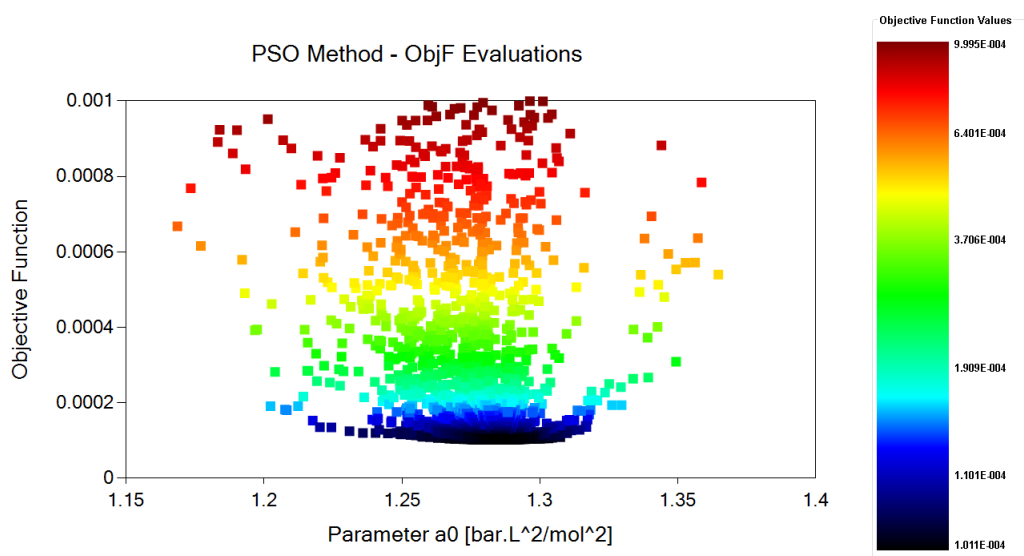


Figure 4.19: Example of scatter plot. Parameter  $a_0$  versus objective function evaluations calculated for water using CPA equation of state. All graphics can be zoomed freely to analyse local minima region. The maximum objective function value can be fixed, manipulating the heat color map to make the visualization easier.

Another possible PSO result plot is the parametric analysis, which is similar to the scatter plot. The difference lies on the fact that, in this case, both x-axis and y-axis are composed of manipulated parameters. Figure 4.20 shows an example from the same calculation as Figure 4.19.

The parametric analysis is useful to perform statistical studies. The maximum value of the objective function, to be used as a criterion to select the parameter sets calculated from the PSO, can be specified or calculated from statistical tests such as chi-square or t-student.

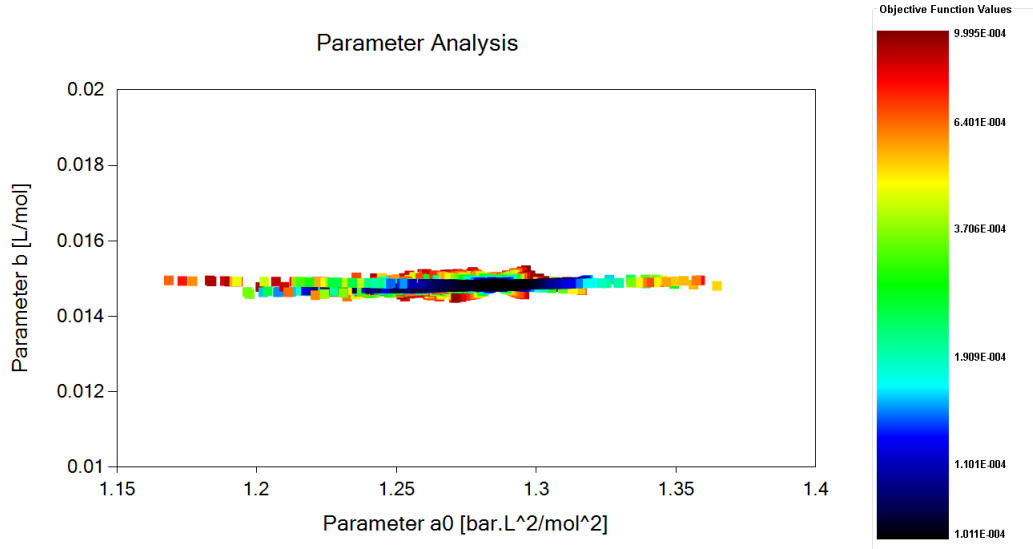


Figure 4.20: Example of parameter analysis. Parameter  $a_0$  versus  $b$ , calculated for water using CPA equation of state. This plot shows clearly that possible solutions for the parameter  $b$  lie on a narrow range, being in agreement with KONTOGEOGRIS *et al.* (2006a).

### Statistical Report

As mentioned earlier in this Section, statistical analyses can be performed from the values stored in  $x_{int}$  and  $S_{int}$ . From them it is possible to predict bounds for the estimable parameters inside which the optimized value would probably be. Thus, the following calculations were implemented for the Pure Component Tab regarding the statistical report:

- A confidence interval analysis, in which the chi-square test (SCHWAAB and PINTO, 2007) was implemented. The user inputs the desired confidence interval  $CI$ , and the program calculates the maximum value of the objective function  $S_{max}$ , as in Equation (4.1):

$$S_{max} = \frac{\chi^2(Prob)}{n_e} \quad (4.1)$$

Where  $\chi^2(Prob)$  is the value of the chi-square expression which results in a probability  $Prob = 0.5(1 + CI)$ , and  $n_e$  is the number of experimental points. This analysis can only be done when the objective function contains only one term (saturation pressure) and all variances are equal. The program searches in the PSO intermediate values with  $S \leq S_{max}$  and reports the parameters' limits and deviations.

- A maximum error analysis, when both terms of the objective functions are active. This analysis takes advantage of the fact that pure parameter

estimations in the literature usually consider correlated data such as DIPPr (DIADEM, 2004), all of which reporting maximum deviations for each expression. SANTOS *et al.* (2015c) discussed in their work an expression for the objective function when the user knows the maximum errors for each variable. Applying them to the Equation (3.30), Equation (4.2) is formed:

$$S_{max} = Err_{max,P}^2 + Err_{max,\rho}^2 \quad (4.2)$$

where  $Err_{max,P}$  and  $Err_{max,\rho}$  are the maximum deviations for saturation pressure and liquid density, respectively. Thus, it has been made possible to generate a similar report for this generalized case.

Figure 4.21 presents the layouts of both reports.

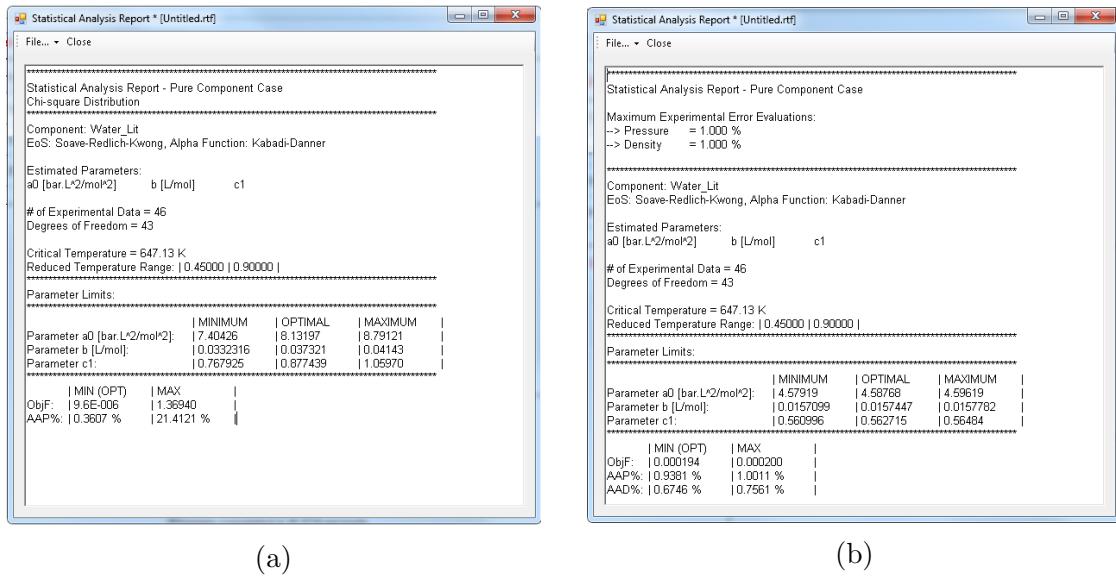


Figure 4.21: Examples of statistical reports generated by *ThermOpt* regarding a parameter estimation of water using the SRK EoS with the Kabadi-Danner  $\alpha$  function. (a) Chi-square test with confidence interval equal to 95%. (b) Maximum error analysis with  $Err_{max,P} = Err_{max,\rho} = 1.0\%$ .

## Simplex Results

Saving intermediary values of the objective function into  $x_{int}$  and  $S_{int}$  also made it possible to generate analogous graphics for the Simplex method (Figure 4.22).

Also, even though this is a result of a 'refining' of the PSO method, it is possible the final solution to be far from the initial guess, depending on the expansion factor of the Simplex selected by the user.

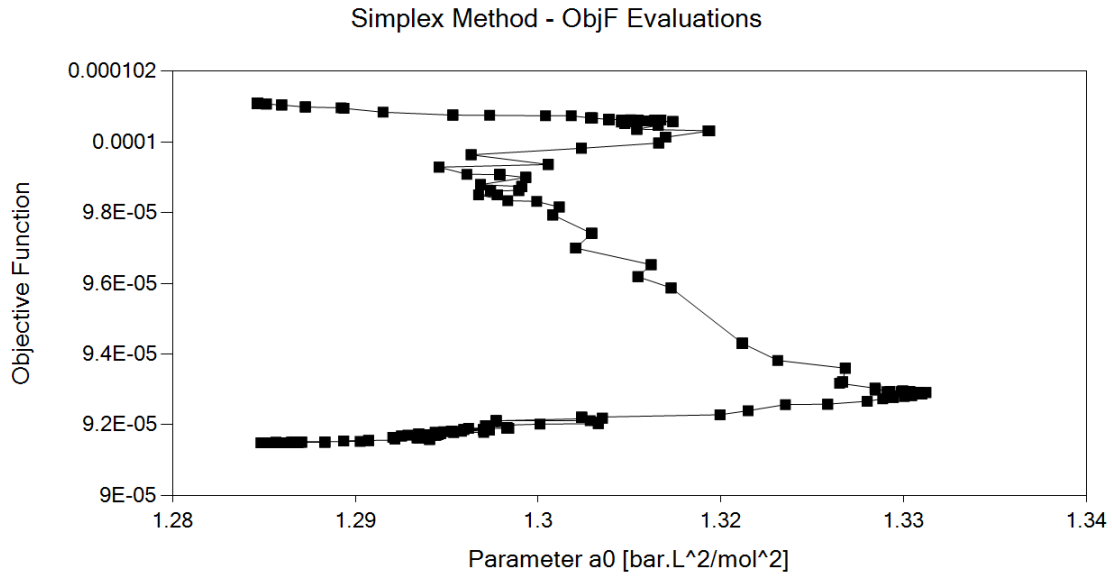


Figure 4.22: Parameter  $a_0$  values versus the objective function, calculated for water using CPA EoS, in a Simplex method executed just after the PSO from figures 4.19 and 4.20.

## General Results

Besides intermediary results, it is possible to view graphics regarding the final solution, such as phase equilibrium variable deviations [%], saturation curves and experimental versus calculated variables. Figures 4.23 to 4.27 show examples of each case.

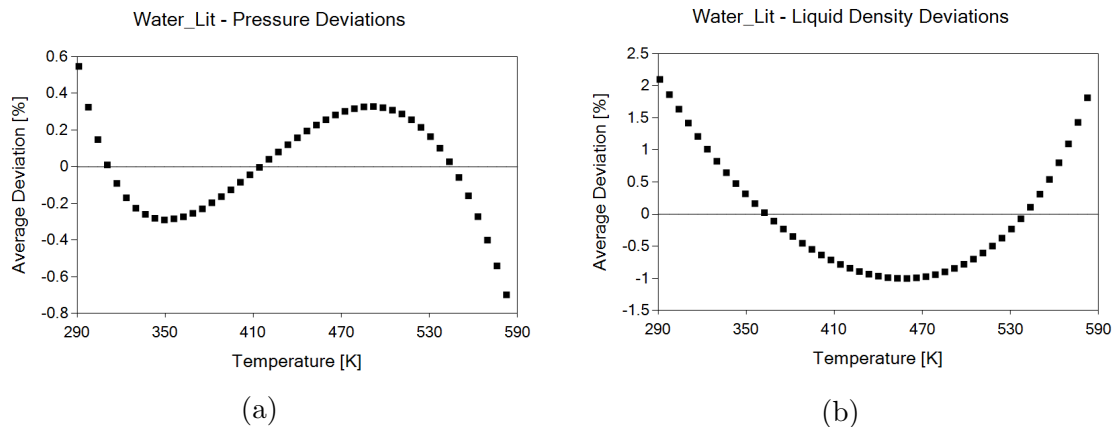


Figure 4.23: Pressure (a) and density (b) deviations [%] for water calculated by CPA equation of state. Experimental data from DIPPr (DIADDEM, 2004).

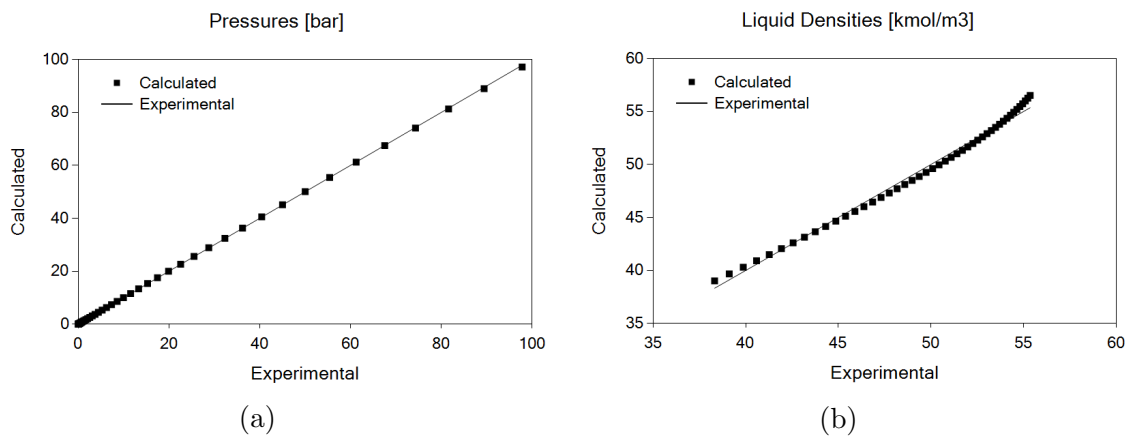


Figure 4.24: Experimental versus calculated values of pressure (a) and density (b) calculated for water using CPA equation of state. Experimental data from DIPPr (DIADDEM, 2004).

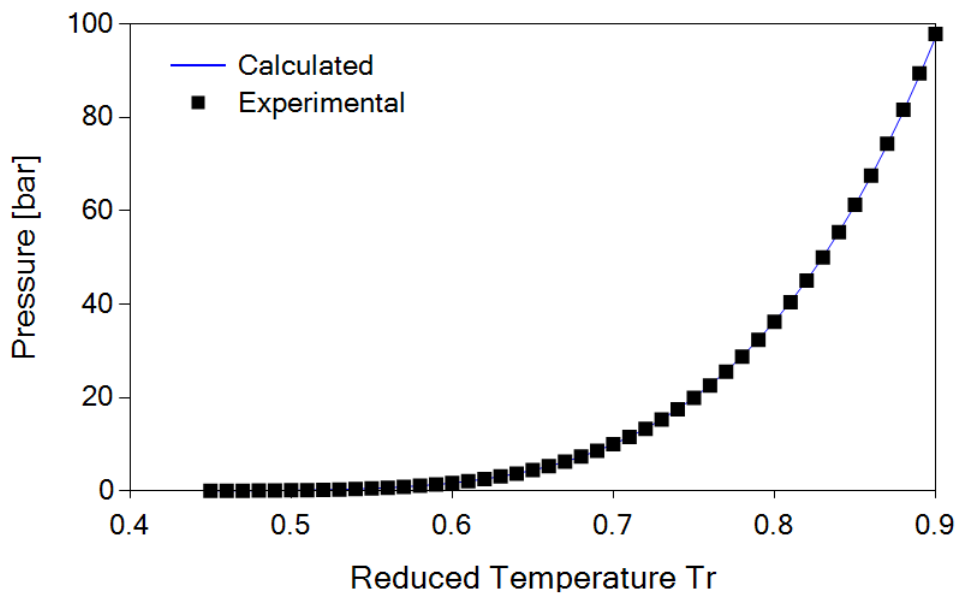


Figure 4.25: Saturation curve – reduced temperature versus pressure – calculated for water using CPA equation of state. Experimental data from DIPPr (DIADDEM, 2004).

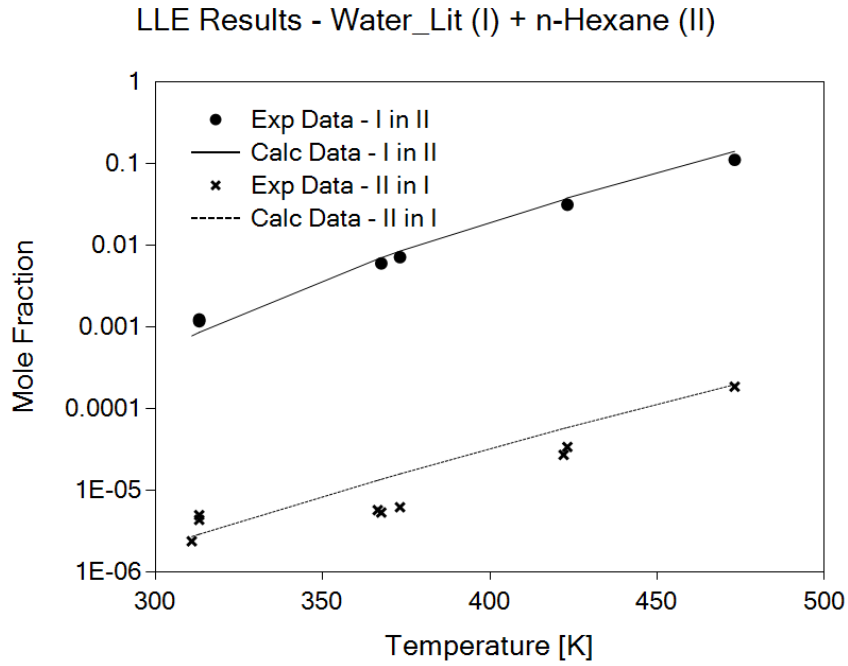


Figure 4.26: Chart reporting liquid-liquid equilibria compositions versus temperature of the binary mixture n-Hexane-Water, calculated by CPA equation of state with  $k_{ij} = 0$  and water parameters from KONTOGEORGIS *et al.* (1999), comparing to experimental data (TSONOPOULOS and WILSON, 1983).

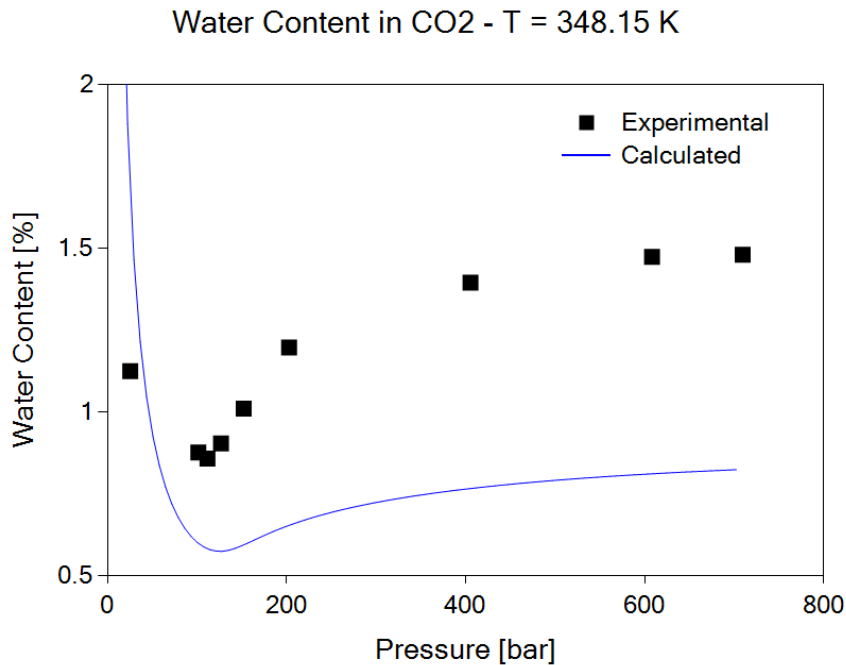


Figure 4.27: Chart reporting dew pressures versus water content of the mixture CO<sub>2</sub>-Water, calculated by CPA equation of state using  $k_{ij} = 0$  and  $\beta^{A_i B_j} = \beta_{water} = 0.0692$ , with water parameters from KONTOGEORGIS *et al.* (1999) and  $T = 348.15K$ . Experimental data are from VALTZ *et al.* (2004).

### 4.3.3 Tables

For each case described in Section 4.3.2 there is a table with all values used or calculated. They can be promptly copied to an Excel sheet, for example. Figure 4.28 to 4.30 show the tables corresponding to aforementioned cases for the pure component.

PSO Method - Variables Table (16100 Total Function Evaluations)						
	Parameter a0 [bar.L <sup>2</sup> /mol <sup>2</sup> ]	Parameter b [L/mol]	Parameter c1	Parameter eps/R [K]	Parameter 1000*beta	Objective Function
▶	1.1956	0.0121663	1.12274	2056.16	132.535	0.742463
	1.53274	0.0134864	0.882059	1624.58	69.2057	0.944251
	1.85947	0.0119472	1.44558	1709.38	90.5529	0.740895
	1.53522	0.0132887	0.65965	1518.38	85.9688	3.34756
	1.36695	0.0103947	0.860243	2192.61	110.484	1.11894
	1.73299	0.0124419	0.735639	1573.82	125.796	0.183115
	1.53103	0.0198223	1.02845	1910.32	79.3601	0.115508
	1.7861	0.0127916	1.1397	1939.76	112.162	0.820022
	1.56043	0.0120385	1.24624	2005.39	88.6797	0.772712
	1.29103	0.0109323	0.585827	1760.41	132.866	0.311079
	1.25347	0.0144386	1.23448	1842.22	111.831	0.199878
	1.53421	0.0100716	1.40564	1882.79	55.6464	0.844443
	1.00667	0.0107029	0.965483	1801.91	97.36	0.1753
	1.1664	0.0101808	1.30883	1978.09	149.91	1.07355
	1.69288	0.0119333	0.879286	2111.1	86.8149	0.865726
	1.42022	0.01914	0.681973	2060.13	64.34	0.0906915

Figure 4.28: Variables table for the PSO results case mentioned on Section 4.3.2. Number of 'Total Function Evaluations' stands for the number of converged objective function evaluations.

Simplex Method - Variables Table (733 Total Function Evaluations)						
	Parameter a0 [bar.L <sup>2</sup> /mol <sup>2</sup> ]	Parameter b [L/mol]	Parameter c1	Parameter eps/R [K]	Parameter 1000*beta	Objective Function
	1.28614	0.0148196	1.22441	1678.75	114.707	0.000101075
	1.28614	0.0148196	1.22441	1678.75	114.707	0.000101075
	1.28715	0.0148196	1.22382	1678.44	114.682	0.000101049
	1.28715	0.0148196	1.22382	1678.44	114.682	0.000101049
	1.28715	0.0148196	1.22382	1678.44	114.682	0.000101049
	1.2887	0.0148216	1.22284	1678.09	114.66	0.000100992
	1.2887	0.0148216	1.22284	1678.09	114.66	0.000100992
	1.2887	0.0148216	1.22284	1678.09	114.66	0.000100992
	1.29104	0.0148239	1.22169	1677.6	114.547	0.000100969
	1.29125	0.0148214	1.22122	1677.41	114.585	0.000100954
	1.29381	0.0148263	1.21992	1677.02	114.474	0.000100845
	1.29839	0.0148319	1.21701	1675.8	114.416	0.000100764
	1.29839	0.0148319	1.21701	1675.8	114.416	0.000100764
	1.29839	0.0148319	1.21701	1675.8	114.416	0.000100764
	1.30081	0.0148309	1.21539	1675.2	114.358	0.000100757
	1.30448	0.0148371	1.21352	1674.51	114.229	0.000100744
	1.30617	0.0148366	1.21225	1673.89	114.243	0.000100743

Figure 4.29: Variables table for the Simplex results case mentioned on Section 4.3.2. Again, number of 'Total Function Evaluations' stands for the number of converged objective function evaluations.



Variables Table					
	Temperature [K]	Experimental Pressures [bar]	Calculated Pressures [bar]	Experimental Liquid Densities [kmol/m <sup>3</sup> ]	Calculated Liquid Densities [kmol/m <sup>3</sup> ]
▶	291.209	0.0207214	0.0208278	55.3499	56.5075
	297.68	0.0308256	0.0309177	55.2237	56.248
	304.151	0.0449824	0.0450404	55.0892	55.9862
	310.622	0.0644724	0.0644702	54.9463	55.7218
	317.094	0.0908701	0.09078	54.7948	55.4547
	323.565	0.126083	0.125864	54.6346	55.1848
	330.036	0.172392	0.172001	54.4655	54.9117
	336.508	0.232487	0.231891	54.2876	54.6354
	342.979	0.309512	0.308657	54.1006	54.3557
	349.45	0.407089	0.405938	53.9043	54.0724
	355.922	0.529361	0.527906	53.6987	53.7851
	362.393	0.681016	0.679229	53.4836	53.494
	368.864	0.867316	0.86521	53.2587	53.1985
	375.335	1.09411	1.09174	53.0241	52.8987
	381.807	1.36788	1.36536	52.7794	52.5942
	388.278	1.69571	1.69316	52.5244	52.2848
	394.749	2.08534	2.08297	52.2591	51.9704
	401.221	2.54514	2.54331	51.9831	51.6506
	407.692	3.08415	3.08316	51.6963	51.3253

Figure 4.30: Variables table for general results (phase equilibrium variables) case described in the Section 4.3.2.

## 4.4 General Features

### 4.4.1 Diagnostics Region

It consists of the following components:

- A rich text-box containing messages about the calculation progress, or intermediate values of the objective function if selected on 'Options' window;
- Progress bars exhibiting in which iteration the program is compared to total;
- An 'Abort Calculations' button for emergencies. It is possible to click on this button to stop the execution and input the right data if a mistake is identified.

This region is visible in all tabs, either pure or mixtures, input or output.

### 4.4.2 Miscellaneous Region

This menu consists of general commands. It appears in all tabs of the program. They are:

#### Load/Save

With commands, one can load or save the input data from or to a .txt file. In the current version, these files have specific formats, with words separated by tabulation ('Tab' button of keyboard), as can be seen below. Also, Figures 4.31 to 4.34 show examples of the input files for each case.

- For a pure component (the created file will be saved in 'Pure' folder):

Name [Component name]

*unitT* [Temperature units – C, F, K or R. Default: K]

*unitP* [Pressure units – kPa, Pa, atm or bar. Default: bar]

*Tc* [Critical temperature value in *unitT*]

*Pc* [Critical pressure value in *unitP*]

*w* [Acentric factor value]

Texp Pexp Rhoexp

[Experimental temperatures] [Experimental pressures] [Experimental densities  
(currently fixed in kmol/m<sup>3</sup>)]

```
% Experimental data for component water|
% Ref: DIPPr (DIADEM, 2004)
% Tr(min) = 0.45; Tr(max) = 0.90
% ErrMax(Psat) = 0.2%; ErrMax(rhosat) = 1%
Name      Water_Lit
unitT     K
unitP     kPa
Tc        647.13
Pc        22055
w         0.3449
Texp      Pexp      Rhoexp
291.209  2.072135985  55.34992
297.680  3.082561897  55.22374
304.151  4.498241975  55.08923
310.622  6.447242083  54.94627
317.094  9.087006008  54.79475
323.565  12.60829771  54.63455
330.036  17.23915043  54.46554
336.508  23.24874717  54.28759
342.979  30.95116042  54.10056
349.450  40.70888435  53.90432
355.922  52.9361015   53.69870
362.393  68.10163545  53.48357
368.864  86.73155261  53.25874
375.335  109.411388   53.02407
381.807  136.7879817  52.77935
388.278  169.5709252  52.52442
394.749  208.5336258  52.25906
401.221  254.5140101  51.98308
407.692  308.4148925  51.69625
```

Figure 4.31: Example of input .txt file of a pure component. Note that experimental values can be copied directly from an Excel sheet, and any text written after the character '%' will not be read, being used to comment the data.

- For binary pairs with VLE calculations (the created file will be saved in 'Binary' folder):

Component1 [name of component 1 – if it is water then it must end with '\*']

Component2 [name of component 2 – if it is water then it must end with '\*']  
 unitT [Temperature units – C, F, K or R. Default: K]  
 unitP [Pressure units – kPa, Pa, atm or bar. Default: bar]  
 VLE  
 Texp Pexp x1 y1  
 [experimental temperatures] [experimental pressures] [experimental liquid  
 composition of component 1] [experimental vapour composition of component  
 1]

```

%
% VLE between CO2 and water. Ref:
%
% Valtz, A.; Chapoy, A.; Coquelet, C.; Paricaud, P.; Richon, D.
% Vapour-liquid Equilibria in the Carbon Dioxide-Water System,
% Measurement and Modelling from 278.2 to 318.2 K.
% Fluid Phase Equilibria, v. 226, 2004, pp. 333-344.
%
Component1      CO2_Lit
Component2      Water_Lit
unitT          K
unitP          bar
VLE
Texp  Pexp   x1    y1
278.22  5.010  0.00585  0.9985
278.22  7.550  0.00852  0.9989
278.22  10.16  0.01111  0.9993
288.26  4.960  0.00401  0.9969
288.26  11.03  0.00867  0.9986
288.26  19.41  0.01434  0.9991
298.28  5.040  0.00314  0.9935
298.28  10.07  0.00614  0.9962
298.28  14.96  0.00887  0.9972
298.28  24.83  0.01356  0.9986
298.28  34.91  0.01772  0.9987
308.2   5.790  0.00276  0.9904
308.2   18.89  0.00856  0.9966
  
```

Figure 4.32: Input .txt file to a binary pair CO<sub>2</sub> - water with VLE data. Note that any text written after the character '%' will not be read, being used to comment the data.

- For binary pairs with LLE calculations (the created file will be saved in 'Binary' folder):

Component1 [name of component 1 – if it is water then it must end with '\*']  
 Component2 [name of component 2 – if it is water then it must end with '\*']  
 unitT [Temperature units – C, F, K or R. Default: K]  
 unitP [Pressure units – kPa, Pa, atm or bar. Default: bar]

LLE

Temp Pexp xI-II xII-I

[experimental temperatures] [experimental pressures] [experimental composition of component 1 in phase rich in component 2] [experimental composition of component 2 in phase rich in component 1]

There is no need to insert each pure component's parameters because *ThermOpt* will look for it inside the Component Data Bank, if available.

```
%
%
% LLE between water and n-hexane. Ref:
% Tsonopoulos, C.; Wilson, G. M.
% High-Temperature Mutual Solubilities of Hydrocarbons and Water.
% Part 1: Benzene, Cyclohexane and n-Hexane.
% AIChE Journal, v. 29(6), pp. 990-999, 1983.
%
%
Component1      Water_Lit
Component2      n-Hexane
unitT           K
unitP           bar
LLE
Temp  Pexp    xI-II      xII-I
310.93      0.000000    0.000000    2.380E-06
313.15      0.4537    1.23E-03    4.350E-06
313.15      1.17E-03    4.975E-06
366.48      0.000000    5.730E-06
367.55      5.95E-03    5.350E-06
373.15      3.4820    7.09E-03    6.210E-06
422.04      0.000000    2.710E-05
423.15      12.548    3.11E-02    3.390E-05
473.15      35.160    1.10E-01    1.850E-04
```

Figure 4.33: Input .txt file to a binary pair water - n-hexane with LLE data. Also, as pressure is not an obligatory variable, it is acceptable to have gaps in this field.

- For multicomponent mixtures (the program created file will also be saved in 'Multicomponent' folder):

Components [Name of water component – it must end with '\*'] [Name of dry gas component 1] [Name of dry gas component 2] [...]

unitT [Temperature units – C, F, K or R. Default: K]

unitP [Pressure units – kPa, Pa, atm or bar. Default: bar]

Temp Pexp yH2O% mol-frac-drygas

[Experimental temperatures] [Experimental pressures] [% of water in gas]

[Composition of dry gas in the same order as above]

Components	Water $\theta^*$	CO2	H2S	Methane
unitT	K			
unitP	bar			
Texp	Pexp	yH2O%	mol_frac_drygas	
310.93	137.90	0.0855	0.1100	0.0000
344.26	68.95	0.6023	0.1100	0.0000
310.93	137.90	0.0855	0.2000	0.0000
344.26	68.95	0.5939	0.2000	0.0000
327.59	103.42	0.2338	0.0000	0.0800
344.26	94.25	0.5202	0.0000	0.2750
344.26	68.95	0.6150	0.0000	0.1700
310.93	75.84	0.1706	0.6000	0.1000
310.95	48.20	0.1910	0.5955	0.1000
310.95	76.00	0.1710	0.5980	0.0984
380.35	83.60	2.2500	0.6044	0.0987
380.35	129.30	1.9600	0.6033	0.0981
380.35	171.70	1.7900	0.6024	0.0988
310.95	62.60	0.2140	0.1742	0.5038
338.75	84.30	0.8660	0.1497	0.6615
380.35	75.60	2.5300	0.1137	0.7654
449.85	110.00	9.3800	0.1189	0.7606
449.85	118.00	9.5000	0.6151	0.0936
449.85	173.10	8.4800	0.6031	0.0951

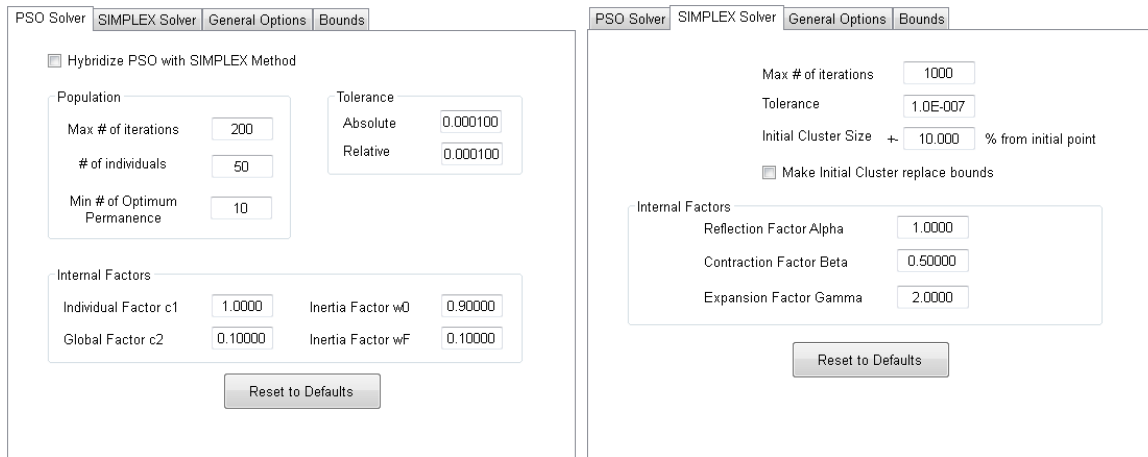
Figure 4.34: Input .txt file for a multicomponent mixture of water, CO<sub>2</sub>, H<sub>2</sub>S and methane.

As a suggestion for future works, new and more efficient ways of saving input data can be implemented.

## Options

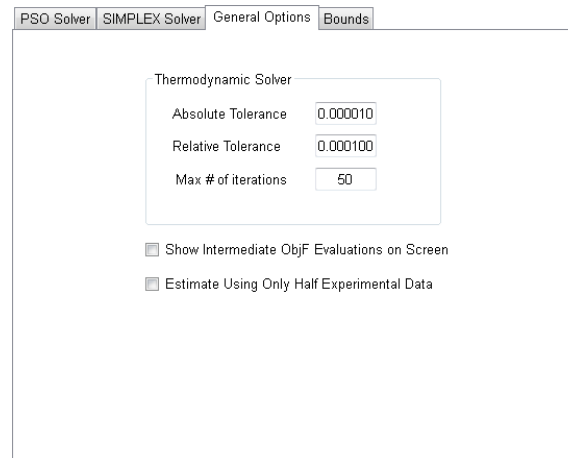
This button contains general options of the optimization solver and bounds to all estimable parameters. Figures 4.35 shows the current visualization of the optimization methods' internal parameters, as explained in Chapter 3.

However, the Simplex method needed a new option, which is the size of the initial cluster formed, in order to minimize the chances of non converging the thermodynamic calculations, as well as to set a degree of refining related to the initial guess (which was the solution of a PSO method). In order to find a solution obligatorily next to the initial point, the option 'Do not go past Initial Cluster' was implemented, substituting the previous bounds of all variables when checked. On the other hand, when unchecked, the initial cluster formed cannot violate these bounds.



(a)

(b)



(c)

Figure 4.35: Solvers in the 'Options' interface of *ThermOpt*. (a) PSO method solver options. (b) Simplex method solver options. (c) General options, such as thermodynamic tolerances.

As for the option 'Show Intermediate ObjF Evaluations on Screen', it is useful to check in real time the progress of the optimization, and 'Estimate Using Only Half Experimental Data' can be used in cases where there is a vast quantity of experimental data. In these cases, it is interesting to calculate half of the experimental points, alternating which will be calculated or ignored, and in the end calculate the deviations with all of the points to check whether or not the EoS is predicting them correctly.

In addition to that, Figure 4.36 shows the visualization of all the estimable parameter bounds of the program. In the current version, for multicomponent mixtures, all estimating binary pairs have the same bounds, defined in this tab.

PSO Solver			SIMPLEX Solver			General Options			Bounds		
						Lower Bounds			Upper Bounds		
▶ Parameter a0 [bar.L <sup>2</sup> /mol <sup>2</sup> ]						-			-		
Parameter b [L/mol]						-			-		
Parameter c1						-			-		
Parameter eps/R [K]						100.00			3000.00		
Parameter 1000*beta						1.0000			1000.00		
Binary Constant Parameter Kij0						-1.0000			1.0000		
Binary T-dependent Parameter Kij1						-			-		
Binary CPA Parameter beta_Cross						0.001000			1.0000		
Binary CPA Parameter eps/R_Cross						100.00			3000.00		
<b>Pure Component Critical Region Penalization</b>											
Weight w1						Weight w2					
<input type="text" value="0.010000"/>						<input type="text" value="0.001000"/>					

Figure 4.36: Estimable parameter bounds inside the *ThermOpt* options.

## Run...

This button contains all the main execution commands:

- Pure component estimation.
- Binary parameter estimation by pressure or liquid composition.
- Binary parameter estimation by water content (multicomponent mixture).
- Pure component + Binary parameter estimation by VLE + LLE methodology.
- Pure component penalization analysis.
- Pure component PSO histogram generator.

The former three commands are just direct estimation calculations, but the latter three commands are special analyses implemented to improve the results of the pure component parameter estimation procedure.

The combined pure component + binary parameter estimation by VLE + LLE methodology executes the calculation according to the Section 3.3.3. There is no dedicated interface to this procedure yet, so after the calculations *ThermOpt* automatically opens a table with all the results.

Penalization analysis is a set of 'Pure component estimation' executions with penalization turned on, varying the weights in a mesh. See Chapter 5 for results of this analysis.

PSO histogram generator is a feature where, for a specified input data, a number of independent PSO executions are performed in order to check if the solutions are tending to the same region. It is an efficient way to check if its internal parameters ( $c_1$ ,  $c_2$ ,  $w_0$ ,  $w_f$ ) are well calibrated and if the method is stable. Figure 4.37 shows an example of histogram.

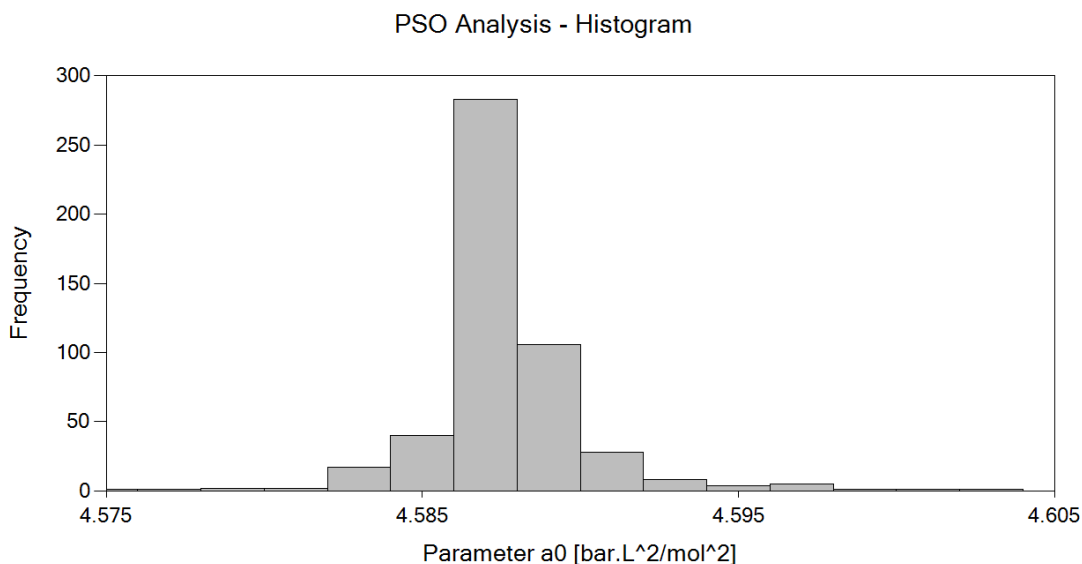


Figure 4.37: Example of histogram generated, analysing the parameter  $a_0$  of water calculated by SRK equation of state and Kabadi-Danner  $\alpha$  function. The optimal solution in this case lies on  $a_0 \approx 4.587$  bar.L<sup>2</sup>/mol<sup>2</sup>.

## Component Data Bank

The last feature of *ThermOpt* to be described in this work is a window containing all estimated parameters for pure components by the user. When saving pure component data, there is a sub-button called 'Output' inside the menu (see Figure 4.38).

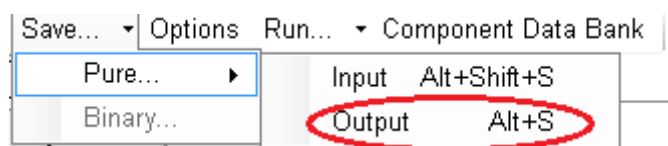


Figure 4.38: Option to save results into the data bank.

This command saves estimated parameters and the equation of state used in a .txt file in the folder named 'Bank', with the following format:

```
[Name of the component – if it is water then it must end with '*']
[Critical temperature in K]
[Critical pressure in bar]
```



[Acentric factor]

[Parameter  $a_0$  in  $bar.L^2/mol^2$ ]

[Parameter  $b$  in  $L/mol$ ]

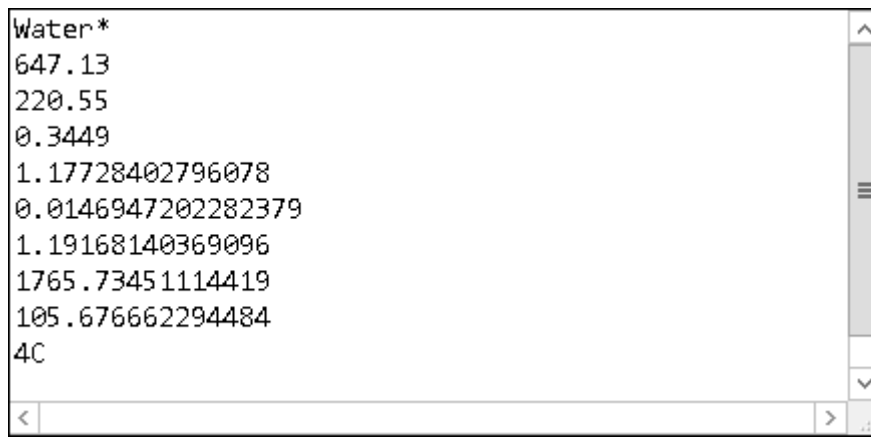
[Parameter  $c_1$ ]

[Parameter  $\varepsilon/R$  in K if CPA, or parameter  $c_2$  if cubic]

[Parameter  $1000\beta$  if CPA, or parameter  $c_3$  if cubic]

[CPA association scheme, if needed]

The name of the file will be '[Name of the component - does not need to be the same as the file]\_[Equation of State used].txt'. An example is shown in Figure 4.39, by the file named 'Water\_CPA.txt'.



```
Water*
647.13
220.55
0.3449
1.17728402796078
0.0146947202282379
1.19168140369096
1765.73451114419
105.676662294484
4C
```

Figure 4.39: .txt file to the data bank, named 'Water\_CPA.txt'.

# Chapter 5

## Results and Discussion

In this Chapter, the results obtained in this work will be discussed: a PSO performance analysis; penalization analysis related to the critical point behaviour of water using the SRK EoS; pure parameter estimation of polar components from saturation pressure and liquid density, with subsequent validation using liquid-liquid equilibria data to select a parameter set for water; a binary parameter estimation using the metrics described in Chapter 3; and finally the application to a dehydration unit using MEG, comparing the optimized results with commercial simulators.

### 5.1 PSO Performance Analysis

Before applying the *ThermOpt* to real systems, it is necessary to perform a series of procedures to evaluate it. The first study conducted in this work was the evaluation of the thermodynamic calculations' speed. After each execution, the diagnostics text-box displays the time elapsed, as shown in Figure 5.1.

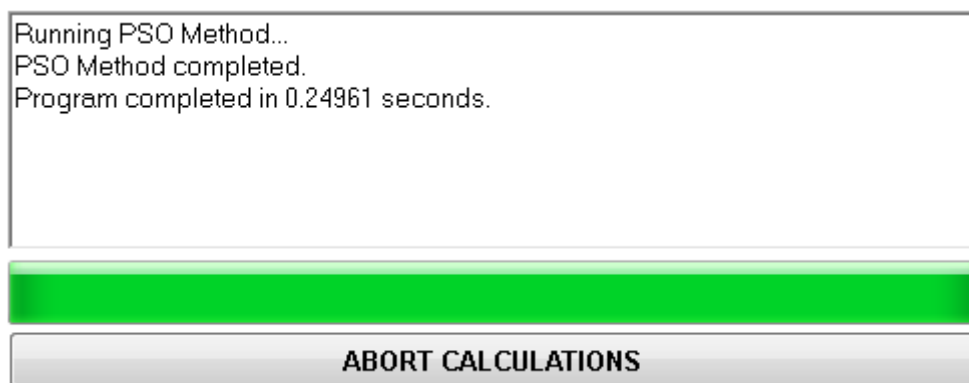


Figure 5.1: Diagnostics text-box showing a result for a parameter estimation procedure by the PSO method.

In order to perform such study, a PSO method was executed with specific options to certify that it would use up a certain amount of iterations, so that tolerance values

and internal factors can be ignored in all of the executions. As a consequence, the program performs a fixed number of thermodynamic calculations, allowing this analysis to be carried out. An example of these options in the interface is presented by Figure 5.2.

PSO Solver | SIMPLEX Solver | General Options | Bounds

Hybridize PSO with SIMPLEX Method

**Population**

Max # of iterations: 100

# of individuals: 1

Min # of Optimum Permanence: 100

**Tolerance**

Absolute: 0.000100

Relative: 0.000100

**Internal Factors**

Individual Factor c1: 1.0000

Global Factor c2: 0.10000

Inertia Factor w0: 0.90000

Inertia Factor wF: 0.10000

Figure 5.2: PSO options used for performance analysis for a case with 100 max iterations and 1 particle per iteration. The minimum number of iteration in optimum permanence must be the same as the maximum number of iterations in order to make the solver ignore the tolerances.

The pure component used to perform this analysis was water, whose experimental data was taken from DIPPr correlated data (DIADDEM, 2004), using 100 points from its triple point to the critical point. The objective function used was the one defined by the Equation (3.30), with the pressure term only and without the penalization effect ( $F_W = 0$ ), using the CPA EoS.

In this Section, as the optimized parameters' values are not relevant, the focus was on the time elapsed. For each case in Table 5.1, the execution time presented was calculated using the mean of three successive executions. Also, the computer used in this test has the following features:

- Processor: Intel Core i7 2.90 GHz
- RAM Memory: 8 Gb
- Operational System: Windows 7 64 bits

It is important to notice that the calculations using the CPA EoS include a internally implemented stability analysis in order to check if the desired phase is found, contributing to the time consumed.

Table 5.1: PSO performance analysis results. Each objective function (ObjF) evaluation contains 100 saturation pressure (PSAT) calculations due to the number of experimental data inserted.

#Iterations	#Particles / Iteration	#ObjF Evaluations	#PSAT Evaluations	Time [s]
10	1	10	$1.0 \times 10^3$	0.26
10	10	100	$1.0 \times 10^4$	2.17
50	10	500	$5.0 \times 10^4$	8.72
100	10	1000	$1.0 \times 10^5$	16.88
50	50	2500	$2.5 \times 10^5$	44.19
100	50	5000	$5.0 \times 10^5$	83.46
100	100	1.0e4	$1.0 \times 10^6$	169.27
200	100	2.0e4	$2.0 \times 10^6$	315.76
500	100	5.0e4	$5.0 \times 10^6$	742.72

Thus, the results from the Table 5.1 show that *ThermOpt* can do about 5000 thermodynamic calculations per second in the tested computer (#PSAT Evaluations / Time), which is a potential to do long studies such as the calculations described in the following sections.

## 5.2 Pure Parameter Estimation

In this Section results for pure parameter estimation will be presented for: water (with and without penalization effect), ethylene glycol (MEG), diethylene glycol (DEG), triethylene glycol (TEG) and 1,2-propylene glycol (PG).

### 5.2.1 Penalization Analysis for Water (SRK EoS + Kabadi-Danner $\alpha$ Function)

As explained in Chapter 3, it was decided to insert an optional penalization term to the objective function described in Section 3.3.1. The goal of this implementation was to check the tendencies of the parameter sets obtained and to select the one that resulted in the lowest deviations from the low temperature desired up to the critical point.

In this work, the penalization analysis was performed as a series of executions of the parameter estimation procedure according to Equations (3.30) and (3.32) varying the weights  $w_1$  and  $w_2$ , forming a mesh. Each solution is then stored into an array in order to show their plots after these executions.

To illustrate this study, this analysis was conducted for water. The main purpose was to investigate the behaviour of this component using the SRK equation of state,

along with the Kabadi-Danner  $\alpha$  function to improve the results. Also, only the pressure term was applied in the objective function, besides the penalty term itself, as can be seen in Figure 5.3. Moreover, Figures 5.4 to 5.6 show the solver options and Table 5.2 the variables' bounds applied. Table 5.3 summarizes the experimental data used and Table 5.4 the weights' values.

**Input Data**

Component Name: Water  Is Water

Critical Temperature [K]: 647.13    Critical Pressure [bar]: 220.55    Acentric Factor  $w$ : 0.3449

#	Temperature [K]	Pressure [bar]
1	273.15	0.006105...
2	279.631	0.009660...
3	286.103	0.01492849
4	292.574	0.022570...
5	299.045	0.033436...
6	305.517	0.048602...
7	311.988	0.069408...

**Thermodynamic Model**

Equation of State: Soave-Redlich-Kwong    Alpha Function: Kabadi-Danner

$$P = \frac{RT}{V-b} - \frac{a_0 \alpha(c_1, T)}{V(V+b)}$$

Fix a0 / b Parameters

If Water:  $\alpha(c_1, T_r) = [1 + c_1(1 - T_r^{0.8})]^2$   
Else:  $\alpha(c_1, T_r) = [1 + c_1(1 - T_r^{0.5})]^2$

**Objective Function**

Pressure: 
$$\frac{1}{N_{exp}} \sum_{i=1}^{N_{exp}} \frac{(p_{calc} - p_i^{exp})^2}{(p_i^{exp})^2}$$

Density (press to activate)

Critical Region Penalization:

$$+ w_1 \left[ \frac{V_c}{P_c} \left( \frac{\partial P}{\partial V} \right)_{T_c} \right]^2 + w_2 \left[ \frac{V_c^2}{P_c} \left( \frac{\partial^2 P}{\partial V^2} \right)_{T_c} \right]^2$$

Variations:  Experimental Point     Fixed

**Parameters to be Estimated**

$\alpha_0$      $b$      $c_1$     Calculate Objective Function...

ABORT CALCULATIONS

Figure 5.3: Input interface in the case studied in the Section 5.2.1.

**Thermodynamic Solver**

Absolute Tolerance: 0.000010

Relative Tolerance: 0.000100

Max # of iterations: 50

Figure 5.4: Thermodynamic options for the case studied in the Section 5.2.1.

PSO Solver
  SIMPLEX Solver
  General Options
  Bounds

---

Hybridize PSO with SIMPLEX Method

Population

Max # of iterations

# of individuals

Min # of Optimum Permanence

Tolerance

Absolute

Relative

Internal Factors

Individual Factor c1       Inertia Factor w0

Global Factor c2       Inertia Factor wF

Figure 5.5: PSO options for the case studied in the Section 5.2.1.

PSO Solver
  SIMPLEX Solver
  General Options
  Bounds

---

Max # of iterations

Tolerance

Initial Cluster Size +  % from initial point

Make Initial Cluster replace bounds

Internal Factors

Reflection Factor Alpha

Contraction Factor Beta

Expansion Factor Gamma

Figure 5.6: Simplex options for the case studied in the Section 5.2.1.

Table 5.2: Parameter bounds for the case studied in the Section 5.2.1. These values were obtained by trial and error in order to select bounds that contain all of the possible solutions achieved in this Section.

Parameter	Lower Bounds	Upper Bounds
$a_0$ [bar.L <sup>2</sup> /mol <sup>2</sup> ]	4.0000	8.0000
$b$ [L/mol]	0.01500	0.03500
$c_1$	0.5000	1.0000

Table 5.3: Input summary for the case studied in the Section 5.2.1.

Data Type	Saturation Pressure
Penalization	Yes
Source	DIPPr Correlation (DIADEM, 2004)
Variance	Experimental Points
$T_R$ Range	0.42 - 1.00
$\Delta T_R$	0.01

Table 5.4: Minimum and maximum weights' values used in the Section 5.2.1, as well as their variation between each execution ( $\Delta w$ ).

Weight	Minimum Value	Maximum Value	$\Delta w$
$w_1$	0.000	1.000e-3	2.500e-5
$w_2$	0.000	1.000e-3	2.500e-5

For each value of  $w_2$ ,  $w_1$  was varied by a fraction of its range as follows:  $[w_1, w_2] = [0, 0]$ ,  $[w_1, w_2] = [2.5e-5, 0]$ ,  $[w_1, w_2] = [5.0e-5, 0]$ , ...,  $[w_1, w_2] = [1.0e-3, 1.0e-3]$ , generating a total of 1681 executions.

Table 5.5 shows some of the results obtained with these values.  $AAP$  is the average absolute deviation of the pressures, defined by Equation (5.1):

$$AAP = \frac{100\%}{n_e} \sum_{i=1}^{n_e} \frac{|P_i^e - P_i^*|}{P_i^e} \quad (5.1)$$

where  $P$  is the saturation pressure,  $n_e$  the number of experimental points, the superscript  $e$  means experimental data and  $*$  means calculated value.

Table 5.5: Penalization analysis' results obtained from different values of weights. SRK-KD original parameters: calculated from critical properties and  $c_1$  proposed by KABADI and DANNER (1985).

$w_1$	$w_2$	$a_0$ [bar.L <sup>2</sup> /mol <sup>2</sup> ]	$b$ [L/mol]	$c_1$	$S$	$AAP$ [%]
0.0	0.0	7.4815	0.0327	0.8186	9.135e-6	0.2281
1.0e-4	0.0	6.7759	0.0280	0.7577	4.145e-5	0.3522
5.0e-4	0.0	5.9958	0.0233	0.6904	7.456e-5	0.6105
0.0	1.0e-4	5.7278	0.0218	0.6701	9.397e-5	0.8317
0.0	5.0e-4	5.6749	0.0215	0.6655	9.583e-5	0.8551
5.0e-4	5.0e-4	5.6667	0.0215	0.6647	9.624e-5	0.8543
1.0e-3	1.0e-3	5.6581	0.0214	0.6639	9.661e-5	0.8547
SRK-KD Original Parameters		5.6113	0.0211	0.6620	2.111e-4	1.2129

When comparing to the pressure term of the metric, the penalization effect is

strong (Table 5.5). This occurs especially for the second derivatives of the pressure, weighted by  $w_2$ . When values in order of  $10^{-4}$  are applied for  $w_2$ , the parameters' values change abruptly, and the objective function values tend to increase together with the respective deviations.

It is also important to mention that a higher value of the weights implies in an increase of the penalization effect, and the parameter set calculated gets closer to the SRK-KD original parameters. This is expected because, as detailed in Chapter 2, these original parameters are the analytical solution for Equation (2.3), which is the foundation of the penalization function  $F_W$  described in Equation (3.30), showing consistency in the results obtained.

When plotting individual pressure deviations for each case, as shown in Figure 5.7, this effect becomes clear. Even though the  $AAP\%$  when  $w_1 = w_2 = 0$  (0.23 %) is lower than when  $w_1 > 0$  and  $w_2 > 0$  (up to 0.85%), the restrictions presented in Equation (2.3) are violated (critical point region). On the other side, when  $w_1 > 0$  and  $w_2 > 0$  the critical region is better adjusted at the cost of losing accuracy for the other regions.

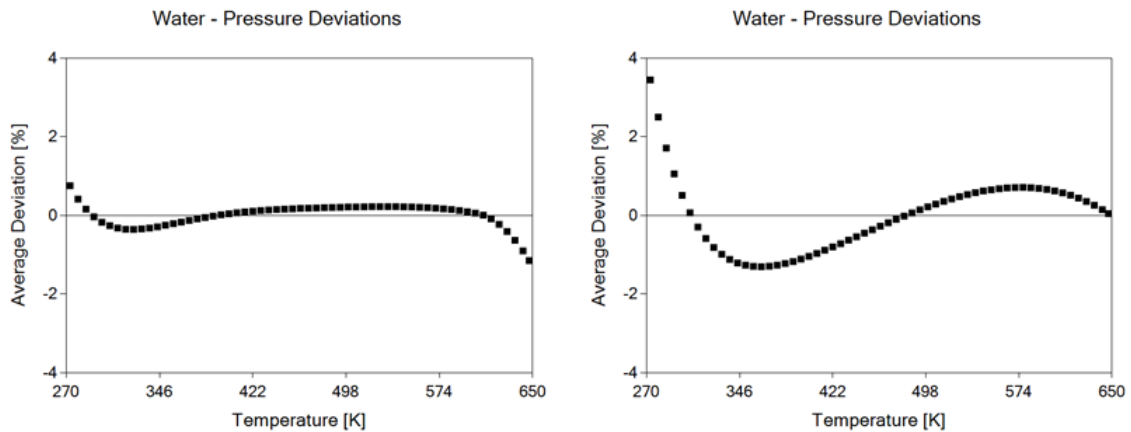


Figure 5.7: Pressure deviations for two of the cases listed in Table 5.5. Left:  $w_1 = w_2 = 0$  ( $AAP = 0.2281\%$ ). Right:  $w_1 = w_2 = 0.001$  ( $AAP = 0.8547\%$ ). Experimental data: DIPPr correlations (DIADDEM, 2004). Critical temperature used for water = 647.13 K. Images taken directly from *ThermOpt*.

In conclusion, there should be a compromise between the  $AAP\%$  and the accuracy near the critical point region. In *ThermOpt* the user can decide the temperature range to be focused in, and whether the penalization should be applied or not. Also, there is the possibility of performing Pareto analyses when varying  $w_1$  and  $w_2$  simultaneously, correlating them into a single weight  $w$ . We consider that this can be a contribution from this work, since the parameters can be adjusted specifically for each engineering application.

This study could be extended to other equations of state, specially the CPA, for which there is no analytic solution to the critical region restrictions. Besides, a



common limitation to this thermodynamic model is the difficulty to correctly predict its properties near the critical point. Therefore, a set of parameters that could satisfactorily calculate in this region without losing the overall accuracy would be absolutely sought by the researchers.

However, due to high interactions between its parameters, this analysis becomes particularly complex, which is out of the scope of this dissertation. With the availability of the tool developed in this work to the academic community, a suggestion for future works is to perform this penalization analysis for polar components using the CPA equation of state.

## 5.2.2 Parameter Estimation for Polar Components Without Penalization (CPA EoS)

The second case studied in this work is the CPA equation of state parameter estimation of polar components. The metric used is composed of saturation pressure and liquid density, with no penalization effects. The components selected were ethylene glycol (MEG), diethylene glycol (DEG), triethylene glycol (TEG), 1,2-propylene glycol (PG) and water. The 4C association scheme (HUANG and RADOSZ, 1990) was applied to all self-associating compounds, and the Table 5.6 resumes the general data used.

Table 5.6: Summary of the general data used for the parameter estimation procedure of MEG, DEG, TEG, PG and water (CPA EoS).

Data Type	Saturation Pressure and Liquid Density
Penalization	No
Source	DIPPr Correlations (DIADEM, 2004)
Variance	Experimental Points
$\Delta T_R$	0.01

The goal of this analysis was to find the optimal solution of each case, regardless of analysing the parameter search space. Therefore, it was decided to execute the parallel PSO + Simplex optimization (described in Chapter 3) for all the results presented in this Section.

Figures 5.8 to 5.10 show the parameters used in the 'Options' visualization for each optimization method, as well as the thermodynamic specifications for these calculations.

PSO Solver | SIMPLEX Solver | **General Options** | Bounds

Hybridize PSO with SIMPLEX Method

Population		Tolerance	
Max # of iterations	200	Absolute	0.000100
# of individuals	50	Relative	0.000100
Min # of Optimum Permanence	10		

Internal Factors			
Individual Factor c1	1.0000	Inertia Factor w0	0.90000
Global Factor c2	0.10000	Inertia Factor wF	0.10000

Figure 5.8: PSO options used in the parameter estimation procedures executed in the Section 5.2.2.

PSO Solver | SIMPLEX Solver | **General Options** | Bounds

Max # of iterations: 1000

Tolerance: 1.0E-007

Initial Cluster Size: +/- 90.000 % from initial point

Make Initial Cluster replace bounds

Internal Factors	
Reflection Factor Alpha	1.0000
Contraction Factor Beta	0.50000
Expansion Factor Gamma	2.0000

Figure 5.9: Simplex options used in the parameter estimation procedures executed in the Section 5.2.2.

Thermodynamic Solver

Absolute Tolerance

Relative Tolerance

Max # of iterations

Figure 5.10: Thermodynamic options used in the parameter estimation procedures executed in the Section 5.2.2.

### Validating the Results: MEG

In the specific case of MEG, DERAWI *et al.* (2003) selected results using saturation pressure and liquid density as well. Therefore, this component was used to validate the optimization capabilities of *ThermOpt*. The parameters' bounds used are shown in Table 5.7.

Table 5.7: Parameters' bounds used for MEG parameter estimation (CPA EoS), obtained by a previous trial and error method.

Parameter	Lower Bounds	Upper Bounds
$a_0$ [bar.L <sup>2</sup> /mol <sup>2</sup> ]	5.0000	20.000
$b$ [L/mol]	0.0300	0.0700
$c_1$	1.0000	2.0000
$\varepsilon/R$ [K]	1000.0	3000.0
$1000\beta$	1.0000	100.00

Table 5.8 shows the comparison between literature and calculated parameters using the same reduced temperature range for the experimental data in each set.  $AAP$  is calculated by Equation (5.1) and  $AAP\rho$ , the average absolute deviation of the liquid densities, is defined by Equation (5.2):

$$AAP\rho = \frac{100\%}{n_e} \sum_{i=1}^{n_e} \frac{|\rho_i^e - \rho_i^*|}{\rho_i^e} \quad (5.2)$$

where  $\rho$  is the liquid density,  $n_e$  the number of experimental points, the superscript  $e$  means experimental data and  $*$  means calculated values.

Table 5.8: Comparison between the literature parameters for MEG (DERAWI *et al.*, 2003) and the calculated ones from *ThermOpt*. The difference between 'Set 01' and 'Set 02' lies on the  $T_R$  range of the experimental data used in each case.

	Set 01		Set 02	
	Literature	Calculated	Literature	Calculated
$a_0$ [bar.L <sup>2</sup> /mol <sup>2</sup> ]	7.1420	7.1404	14.697	14.691
$b$ [mol/L]	0.0510	0.0510	0.0525	0.0525
$c_1$	1.7333	1.7360	1.1099	1.1104
$\varepsilon/R$ [K]	1662.7	1660.2	1215.1	1214.2
$1000\beta$	83.900	84.216	18.400	18.473
$T_R$ range	0.40 - 0.90		0.45 - 0.99	
$AAP$ [%]	1.069	1.067	1.153	1.153
$AA\rho$ [%]	0.502	0.506	0.716	0.715

Slight differences are expected between the literature and calculated parameters due to specificities of the implementation of the saturation pressure calculation such as tolerances, convergence criteria etc. Hence, it can be inferred that *ThermOpt*'s calculations for pure components are performed properly.

### Applying to the Other Compounds (DEG, TEG, PG and water)

The same optimization approach was executed for the remaining components studied. Table 5.9 contains the respective bounds included in the optimizer and table 5.10 shows the results obtained by *ThermOpt*.

Table 5.9: Bounds for the parameters to be estimated for DEG, TEG, PG and water, as well as their temperature range for the experimental data (DIADEM, 2004).

	DEG	TEG	PG	Water
$a_0$ [bar.L <sup>2</sup> /mol <sup>2</sup> ]	20.00 - 40.00	30.00 - 60.00	1.000 - 20.00	1.000 - 2.000
$b$ [mol/L]	0.050 - 0.100	0.100 - 0.150	0.050 - 0.100	0.010 - 0.020
$c_1$	0.500 - 1.500	0.500 - 1.500	0.500 - 3.500	0.500 - 1.500
$\varepsilon/R$ [K]	1000 - 3000	1000 - 3000	1000 - 3000	1000 - 3000
$1000\beta$	0.100 - 50.00	0.100 - 50.00	10.00 - 150.0	50.00 - 150.0
$T_R$ range	0.49 - 0.86	0.49 - 0.82	0.44 - 0.77	0.42 - 0.95

Table 5.10: Parameters estimated by *ThermOpt*, using saturation pressure and liquid density, for DEG, TEG, PG and water.

	DEG	TEG	PG	Water
$a_0$ [bar.L <sup>2</sup> /mol <sup>2</sup> ]	30.499	47.480	4.4228	1.1534
$b$ [mol/L]	0.0918	0.1312	0.0647	0.0147
$c_1$	1.0108	1.0864	3.1473	1.2323
$\varepsilon/R$ [K]	2274.1	2463.3	1904.5	1758.1
$1000\beta$	1.0939	0.4381	108.71	108.66
$AAP$ [%]	0.549	0.504	1.890	0.305
$AA\rho$ [%]	0.596	0.891	1.508	1.147

As mentioned in Chapter 2, using only saturation pressure and liquid density in the objective function are not enough to attain a set of parameters that is capable to correctly predict the behaviour of mixtures, specially when they are in liquid-liquid equilibrium (LLE). When applied to these mixtures, frequently the optimized set failed to predict the experimental data (DERAWI *et al.*, 2003). SANTOS *et al.* (2015c) proposed in their publication a combination of objective functions using VLE and LLE variables to guide this selection, weighted by a user defined number. A slight variation of this methodology was implemented in *ThermOpt* to be applied in this work, explained in details in Chapter 3.

Therefore, the parameters obtained in the Table 5.10 were used as initial guesses to define the optimal parameters presented in the Section 5.3.

### 5.3 VLE + LLE Methodology for CPA EoS Parameter Estimation

Table 5.8 evidences the steep difference between the parameters in Set 01 and Set 02 for MEG, with both of them providing low deviations from DIPPr correlations. The reason for this lies on the large uncertainty of the DIPPr correlations (DERAWI *et al.*, 2003).

Hence, it is common to add LLE restrictions to the sets of parameters previously generated (KONTOGEOGRIS *et al.*, 2006a,b). However, this 'selection' may be a very time consuming process. Therefore, the henceforth called the VLE + LLE Methodology was implemented in this work to improve the effectiveness of this procedure.

Firstly, the glycols were analysed in order to validate this procedure, and after that this methodology was applied to water in order to select a new set of parameters using specific criteria, besides further validating the calculations.

The common options for all of the components studied in this Section are shown in Figure 5.11.

PSO Solver
SIMPLEX Solver
General Options
Bounds

Max # of iterations

Tolerance

Initial Cluster Size +/-  % from initial point

Make Initial Cluster replace bounds

Internal Factors

Reflection Factor Alpha

Contraction Factor Beta

Expansion Factor Gamma

Figure 5.11: Simplex options used in the parameter estimation procedures executed in the Section 5.3.

The parameters' bounds were also the same for all cases. In this case, the optimization procedure consists of solely one method (Simplex) executed repeatedly with well-defined initial guesses (Table 5.10). Consequently, large bounds (Table 5.11) are adequate in order to limit the maximum size of the Simplex.

Table 5.11: Parameter bounds for the case studied in the Section 5.3.

Parameter	Lower Bounds	Upper Bounds
$a_0$ [bar.L <sup>2</sup> /mol <sup>2</sup> ]	1.0000	80.000
$b$ [L/mol]	0.0010	1.0000
$c_1$	0.1000	4.0000
$\varepsilon/R$ [K]	100.00	4000.0
$1000\beta$	0.1000	200.00
$k_{ij}$	-1.0000	1.0000

The objective function term  $S_{LLE}$  was calculated from Equation (3.33). The variances were considered to be the own experimental points in order to ensure that the optimized solutions would generate the lowest possible deviations.

When applying the algorithm recommended in the Section 3.3.3, it was noted that, in all cases, the curve formed by the objective function of the LLE term ( $S_{LLE}$ ) versus the objective function of the pure VLE term ( $S_{pure}$ ) took the form of rational-type functions in the positive quadrant. That is,  $S_{pure}$  and  $S_{LLE}$  were inversely proportional.

Therefore, it was possible to determine a better set of parameters by choosing the point placed on an intermediate position, where an increase of  $S_{pure}$  would result in a lower decrease of  $S_{LLE}$  and vice-versa.

### 5.3.1 Glycols

The selected alkane to evaluate LLE with all glycols studied in this Section was the n-heptane (DERAWI *et al.*, 2002).

For each compound, the following sets of parameters were chosen to the analysis:

- Set of Parameters 01 ('Set 01'). Generated by only saturation pressure and liquid density (VLE variables). Its weight  $w$  on Equation (3.35) is equal to zero.
- Set of Parameters 02 ('Set 02'). Obtained graphically, from an intermediate position of the curve.
- Set of parameters 03 ('Set 03'). Calculated from the maximum allowed value of  $S_{pure}$ . It is obtained from the maximum errors reported by the corresponding DIPPr correlation (DIADEM, 2004), according to Equation (5.3). These maximum error values can be seen in Table 5.12.

$$S_{max,pure} = Err_{max,P}^2 + Err_{max,\rho}^2 \quad (5.3)$$

Table 5.12: Maximum errors in DIPPr correlations (DIADEM, 2004) for each studied component in the Section 5.3.1.

	MEG	DEG	TEG	PG
Error % in $P^{SAT}$	3.00	10.0	10.0	5.00
Error % in $\rho^{SAT}$	1.00	3.00	3.00	3.00
$S_{max,pure}$	1.00e-3	1.09e-2	1.09e-2	3.40e-3

### MEG

Figures 5.12 and 5.13 show the corresponding objective functions curve obtained for MEG. The former shows the whole region analysed, from the solution of Equation (3.35) with  $w = 0$  ('Set 01') to the solution where  $S_{pure} = S_{pure,max}$  ('Set 03'), and the latter focus on the region where the Set of Parameters 02 was chosen, comparing to where would be situated the literature data (DERAWI *et al.*, 2003).

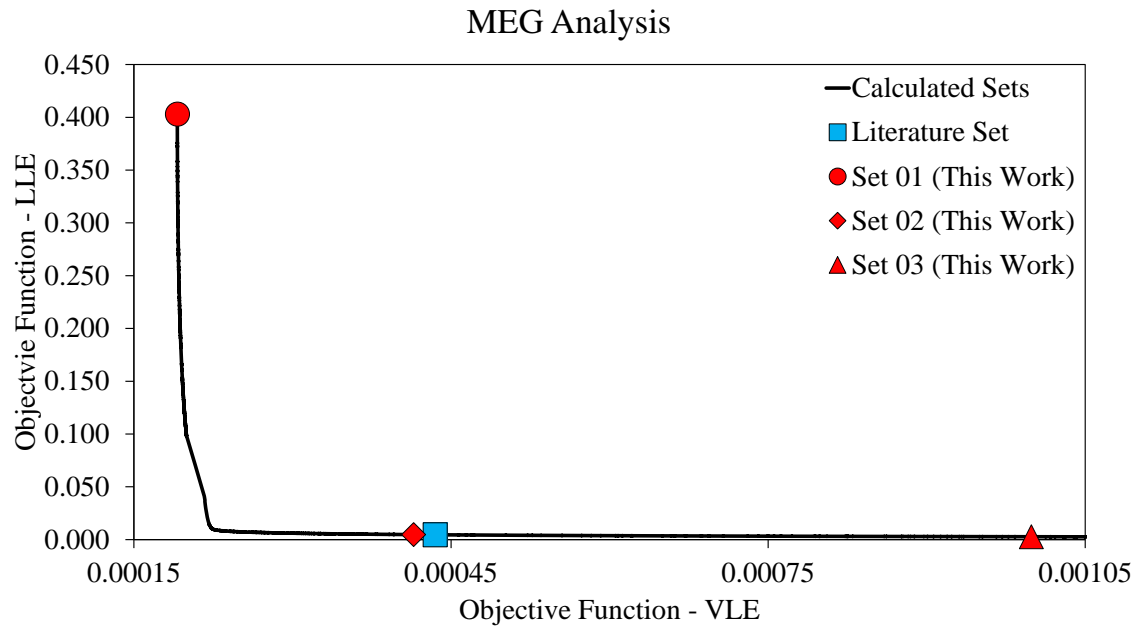


Figure 5.12: Pareto analysis containing both objective function terms of Equation (3.35) for MEG, as seen throughout the studied region, showing the 'Set 01', with  $w = 0$  (red circle). Literature Set of parameters was taken from DERAWI *et al.* (2003).

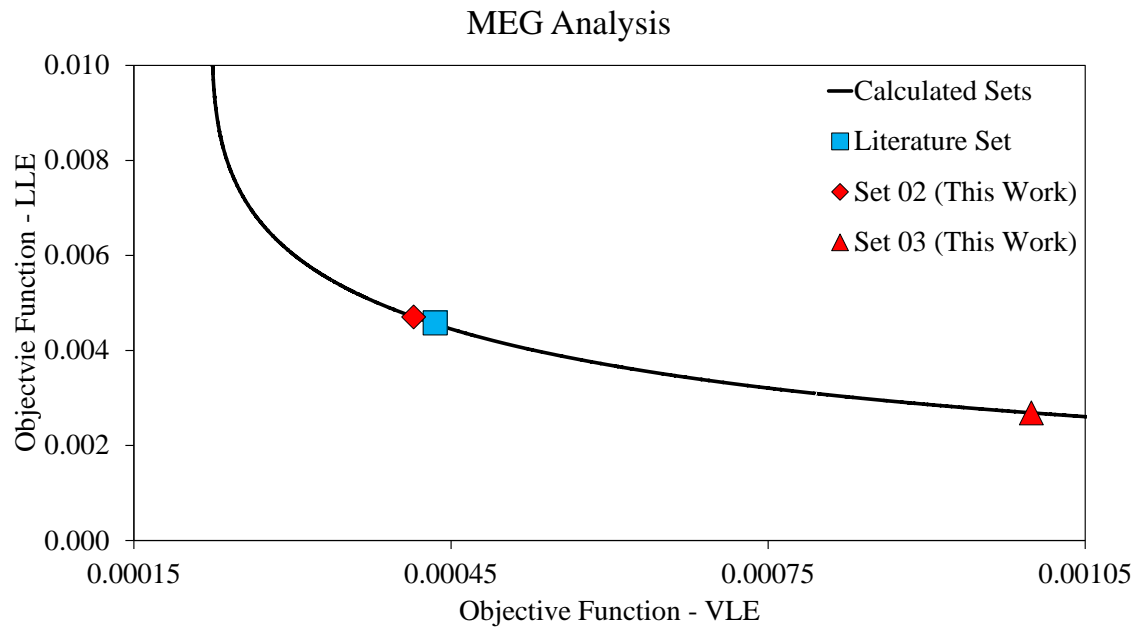


Figure 5.13: Pareto analysis containing both objective function terms of Equation (3.35) for MEG, focusing on the region where the 'Set 02' was selected (diamond), comparing to the actual location of the Literature Set (DERAWI *et al.*, 2003), marked as a square.

Also, Table 5.13 summarizes the selected sets, comparing them to the one found in the literature. Furthermore, another set of parameters was inserted in this table,



'Set 00', which is the calculated set with  $S_{pure}$  closest to the literature set, in order to validate the methodology proposed in this work.

Table 5.13: Parameters chosen using the VLE + LLE Methodology for MEG ( $S_{max,pure} = 1.0e - 3$ ), comparing to the parameters from the literature (DERAWI *et al.*, 2003).  $w$  consists of the weight inserted on Equation (3.35).

	Literature	Set 00	Set 01	Set 02	Set 03
$w$	-	0.143	0.000	0.129	0.611
$a_0$ [bar.L <sup>2</sup> /mol <sup>2</sup> ]	10.819	10.834	7.1404	10.771	11.738
$b$ [mol/L]	0.0514	0.0514	0.0510	0.0514	0.0512
$c_1$	0.6744	0.6730	1.7360	0.6834	0.5155
$\varepsilon/R$ [K]	2375.8	2376.8	1660.2	2369.2	2498.6
$1000\beta$	14.100	14.054	84.216	14.381	9.8107
$S_{pure}$	4.35e-4	4.33e-4	1.91e-4	4.15e-4	9.99e-4
$AAP$ [%]	0.906	0.906	1.067	0.848	1.929
$AA\rho$ [%]	1.581	1.582	0.506	1.569	1.948

Besides, the sets presented in the Table 5.13 were compared to literature parameters when applying to various LLE binary mixtures, as stated in Tables 5.14 to 5.17. The 'Set 00' was excluded from these tables because their results are similar to the literature set of parameters. In these tables,  $AAX_{*,HC}$  and  $AAX_{HC,*}$ , which are the average absolute deviations for the compositions in LLE, are defined by Equations (5.4) and (5.5).

$$AAX_{*,HC} = \frac{100\%}{n_e} \sum_{i=1}^{n_e} \frac{|x_{*,HC}^e - x_{*,HC}^*|}{x_{*,HC}^e} \quad (5.4)$$

$$AAX_{HC,*} = \frac{100\%}{n_e} \sum_{i=1}^{n_e} \frac{|x_{HC,*}^e - x_{HC,*}^*|}{x_{HC,*}^e} \quad (5.5)$$

In the subscripts, 'HC' stands for 'hydrocarbon' and '\*' is the polar component, which is MEG in this case. Also, it is important to point out that all of the binary parameters were optimized in *ThermOpt*, even when they were available in the literature, in order to standardize the comparisons.

Table 5.14: Results for the binary mixture MEG + n-heptane (DERAWI *et al.*, 2002).  $AAX_{MEG,HC}$  and  $AAX_{HC,MEG}$  are calculated from Equations (5.4) and (5.5).

	Literature	Set 01	Set 02	Set 03
$k_{ij}$	0.0471	0.0488	0.0471	0.0458
$S_{otim}$	4.58e-3	4.03e-1	4.71e-3	2.69e-3
$AAX_{MEG,HC}$ [%]	1.172	40.18	1.245	0.642
$AAX_{HC,MEG}$ [%]	5.351	46.04	5.415	4.030

Table 5.15: Results for the binary mixture MEG + n-hexane (DERAWI *et al.*, 2002).  $AAX_{MEG,HC}$  and  $AAX_{HC,MEG}$  are calculated from Equations (5.4) and (5.5).

	Literature	Set 01	Set 02	Set 03
$k_{ij}$	0.0592	0.0609	0.0592	0.0586
$S_{otim}$	1.98e-2	4.02e-1	1.97e-2	2.54e-2
$AAX_{MEG,HC}$ [%]	11.65	38.60	11.57	13.95
$AAX_{HC,MEG}$ [%]	5.815	49.09	5.854	5.529

Table 5.16: Results for the binary mixture MEG + benzene (FOLAS *et al.*, 2006b).  $AAX_{MEG,HC}$  and  $AAX_{HC,MEG}$  are calculated from Equations (5.4) and (5.5).

	Literature	Set 01	Set 02	Set 03
$k_{ij}$	0.0480	0.0251	0.0479	0.0484
$\beta_{ij}^{cross}$	0.0387	0.0517	0.0390	0.0331
$S_{otim}$	2.75e-2	5.75e-2	2.77e-2	2.39e-2
$AAX_{MEG,HC}$ [%]	3.692	11.00	3.798	2.553
$AAX_{HC,MEG}$ [%]	14.52	19.08	14.56	13.63

Table 5.17: Results for the binary mixture MEG + toluene (FOLAS *et al.*, 2006b).  $AAX_{MEG,HC}$  and  $AAX_{HC,MEG}$  are calculated from Equations (5.4) and (5.5).

	Literature	Set 01	Set 02	Set 03
$k_{ij}$	0.0470	0.0244	0.0470	0.0468
$\beta_{ij}^{cross}$	0.0384	0.0547	0.0388	0.0324
$S_{otim}$	1.85e-2	5.12e-2	1.87e-2	1.53e-2
$AAX_{MEG,HC}$ [%]	4.798	6.908	4.777	5.176
$AAX_{HC,MEG}$ [%]	10.20	16.88	10.26	8.896

## DEG

Figures 5.14 and 5.15 present the corresponding objective functions curve for DEG, in the same way as it was shown for MEG. Also, the results of the selected

sets, as well as the LLE binary mixture evaluation with n-heptane, can be seen in Tables 5.18 and 5.19.

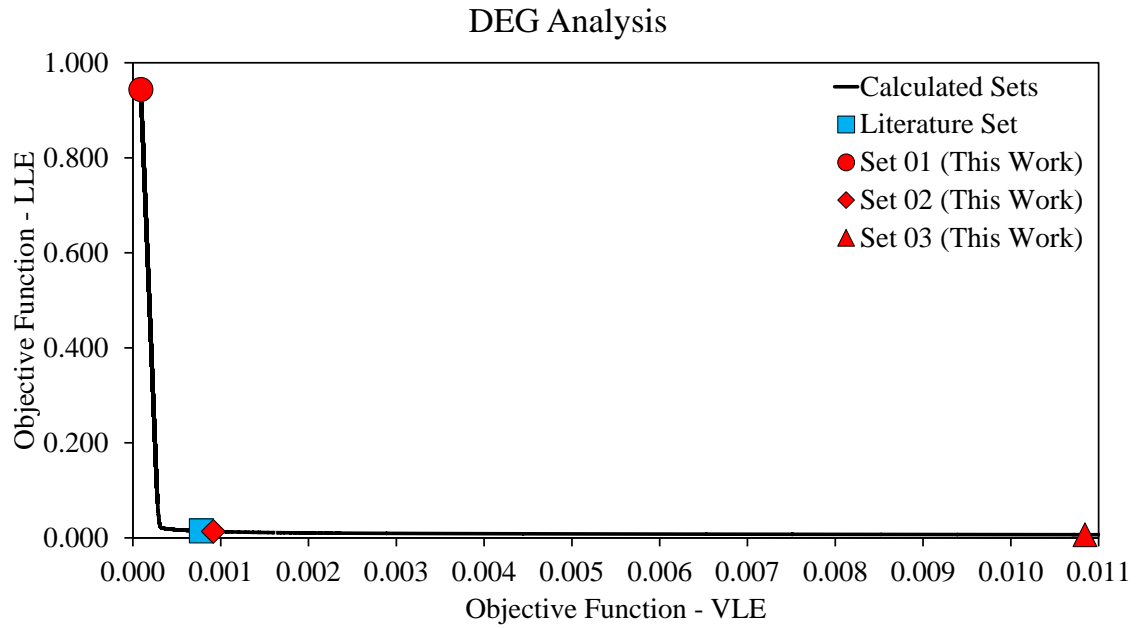


Figure 5.14: Pareto analysis containing both objective function terms of Equation (3.35) for DEG, as seen throughout the studied region, showing the 'Set 01', with  $w = 0$  (red circle). Literature Set of parameters was taken from DERAWI *et al.* (2003)

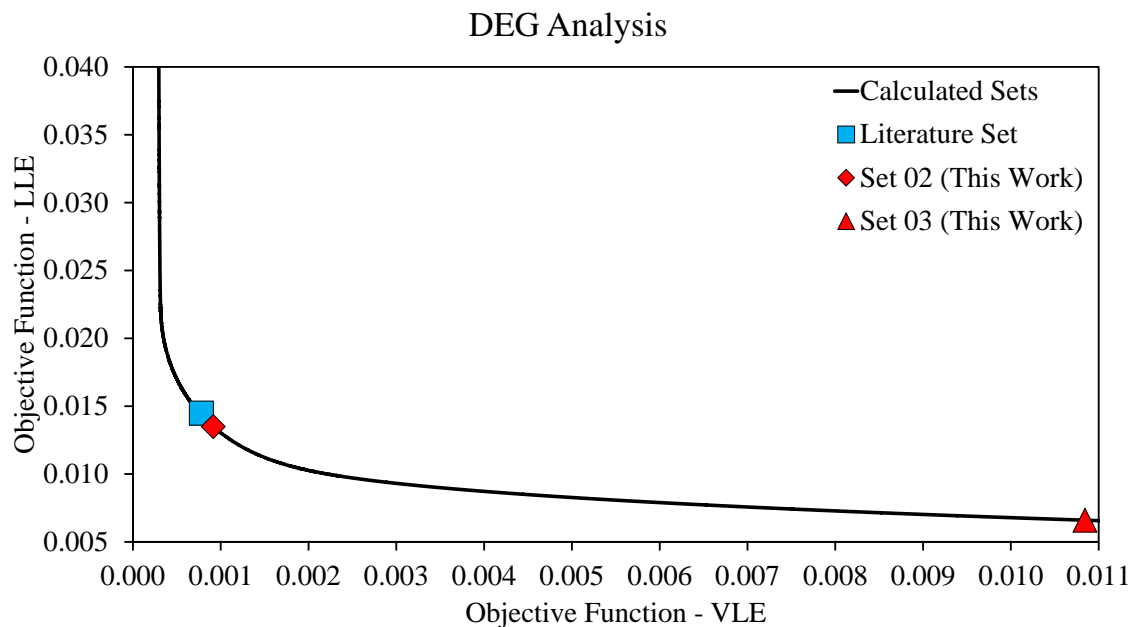


Figure 5.15: Pareto analysis containing both objective function terms of Equation (3.35) for DEG, focusing on the region where the 'Set 02' was selected (diamond), comparing to the location of the set of parameters from the literature (DERAWI *et al.*, 2003), marked as a square.

Table 5.18: Parameter sets chosen using the VLE + LLE Methodology for DEG ( $S_{max,pure} = 1.09e - 2$ ), comparing to the parameters from literature (DERAWI *et al.*, 2003).  $w$  consists of the weight inserted on Equation (3.35).

	Literature	Set 00	Set 01	Set 02	Set 03
$w$	-	0.135	0.000	0.177	4.680
$a_0$ [bar.L <sup>2</sup> /mol <sup>2</sup> ]	26.408	26.405	30.499	25.910	22.538
$b$ [mol/L]	0.0921	0.0921	0.0918	0.0920	0.0862
$c_1$	0.7991	0.7985	1.0108	0.8288	0.8974
$\varepsilon/R$ [K]	2367.4	2368.5	2274.1	2320.0	2092.9
$1000\beta$	6.4000	6.3719	1.0939	7.3901	16.990
$S_{pure}$	7.80e-4	7.51e-4	8.95e-5	9.15e-4	1.08e-2
$AAP$ [%]	1.855	1.773	0.547	2.081	6.192
$AA\rho$ [%]	1.590	1.582	0.596	1.598	7.140

Table 5.19: Results for the binary mixture DEG + n-heptane (DERAWI *et al.*, 2002).  $AAX_{DEG,HC}$  and  $AAX_{HC,DEG}$  are calculated from Equations (5.4) and (5.5).

	Literature	Set 01	Set 02	Set 03
$k_{ij}$	0.0656	0.1585	0.0660	0.0538
$S_{otim}$	1.45e-2	9.44e-1	1.35e-2	6.60e-3
$AAX_{DEG,HC}$ [%]	7.100	10.42	6.416	2.518
$AAX_{HC,DEG}$ [%]	7.712	96.33	2.518	6.820

## TEG

Figure 5.16 shows the corresponding objective functions curve for TEG throughout the analysis, from the solution of the pure VLE case ('Set 01') to the solution with  $S_{pure} = S_{pure,max}$  ('Set 03'), and Figure 5.17 focus on the region where the 'Set 02' was selected in this work.

The results of the chosen sets and the LLE binary mixtures evaluations can be seen in Tables 5.20 and 5.23. These tables present the LLE in the following mixtures: TEG + n-heptane, TEG + benzene and TEG + toluene.

### TEG Analysis

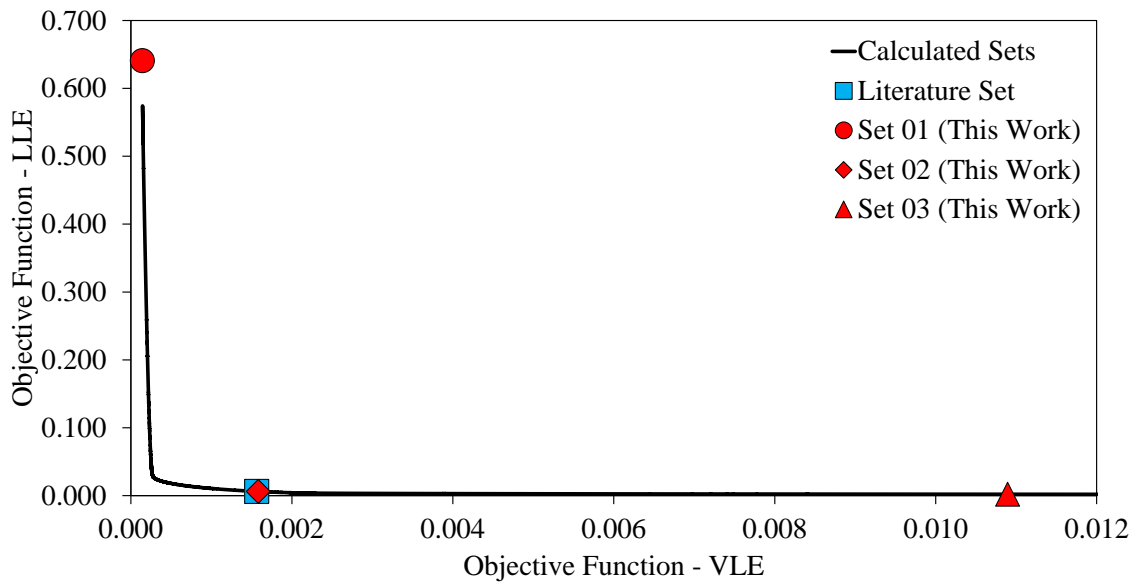


Figure 5.16: Pareto analysis containing both objective function terms of Equation (3.35) for TEG, as seen throughout the studied region, showing the 'Set 01', with  $w = 0$  (red circle). Literature Set of parameters was taken from DERAWI *et al.* (2003)

### TEG Analysis

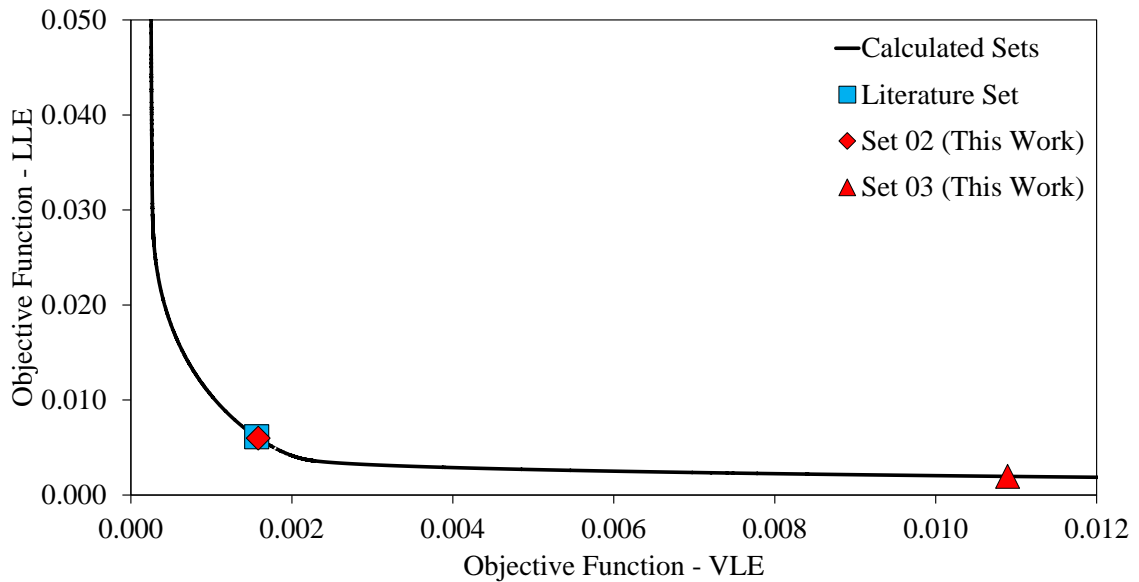


Figure 5.17: Pareto analysis containing both objective function terms of Equation (3.35) for TEG, focusing on the region where the 'Set 02' was selected (diamond), comparing to the location of the set of parameters from the literature (DERAWI *et al.*, 2003), marked as a square.

Table 5.20: Parameter sets chosen using the VLE + LLE Methodology for TEG ( $S_{max,pure} = 1.09e - 2$ ), comparing to the parameters from literature (DERAWI *et al.*, 2003). The weight  $w$  is taken from Equation (3.35).

	Literature	Set 00	Set 01	Set 02	Set 03
$w$	-	0.173	0.000	0.187	11.60
$a_0$ [bar.L <sup>2</sup> /mol <sup>2</sup> ]	39.126	39.124	47.480	39.004	34.320
$b$ [mol/L]	0.1321	0.1321	0.1312	0.1320	0.1239
$c_1$	1.1692	1.1688	1.0864	1.1740	1.2303
$\varepsilon/R$ [K]	1724.3	1725.1	2463.3	1717.7	1509.9
$1000\beta$	18.800	18.802	0.4381	19.256	44.659
$S_{pure}$	1.56e-3	1.56e-3	1.41e-4	1.58e-3	1.09e-2
$AAP$ [%]	3.018	3.042	0.504	3.068	6.464
$AA\rho$ [%]	1.607	1.611	0.891	1.614	6.850

Table 5.21: Results for the binary mixture TEG + n-heptane (DERAWI *et al.*, 2002).  $AAX_{TEG,HC}$  and  $AAX_{HC,TEG}$  are calculated from Equations (5.4) and (5.5).

	Literature	Set 01	Set 02	Set 03
$k_{ij}$	0.0939	0.1339	0.0937	0.0829
$S_{otim}$	6.12e-3	6.41e-1	5.99e-3	1.96e-3
$AAX_{TEG,HC}$ [%]	4.542	19.58	4.490	1.233
$AAX_{HC,TEG}$ [%]	4.497	76.06	4.452	3.390

Table 5.22: Results for the binary mixture TEG + benzene (FOLAS *et al.*, 2006b).  $AAX_{TEG,HC}$  and  $AAX_{HC,TEG}$  are calculated from Equations (5.4) and (5.5).

	Literature	Set 01	Set 02	Set 03
$k_{ij}$	0.0362	0.2102	0.0362	0.0323
$\beta_{ij}^{cross}$	0.0987	0.3191	0.0999	0.1502
$S_{otim}$	2.54e-3	4.15e-2	2.54e-3	2.91e-3
$AAX_{TEG,HC}$ [%]	4.459	7.906	4.467	4.731
$AAX_{HC,TEG}$ [%]	1.308	17.22	1.300	1.026

Table 5.23: Results for the binary mixture TEG + toluene (FOLAS *et al.*, 2006b).  $AAX_{TEG,HC}$  and  $AAX_{HC,TEG}$  are calculated from Equations (5.4) and (5.5).

	Literature	Set 01	Set 02	Set 03
$k_{ij}$	0.0374	0.0357	0.0374	0.0324
$\beta_{ij}^{cross}$	0.0465	0.0012	0.0471	0.0751
$S_{otim}$	8.01e-3	2.16e-1	7.85e-3	7.75e-3
$AAX_{TEG,HC}$ [%]	2.381	25.97	2.226	5.241
$AAX_{HC,TEG}$ [%]	7.279	32.21	7.260	5.807

## PG

Figures 5.18 and 5.19, as well as Tables 5.24 and 5.25, show the results for PG, attained as the former studied glycols. The only available alkane to analyse the LLE with propylene glycol was the n-heptane.

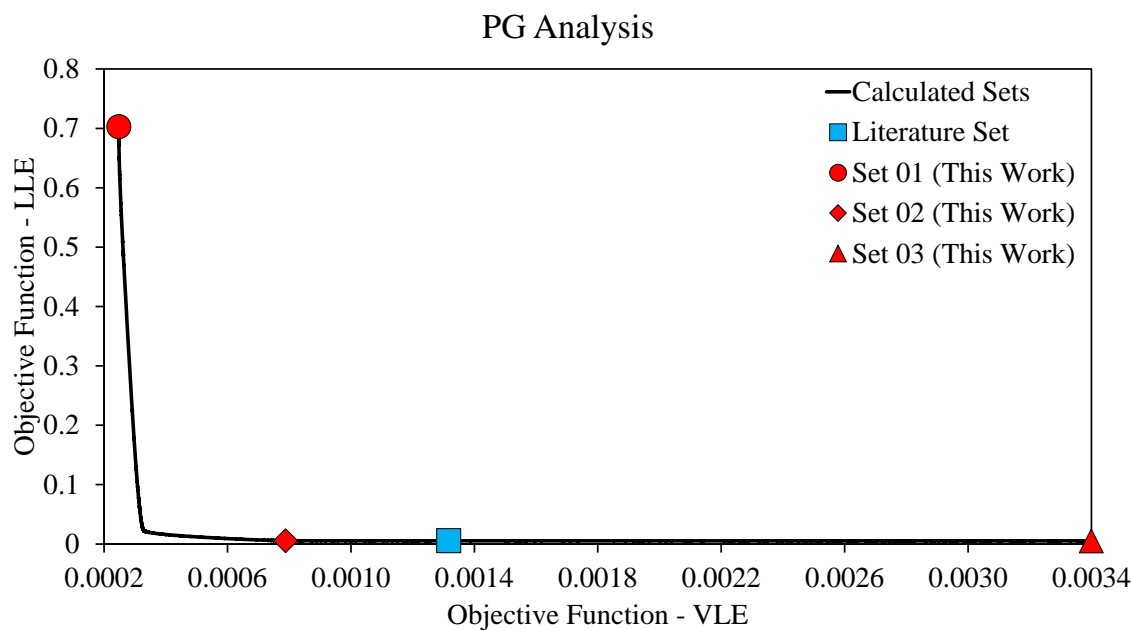


Figure 5.18: Pareto analysis containing both objective function terms of Equation (3.35) for PG, as seen throughout the studied region, showing the 'Set 01', with  $w = 0$  (red circle). Literature Set of parameters was taken from DERAWI *et al.* (2003)

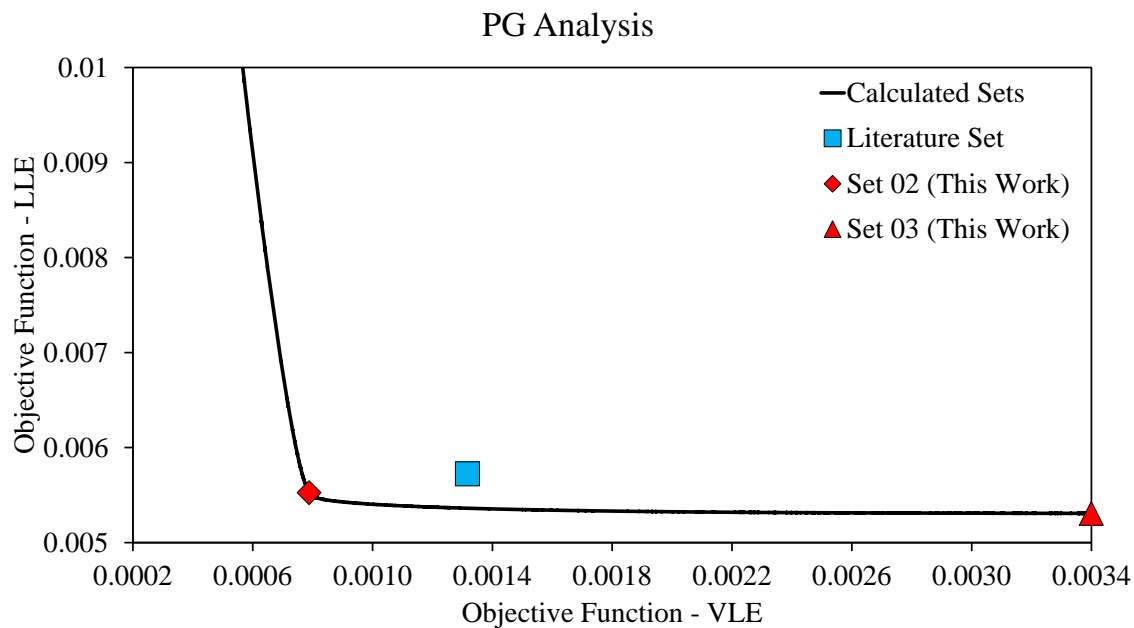


Figure 5.19: Pareto analysis containing both objective function terms of Equation (3.35) for PG, focusing on the region where the 'Set 02' was selected (diamond), comparing to the location of the literature set (DERAWI *et al.*, 2003), marked as a square.

Table 5.24: Parameters chosen using the VLE + LLE Methodology for PG ( $S_{max,pure} = 3.40 \times 10^{-3}$ ), comparing to the parameters from literature (DERAWI *et al.*, 2003). The weight  $w$  is taken from Equation (3.35).

	Literature	Set 00	Set 01	Set 02	Set 03
$w$	-	11.10	0.000	0.216	238.25
$a_0$ [bar.L <sup>2</sup> /mol <sup>2</sup> ]	13.836	14.258	4.4228	13.816	14.977
$b$ [mol/L]	0.0675	0.0687	0.0647	0.0676	0.0711
$c_1$	0.9372	0.9288	3.1473	0.9526	0.9129
$\varepsilon/R$ [K]	2097.8	2145.3	1904.5	2112.0	2149.1
$1000\beta$	19.000	15.870	108.72	18.067	14.818
$S_{pure}$	1.32e-3	1.32e-3	2.47e-4	7.88e-4	3.40e-3
$AAP$ [%]	1.890	2.423	1.349	1.869	2.299
$AA\rho$ [%]	1.508	2.019	0.118	1.490	4.971



Table 5.25: Results for the binary mixture PG + n-heptane (DERAWI *et al.*, 2002).  $AAX_{PG,HC}$  and  $AAX_{HC,PG}$  are calculated from Equations (5.4) and (5.5).

	Literature	Set 01	Set 02	Set 03
$k_{ij}$	0.0320	0.0549	0.0318	0.0448
$S_{otim}$	5.72e-3	7.03e-1	5.53e-3	5.31e-3
$AAX_{PG,HC}$ [%]	3.288	83.39	2.959	2.470
$AAX_{HC,PG}$ [%]	6.133	6.480	6.112	5.983

## Discussion

Based on the results obtained, it is possible to infer that the VLE + LLE Methodology implemented in *ThermOpt* succeeded in systematically finding a wide range of CPA sets of parameters which fit satisfactorily the DIPPr correlations as well as LLE experimental data with n-heptane.

Moreover, for MEG, DEG and TEG one of the sets ('Set 00') obtained was similar to the literature counterpart. It has been presented in the results to emphasize that using the methodology proposed in this work it was possible to find, among others, the parameter set presented in the literature depending only on the user's selection criteria.

The only exception lied on the propylene glycol, whose 'Set 00' turned out to be different from the literature set. The most probable reason to this discrepancy was the fact that the temperatures range used by DERAWI *et al.* (2003) had started with low values of pressure of PG (order of  $1 \text{ Pa} = 10^{-5} \text{ bar}$ ), which had greatly affected its calculation, depending on the tolerances used. For instance, these authors reported the pressure and density deviations for PG equal to 4.88% and 1.50%, respectively. *ThermOpt* found 1.89% and 1.51% for the same variables, as seen in Table 5.24. On the other hand, the parameters in 'Set 02' were quite close to the literature counterparts, further validating the methodology even with the prior discrepancies in the pressure calculations.

In addition to that, it is not clear how to define specific criteria with the methodology proposed in this work in order to replicate the parameters obtained by the respective authors (DERAWI *et al.*, 2003; FOLAS *et al.*, 2006a; KONTOGEOGRIS *et al.*, 1999), defined by the 'Set 00' presented previously. Thus, in this study the 'Set 02' for each component was suggested as an independent method to find parameters with potential of predicting LLE with hydrocarbons. As seen specially in the tables of MEG and TEG, which contained results for mixtures of these compounds with other hydrocarbons, the 'Set 02' provided results with deviations as low as in the authors' papers.

Moreover, the 'Set 03' was proposed to demonstrate the limits to this methodology, where the objective function attained the maximum value allowed by the DIPPr correlations' errors. While their deviations in the binary mixtures with n-heptane were lower than the other sets, this trend was not necessarily repeated in the mixtures with other hydrocarbons, when applicable. Therefore, their LLE results do not compensate the higher deviations in the VLE term.

Lastly, it is of crucial importance to point out that 'Set 02' and 'Set 03' were mere examples of possible approaches to select the most suitable parameters. The main goal of this study is to present a tool that provides a systematic methodology to generate a wide range of parameters which corresponds satisfactorily to both VLE and LLE data, thus facilitating the user's decision-making.

### 5.3.2 Water

For water the same analysis was conducted with specific differences:

- The selected hydrocarbon for such study was the n-hexane (TSONOPOULOS and WILSON, 1983), as also stated by KONTOGEORGIS *et al.* (1999).
- TSONOPOULOS and WILSON (1983) presented, in their work, temperature dependent correlations to calculate the liquid compositions of each phase of the mixture water + n-hexane. In order to explore the whole valid temperature region, this correlation was used instead of the actual experimental data. The temperature region selected is from  $T = 273.15$  K to  $T = 473.15$  K.
- The DIPPr correlations errors for water is exceedingly lower than the glycols, as seen in Table 5.26. Were the original 'Set 03' was applied for this case, no solution would be found.

Table 5.26: Maximum errors in DIPPr correlations (DIADEM, 2004) for water.

	Water
Error % in $P^{SAT}$	0.200
Error % in $\rho^{SAT}$	1.00
$S_{max,pure}$	1.04e-4

- Therefore, a new Set of Parameters 03 was proposed for water, due to the availability of the experimental measure of its hydrogen bonds energy (KOH *et al.*, 1993). This property was found to be  $E_H/R = 1813$  K, which can be compared to the parameter  $\varepsilon/R$  (KONTOGEORGIS *et al.*, 1996).

When specifying the parameters for this new 'Set 03', it was found that the variable  $\varepsilon/R$  also decreases when  $S_{LLE}$  increases, as seen in Figure 5.20. If the set containing the value of  $\varepsilon/R$  exactly equal to the experimental findings of KOH *et al.* (1993) (circle) were the selected one, there would be a possibility of crudely predict the behaviour of LLE in aqueous solutions of hydrocarbons.

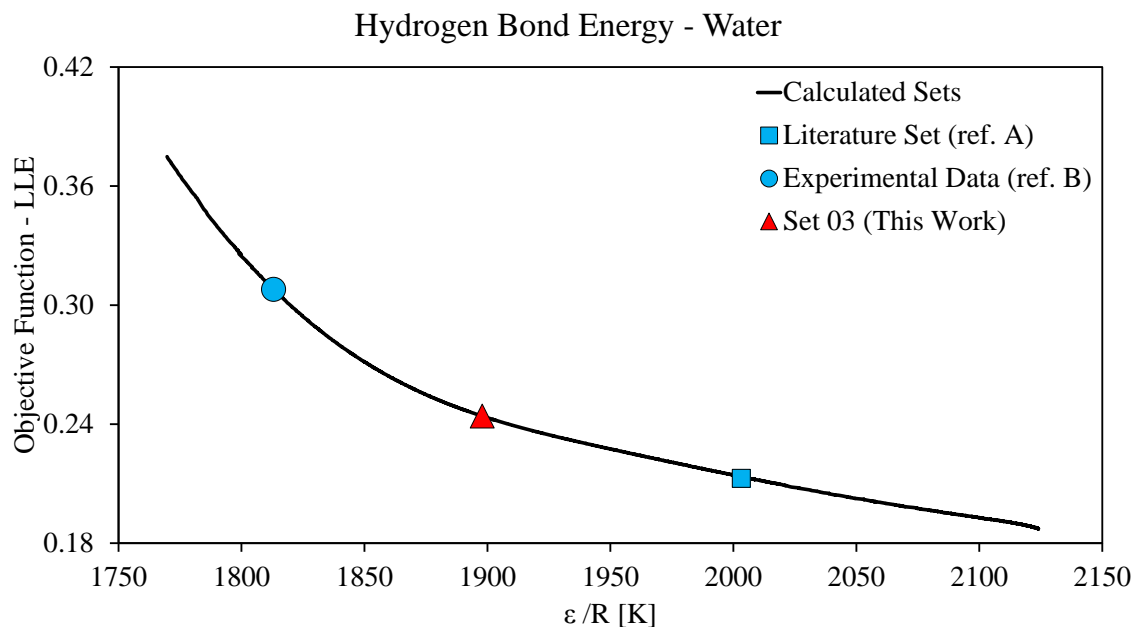


Figure 5.20: Chart containing the values of association energy for water versus  $S_{LLE}$ , comparing with the literature values and the chosen 'Set 03' in this work. Ref. A: KONTOGEORGIS *et al.* (1999). Ref B: KOH *et al.* (1993).

Therefore, the water's new 'Set 03' was selected as an intermediary value between the experimental and the one reported by KONTOGEORGIS *et al.* (1999), being arbitrated with  $\varepsilon/R$  roughly equal to 1900 K.

Figure 5.21 shows the behaviour of all of the solutions in this methodology applied to water, analogously to the glycols, and Table 5.27 presents the main results with the selected sets.

## Water Analysis

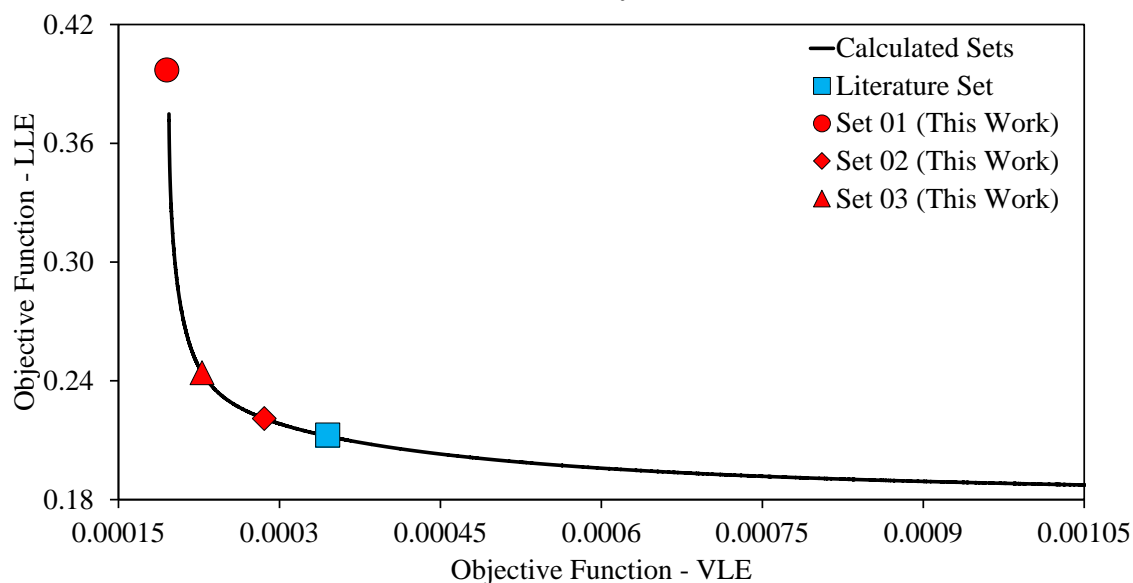


Figure 5.21: Pareto analysis containing both objective function terms of Equation (3.35) for water, showing the 'Set 01', with  $w = 0$  (red circle). Literature Set was taken from KONTOGEORGIS *et al.* (1999).

Table 5.27: Parameter sets chosen using the VLE + LLE Methodology for water, comparing to the parameters from literature (KONTOGEORGIS *et al.*, 1999).  $w$  consists of the weight inserted on Equation (3.35).

	Literature	Set 00	Set 01	Set 02	Set 03
$1000w$	-	8.77	0.00	5.02	1.15
$a_0$ [bar.L <sup>2</sup> /mol <sup>2</sup> ]	1.2278	1.2224	1.1534	1.1631	1.0978
$b$ [mol/L]	0.0145	0.0145	0.0147	0.0145	0.0145
$c_1$	0.6736	0.6650	1.2323	0.7865	1.0120
$\varepsilon/R$ [K]	2003.2	2008.8	1758.1	1974.3	1897.9
$1000\beta$	69.200	68.897	108.66	75.517	89.078
$S_{pure}$	3.45e-4	3.44e-4	1.95e-4	2.86e-4	2.28e-4
$AAP$ [%]	0.784	0.777	0.305	0.755	0.625
$AA\rho$ [%]	1.205	1.223	1.147	1.145	1.108

Also, Tables 5.28 to 5.31 show the results regarding mixtures with the following hydrocarbons: n-octane, benzene and toluene. For the mixture with n-octane, HEIDMAN and TSONOPOULOS (1985) also generated correlations for their experimental data. Therefore, they were also adopted in this work, within the range [297 – 522 K].

Table 5.28: Results for the binary mixture water + n-hexane (TSONOPOULOS and WILSON, 1983).  $AAX_{W,HC}$  and  $AAX_{HC,W}$  are calculated from Equations (5.4) and (5.5).

	Literature	Set 01	Set 02	Set 03
$k_{ij}$	0.0376	0.0108	0.0391	0.0321
$S_{otim}$	2.13e-1	3.97e-1	2.21e-1	2.44e-1
$AAX_{W,HC}$ [%]	12.28	33.36	11.05	10.99
$AAX_{HC,W}$ [%]	34.95	39.91	35.67	37.28

Table 5.29: Results for the binary mixture water + n-octane (HEIDMAN and TSONOPOULOS, 1985).  $AAX_{W,HC}$  and  $AAX_{HC,W}$  are calculated from Equations (5.4) and (5.5).

	Literature	Set 01	Set 02	Set 03
$k_{ij}$	-0.0002	-0.0282	0.0015	-0.0051
$S_{otim}$	1.37e-1	2.54e-1	1.48e-1	1.65e-1
$AAX_{W,HC}$ [%]	9.190	18.83	9.818	5.424
$AAX_{HC,W}$ [%]	29.64	35.46	30.44	32.44

Table 5.30: Results for the binary mixture water + benzene (ANDERSON and PRAUSNITZ, 1986).  $AAX_{W,HC}$  and  $AAX_{HC,W}$  are calculated from Equations (5.4) and (5.5).

	Literature	Set 01	Set 02	Set 03
$k_{ij}$	0.0439	0.0214	0.0461	0.0420
$\beta_{ij}^{cross}$	0.0770	0.0746	0.0830	0.0874
$S_{otim}$	4.06e-3	3.64e-3	3.67e-3	3.37e-3
$AAX_{W,HC}$ [%]	2.045	2.545	2.420	2.821
$AAX_{HC,W}$ [%]	4.381	4.240	4.228	4.153

Table 5.31: Results for the binary mixture water + toluene (ANDERSON and PRAUSNITZ, 1986).  $AAX_{W,HC}$  and  $AAX_{HC,W}$  are calculated from Equations (5.4) and (5.5).

	Literature	Set 01	Set 02	Set 03
$k_{ij}$	0.0194	-0.0061	0.0214	0.0166
$\beta_{ij}^{cross}$	0.0619	0.0548	0.0669	0.0696
$S_{otim}$	8.38e-3	7.29e-3	7.28e-3	6.27e-3
$AAX_{W,HC}$ [%]	1.156	1.084	1.090	1.135
$AAX_{HC,W}$ [%]	5.952	7.007	5.251	5.728

## Discussion

The 'Set 00' was selected as the parameter set with the  $S_{pure}$  closest to the literature set. It has been seen that the selected set was similar to the one presented by KONTOGEORGIS *et al.* (1999), confirming the consistency of the proposed methodology.

All sets, with the exception of 'Set 01' in aqueous solutions with the alkanes, were able to satisfactorily predict the LLE data.

The selection of 'Set 02' depends on a series of factors, such as the limits of the objective functions in the chart where the user can select the best position for each specific application. These limits are defined by the user tolerance on where could be the maximum allowed values of  $S_{pure}$  and  $S_{LLE}$  in each case. The rigorous approach would be to test all sets in a predetermined region for LLE with other components until an optimal set is found. With the methodology presented (VLE + LLE), this analysis may become simpler than what KONTOGEORGIS *et al.* (2006b) published in their paper due to its systematic feature. Consequently, we consider that this is a contribution of this work to the literature.

Nevertheless, we considered the 'Set 03' as the main parameter set to be evaluated and compared against the published binary parameters and experimental data. The main reason for that is the higher theoretical background, with the variable  $\varepsilon/R$  nearer the value reported by KOH *et al.* (1993), without losing accuracy in the LLE predictions.

Finally, as already stated in the Section 5.3.1, it is necessary to state that the objective of this analysis is to provide a systematic guide to facilitate the selection of the best parameters. Hence, a suggestion to future works may be to use this rigorous approach to find the most proper parameters in a specific application. Eventually, the final decision must be taken by the user.

## 5.4 CPA Binary Parameter Estimation Using Water Dew Point

Having validated, optimized and selected parameters for pure components, this Section will present a study of parameter estimation procedures for mixtures using dew point experimental data. It is specifically applied to the natural gas production process.

### 5.4.1 Analysis of the Binary Mixture H<sub>2</sub>O + CO<sub>2</sub>

One of the most studied compounds of the natural gas is the carbon dioxide (CO<sub>2</sub>) due to its particular characteristics, specially its capability to do cross association when mixed with water according to KONTOGEORGIS *et al.* (2006b); LI and FIROOZABADI (2009). The parameter estimation procedure followed the steps listed in the Section 3.4.

- For the pure components, literature parameters (KONTOGEORGIS *et al.*, 1999) and the 'Set 03' from the Section 5.3.2 were used for water, and the parameters from TSIVINTZELIS *et al.* (2010) were set for CO<sub>2</sub>. They are listed in Table 5.32.
- Parameter Estimation A: binary parameters were estimated from dew pressure calculation optimized by PSO+Simplex. This work considers that there is a solvation effect between CO<sub>2</sub> and water, even if the former does not self-associate. The parameters to be optimized are then  $k_{ij}$  and  $\beta_{ij}^{cross}$ .
- Parameter Estimation B: Estimation A's results were used as an initial estimative to re-estimate these parameters using the water content metric (Equation 3.38) by the Simplex method.

Table 5.32: Pure component parameters used in the Section 5.4.1.

	Water (Literature) <sup>a</sup>	Water ('Set 03') <sup>b</sup>	CO <sub>2</sub> <sup>c</sup>
$a_0$ [bar.L <sup>2</sup> /mol <sup>2</sup> ]	1.2278	1.0978	3.5081
$b$ [mol/L]	0.0145	0.0145	0.0272
$c_1$	0.6736	1.0120	0.7602
$\varepsilon/R$ [K]	2003.2	1897.9	-
$1000\beta$	69.200	89.078	-

<sup>a</sup>KONTOGEORGIS *et al.* (1999)

<sup>b</sup>This work

<sup>c</sup>TSIVINTZELIS *et al.* (2010)

Table 5.33 summarizes the experimental data used, and Table 5.34 presents the estimable variables' bounds. The options used are the same as reported in Figures 5.8 to 5.10.

Because of the high pressure values in the work of WIEBE and GADDY (1941), whose values reached up to 700 bar, the Estimation A did not give reliable results. Therefore, only the data of VALTZ *et al.* (2004) could be used in this stage of the calculation. On the other hand, for Estimation B all experimental data could be satisfactorily applied.

Table 5.33: Summary of the data of the mixture studied in this Section.

	Estimation A	Estimation B
Data Type	Dew Pressure	Water Content
Source	VALTZ <i>et al.</i> (2004)	VALTZ <i>et al.</i> (2004) WIEBE and GADDY (1941)
Variance	Experimental Points	
# of Points	24	67

Table 5.34: Bounds for the water + CO<sub>2</sub> parameter estimation in this Section. These values were obtained by trial and error.

Parameter	Lower Bounds	Upper Bounds
$k_{ij}$	-0.5000	0.5000
$\beta_{ij}^{cross}$	0.0100	0.5000

Tables 5.35 and 5.36 display the results of this procedure.  $S_P$  is the objective function calculated by Equation (3.36), and  $S_y$  calculated by Equation (3.38).  $AAP_{dew}$  and  $AAY$  are calculated according to Equations (5.6) and (5.7).

$$AAP_{dew} = \frac{100\%}{n_e} \sum_{i=1}^{n_e} \frac{|P_i^e - P_i^*|}{P_i^e} \quad (5.6)$$

$$AAY = \frac{100\%}{n_e} \sum_{i=1}^{n_e} \frac{|y_i^e - y_i^*|}{y_i^e} \quad (5.7)$$

Table 5.35: Estimation results for water (KONTOGEOORGIS *et al.*, 1999) + CO<sub>2</sub> mixture studied in this Section.

Case	$k_{ij}$	$\beta_{ij}^{cross}$	$S_P$	$S_y$	$AAP_{dew}$ [%]	$AAY$ [%]
Estimation A	-0.2324	0.0677	2.65e-2	3.37e-2	13.02	15.41
Estimation B	0.1542	0.1765	4.98e-2	2.15e-2	18.46	10.81
Literature Data <sup>a</sup>	0.1145	0.1836	5.20e-2	4.01e-2	18.92	16.13

<sup>a</sup>TSIVINTZELIS *et al.* (2011)

Table 5.36: Estimation results for water (Set 03) + CO<sub>2</sub> mixture studied in this Section.

Case	$k_{ij}$	$\beta_{ij}^{cross}$	$S_P$	$S_y$	$AAP_{dew}$ [%]	$AAY$ [%]
Estimation A	-0.2408	0.0718	2.60e-2	3.39e-2	12.88	15.57
Estimation B	0.1701	0.2093	4.86e-2	2.11e-2	18.28	10.71

Based on the results presented in Tables 5.35 and 5.36, it is possible to infer that the dew pressure calculations lead to different parameters when compared with



those obtained by the water content because of its restrictions. In higher pressures, dew pressure calculations become exceedingly complex, affecting its convergence. The work of WIEBE and GADDY (1941) focus on these extreme regions, therefore changing the search space.

However, this issue did not occur in the optimization based on water content, showing the success of the metric proposed (Equation 3.38). According to Table 5.35, the Estimation B's parameters are close to the set published by TSIVINTZELIS *et al.* (2011), but resulting in reduced deviations.

In addition to that, the 'Set 03' obtained for water succeeded to predict the water content with slightly lower deviations than the set selected by KONTOGEORGIS *et al.* (1999). Figures 5.22 to 5.25 illustrate these results with isotherms.

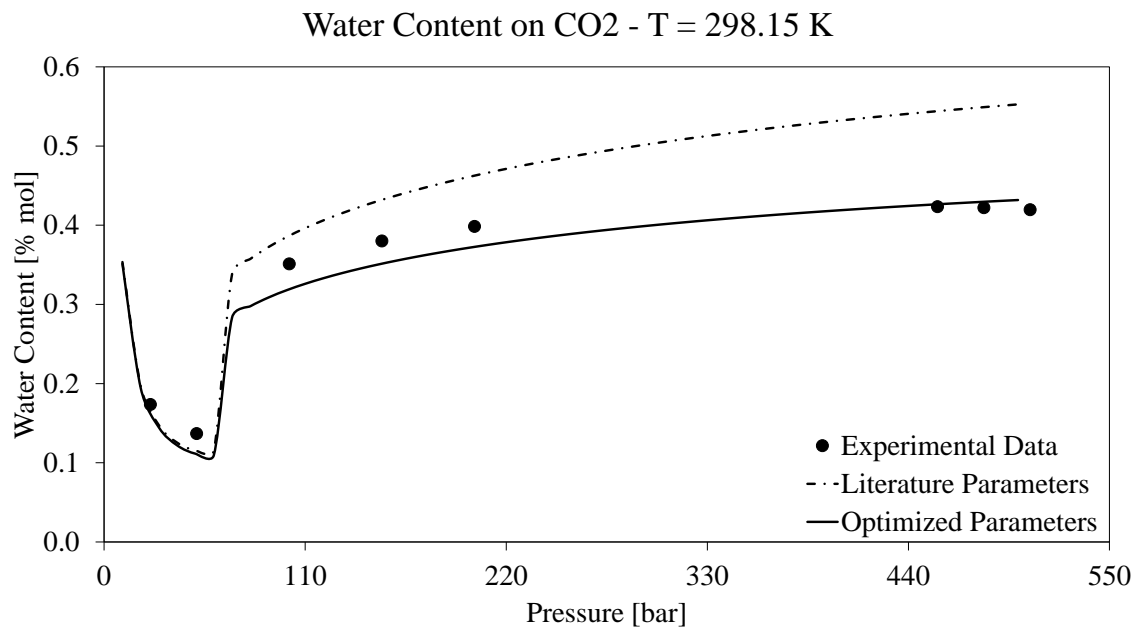


Figure 5.22: Chart containing values of pressure versus water content in dew point for the mixture Water + CO<sub>2</sub> in an isotherm at  $T = 298.15 K$ . Experimental data: WIEBE and GADDY (1941). Literature parameters: KONTOGEORGIS *et al.* (1999) (pure water) and TSIVINTZELIS *et al.* (2011) (binary parameters). Optimized parameters: this work ('Set 03' for pure water).

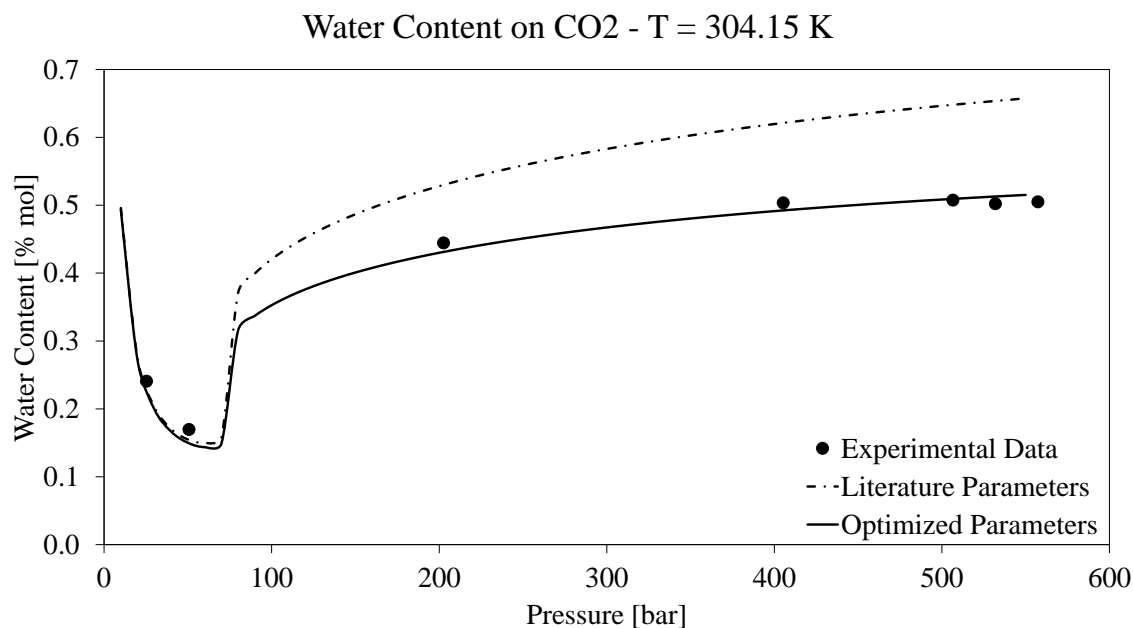


Figure 5.23: Chart containing values of pressure versus water content in dew point for the mixture Water + CO<sub>2</sub> in an isotherm at  $T = 304.15\text{ K}$ . Experimental data: WIEBE and GADDY (1941). Literature parameters: KONTOGEORGIS *et al.* (1999) (pure water) and TSIVINTZELIS *et al.* (2011) (binary parameters). Optimized parameters: this work ('Set 03' for pure water).

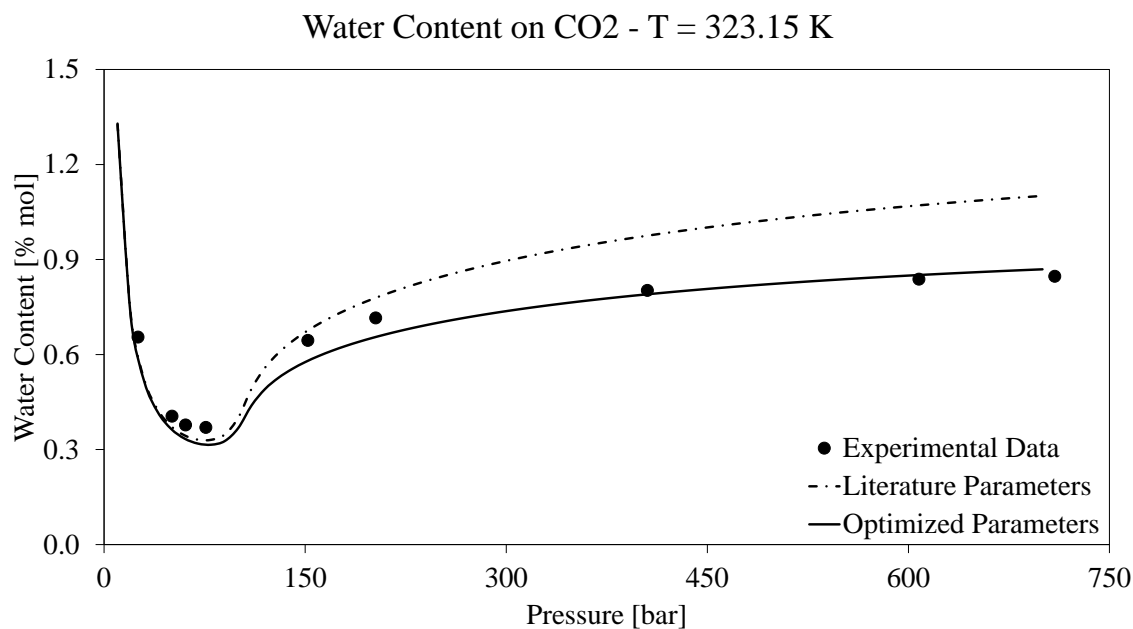


Figure 5.24: Chart containing values of pressure versus water content in dew point for the mixture Water + CO<sub>2</sub> in an isotherm at  $T = 323.15\text{ K}$ . Experimental data: WIEBE and GADDY (1941). Literature parameters: KONTOGEORGIS *et al.* (1999) (pure water) and TSIVINTZELIS *et al.* (2011) (binary parameters). Optimized parameters: this work ('Set 03' for pure water).

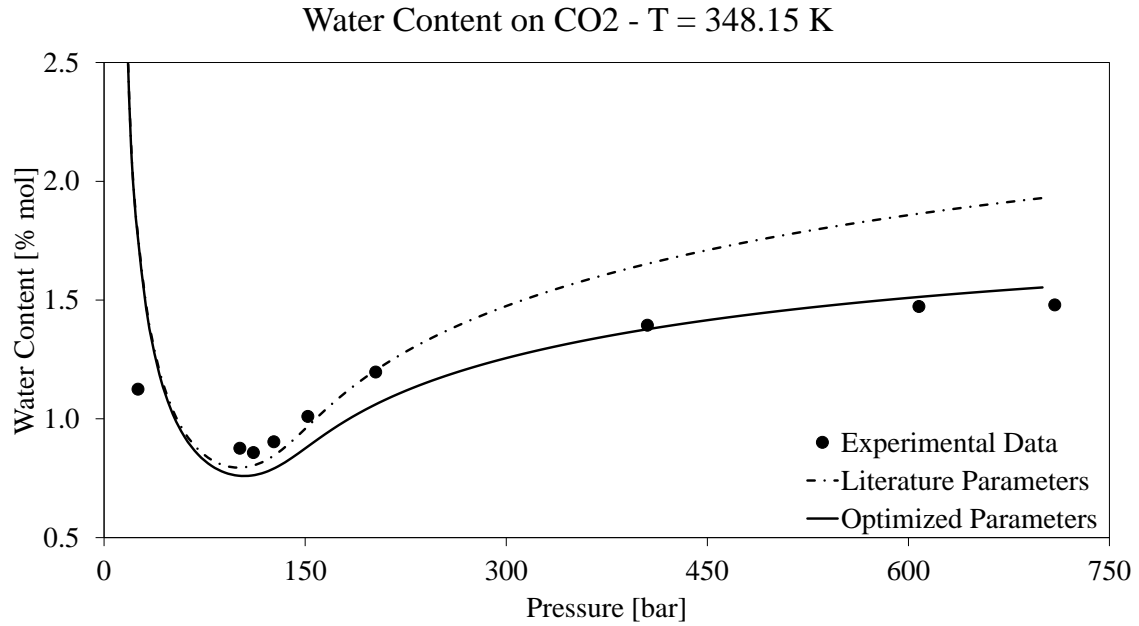


Figure 5.25: Chart containing values of pressure versus water content in dew point for the mixture Water + CO<sub>2</sub> in an isotherm at  $T = 348.15\text{ K}$ . Experimental data: WIEBE and GADDY (1941). Literature parameters: KONTOGEORGIS *et al.* (1999) (pure water) and TSIVINTZELIS *et al.* (2011) (binary parameters). Optimized parameters: this work ('Set 03' for pure water).

Analysing these charts (Figures 5.22 to 5.25), it is concluded that even though all sets of parameters predict the inversion effect of water content when the pressure increases, the potential results of this study seem to be superior than the literature parameters (KONTOGEORGIS *et al.*, 1999; TSIVINTZELIS *et al.*, 2011). Besides, in higher pressures (above 200 bar) the differences between each optimized case and the calculations performed by the set modelled by the literature become more prominent, as presented in Table 5.37. Therefore, it is possible to check if these positive results persist when predicting the water content in multicomponent natural gases.

Table 5.37: Estimation results for water + CO<sub>2</sub> mixture studied in this Section for  $P > 200\text{ bar}$ .

Case	AAY [%]
Literature Data (TSIVINTZELIS <i>et al.</i> , 2011)	23.70
Optimized from water (KONTOGEORGIS <i>et al.</i> , 1999)	3.43
Optimized from water (Set 03)	3.34

Also, the metric selected for the water content calculation was particularly important to the attainment of the lowest deviations. For instance, if the selected variances were equal to 1 for all points, it was observed that the values of the

objective function had had little variation throughout extensive ranges of  $k_{ij}$  and  $\beta_{ij}^{cross}$ . Figures 5.26 and 5.27 illustrate this issue in PSO scatters generated from the optimization for this mixture, using the parameter set 03 for water.

According to these figures, this modified objective function  $S'_y$  varies from 0.58 to 0.61 in the range of  $k_{ij} \approx [-0.5, 0.3]$  and  $\beta_{ij}^{cross} \approx [0.02, 0.35]$ . However, the actual deviations can present a large variation in this region, from lower than 11% to higher than 30%, with the best solution of this specific metric resulting in  $AAY = 22.97\%$ , as presented in Table 5.38.

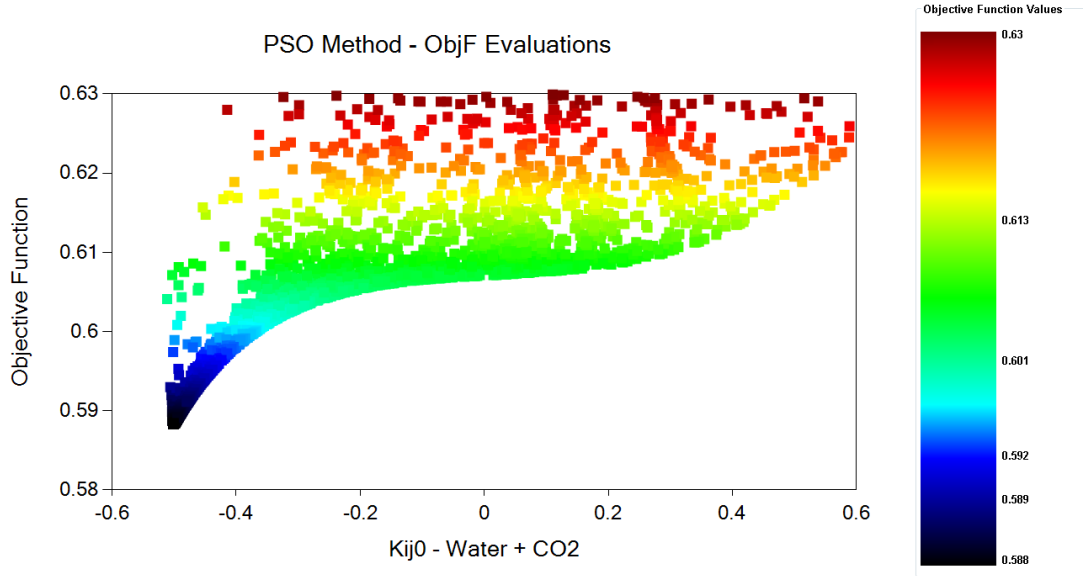


Figure 5.26: Scatter plot of parameter  $k_{ij}$  versus objective function evaluations calculated for the mixture water ('Set 03') +  $\text{CO}_2$  using all  $\sigma_{y,i} = 1$  in Equation (3.38). Image taken directly from *ThermOpt*.

Table 5.38: Estimation results for water (Set 03) +  $\text{CO}_2$  mixture studied in this Section with  $S'_y$  defined by Equation (3.38) with all variances equal to 1.

Case	$k_{ij}$	$\beta_{ij}^{cross}$	$S_y$	$S'_y$	$AAY$ [%]
Minimization of $S'_y$	-0.4902	0.0406	1.00e-1	5.90e-1	22.97
Minimization of $S_y$	0.1701	0.2093	2.11e-2	6.08e-1	10.71

Thus, these discrepancies corroborates the choice to weigh the objective function with the experimental data values as variances in this work ( $AAP_{dew} = 18.28\%$  and  $AAY = 10.71\%$ ).

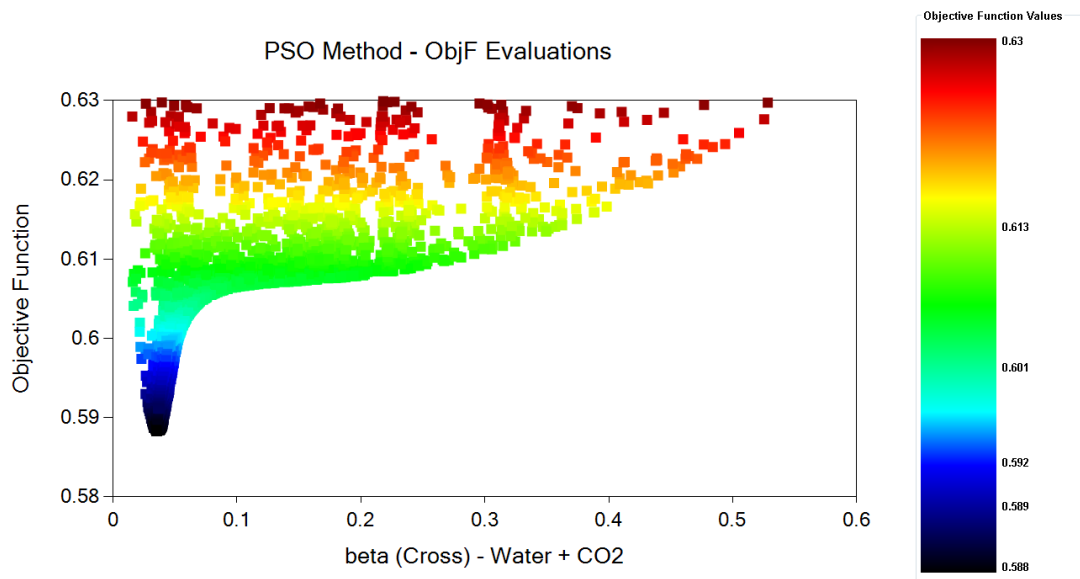


Figure 5.27: Scatter plot of parameter  $\beta_{ij}^{cross}$  versus objective function evaluations calculated for the mixture water ('Set 03') + CO<sub>2</sub> using all  $\sigma_{y,i} = 1$  in Equation (3.38). Image taken directly from *ThermOpt*.

## 5.4.2 Validation through Multicomponent Dew Point Calculations

The same analysis performed in the Section 5.4.1 was replicated for the following compounds: H<sub>2</sub>S, methane, ethane, propane and n-butane, in order to predict the water content in dew point condition of multicomponent mixtures containing these substances. Even though all of these components are not self-associating, H<sub>2</sub>S was considered to perform cross-association with water, as in the case of CO<sub>2</sub> (SANTOS *et al.*, 2015a).

Table 5.39 presents the parameters obtained for these mixtures, compared to the published values in the literature (SANTOS *et al.*, 2015b).

Thereon, they were validated with various multicomponent systems studied in the literature. In this work four mixtures have been studied, with the following compositions in dry basis:

- Natural Gas (NG): 94% methane + 4% ethane + 2% n-butane. Reference: CHAPOY *et al.* (2005).
- Natural Acid Gas 01 (NAG-1): 75% methane + 8% ethane + 4% propane + 13% CO<sub>2</sub>. Reference: MADDOX *et al.* (1988).
- Natural Acid Gas 02 (NAG-2): methane + CO<sub>2</sub> + H<sub>2</sub>S (various compositions). References: GPSA (1998); HUANG *et al.* (1985).

Table 5.39: Estimation results for each aqueous binary mixture studied in this work. All interaction parameters presented within the literature sets were taken from SANTOS *et al.* (2015b), and the 'Set 03' for water was used in the optimized sets from this work. 'mCR-1' means that  $\varepsilon_{ij}^{cross}$  was calculated according to Equation (2.31).

Mixture	Parameters	$k_{ij}$	$\beta_{ij}^{cross}$	$\varepsilon_{ij}^{cross}/R$	$S_y$	AAY [%]
Water + H <sub>2</sub> S <sup>a</sup>	Literature	0.1913	0.0624	1308.3	2.20e-2	11.83
	This Work	0.4093	0.2550	mCR-1	1.39e-2	7.795
Water + Methane <sup>b</sup>	Literature	0.0098	-	-	6.15e-3	5.582
	This Work	0.0449	-	-	5.40e-3	4.765
Water + Ethane <sup>c</sup>	Literature	0.1162	-	-	2.35e-2	10.18
	This Work	0.0721	-	-	1.39e-2	7.980
Water + Propane <sup>d</sup>	Literature	0.1135	-	-	2.96e-2	9.731
	This Work	0.0661	-	-	2.88e-2	10.12
Water + n-Butane <sup>e</sup>	Literature	0.0875	-	-	1.98e-2	11.66
	This Work	0.4522	-	-	1.24e-3	1.954

<sup>a</sup>SELLECK *et al.* (1952)

<sup>b</sup>FOLAS *et al.* (2007); MOHAMMADI *et al.* (2004); OLDS *et al.* (1942)

<sup>c</sup>MOHAMMADI *et al.* (2004); REAMER *et al.* (1943); SONG and KOBAYASHI (1994); ANTHONY and MCKETTA (1967)

<sup>d</sup>KOBAYASHI and KATZ (1953); SONG and KOBAYASHI (1994)

<sup>e</sup>REAMER *et al.* (1944)

- Natural Acid Gas 03 (NAG-3): methane + propane + CO<sub>2</sub> + H<sub>2</sub>S (various compositions). Reference: NG *et al.* (2001).

Table 5.40 shows the deviations in the water content in each case, using the literature and optimized parameters previously described in Table 5.39.

Table 5.40: Mean absolute deviations for water content (AAY [%]) calculated for each of the mixtures studied in this Section. Literature parameters were taken from SANTOS *et al.* (2015b).

AAY [%]	NG	NAG-1	NAG-2	NAG-3
Lit. Parameters	2.578	23.34	9.011	12.18
This Work	1.448	14.50	8.328	18.26

With the exception of NAG-3, it can be inferred that the optimized parameters obtained for binary mixtures have a high potential of predicting the water content of multicomponent mixtures. Also, it is important to emphasize that one of the pairs (water + H<sub>2</sub>S) is calculated in the literature with three parameters ( $k_{ij}$ ,  $\beta_{ij}^{cross}$  and  $\varepsilon_{ij}^{cross}$ ), but in this work it was decided to use only the two former variables to optimize, calculating the latter by Equation (2.31). That is, it was made possible to improve most of the results manipulating less parameters.

The probable reason for the higher deviations in the case of NAG-3 may be the harsher conditions of the experiments (NG *et al.*, 2001), where the pressures reached values up to 690 bar. Simultaneously, for example, the conditions of the experimental data available for water + methane (FOLAS *et al.*, 2007; MOHAMMADI *et al.*, 2004; OLDS *et al.*, 1942) did not surpass 30 bar.

However, if the user wishes to analyse specifically this mixture, it is possible to re-estimate one or all water-containing binary parameters for these conditions. For instance, if the water + H<sub>2</sub>S and water + methane parameters were to be re-estimated using the experimental data on NAG-3 NG *et al.* (2001), keeping the remaining values equal to the ones found in this work, the Simplex procedure of *ThermOpt* would reach the following values:  $k_{water-C_1} = 0.1470$ ,  $k_{water-H_2S} = 0.5265$  and  $\beta_{water-H_2S}^{cross} = 0.2012$ , with  $AAY = 11.60\%$ . Thus, this deviation is lower than the 12.18% calculated using the literature parameters. This further corroborates the importance of a flexible optimizing tool rather than overall optimized parameters.

## 5.5 Application to an Industrial Dehydration Unit

Having validated the CPA EoS parameters obtained and presented in the previous sections, it is possible to apply directly to a fictitious industrial dehydration unit to check if the results follow the expected tendencies of its key variables, such as the dehydrated gas composition.

### 5.5.1 Generating New Parameters for Binary Mixtures With Water

In this unit, the streams' components are water, ethylene glycol (MEG), benzene, CO<sub>2</sub>, N<sub>2</sub> and alkanes up to C<sub>8</sub>. The experimental data of each aqueous pair were taken from the following references:

- Water + MEG: CHIAVONE-FILHO *et al.* (2004)
- Water + Benzene: ANDERSON and PRAUSNITZ (1986); GÓRAL *et al.* (2004)
- Water + CO<sub>2</sub>: VALTZ *et al.* (2004); WIEBE and GADDY (1941)
- Water + N<sub>2</sub>: FOLAS *et al.* (2007)
- Water + Methane: FOLAS *et al.* (2007); MOHAMMADI *et al.* (2004); OLDS *et al.* (1942)

- Water + Ethane: ANTHONY and MCKETTA (1967); MOHAMMADI *et al.* (2004); REAMER *et al.* (1943); SONG and KOBAYASHI (1994)
- Water + Propane: KOBAYASHI and KATZ (1953); SONG and KOBAYASHI (1994)
- Water + n-Butane: REAMER *et al.* (1944)
- Water + n-Pentane: ARLT *et al.* (1979); MACZYNSKI *et al.* (2004)
- Water + n-Hexane: TSONOPOULOS and WILSON (1983) (correlation)
- Water + n-Heptane: MACZYNSKI *et al.* (2004)
- Water + n-Octane: HEIDMAN and TSONOPOULOS (1985) (correlation)

Therefore, all binary parameters between water and each of these components were estimated in this work to be applied in the referred simulation. Table 5.41 presents the metrics and the calculated parameters for each pair.

Table 5.41: All binary CPA EoS parameters obtained for the 'Set 03' parameters of water ('component i') with the components present in the simulation of the MEG unit. All calculations were performed in *ThermOpt*.

Component j	$k_{ij}$	Combining Rule	$\beta_{ij}^{cross}$	Metric
MEG	-0.0221	CR-1	-	Bubble Pressure, Eq. (3.36)
Benzene	0.0183	Solvation	0.0797	LLE Compositions, Eq. (3.33)
CO <sub>2</sub>	0.1701	Solvation	0.2093	Water Dew Content, Eq. (3.38)
N <sub>2</sub>	0.0186	None	-	Water Dew Content, Eq. (3.38)
Methane	0.0449	None	-	Water Dew Content, Eq. (3.38)
Ethane	0.0721	None	-	Water Dew Content, Eq. (3.38)
Propane	0.0661	None	-	Water Dew Content, Eq. (3.38)
n-Butane	0.4522	None	-	Water Dew Content, Eq. (3.38)
n-Pentane	0.0364	None	-	LLE Compositions, Eq. (3.33)
n-Hexane	0.0339	None	-	LLE Compositions, Eq. (3.33)
n-Heptane	0.0258	None	-	LLE Compositions, Eq. (3.33)
n-Octane	-0.0051	None	-	LLE Compositions, Eq. (3.33)

## 5.5.2 The MEG Dehydration Unit

Figure 5.28 presents the scheme of the unit studied in this work.

The feed stream 'HC01' is arbitrated using a standard composition, as well as various conditions in the simulation. Appendix A lists all of them.





water, benzene, methane and/or  $C_{2+}$ ;

- Three-phase vessel V-03 temperature [ $^{\circ}\text{C}$ ] and outlet flows [kgmol/h];
- Reboiler duty (P-02 and P-03) and regenerator condenser duty (P-01) [Gcal/h];
- Pump B-01 power [HP].

Tables 5.42 to 5.44 present the results from the simulators using own internal EoS and parameters. Tables 5.45 to 5.47 show the explicit comparison when executing this simulation with Petrox<sup>®</sup> using its internal parameters (SANTOS *et al.*, 2015b) and the parameters generated in this work.

Table 5.42: Dehydrated gas ('HC02') results for the MEG unit. Simulated at: Hysys<sup>®</sup>, Petro-SIM<sup>®</sup>, ProMax<sup>®</sup> and Petrox<sup>®</sup>.

Variable	Unit	Hysys <sup>®</sup>	Petro-SIM <sup>®</sup>	ProMax <sup>®</sup>	Petrox <sup>®</sup>
Molar Flow	kgmol/h	7578	7988	7731	7901
Temperature	$^{\circ}\text{C}$	17.53	15.70	18.38	18.97
Water Content	ppm	2.08	7.28	3.78	8.33
Benzene Content	ppm	0.99	5.16	1.47	4.15

Table 5.43: Regenerator top outlet conditions ('VENT') results for the MEG unit. Simulated at: Hysys<sup>®</sup>, Petro-SIM<sup>®</sup>, ProMax<sup>®</sup> and Petrox<sup>®</sup>.

Variable	Unit	Hysys <sup>®</sup>	Petro-SIM <sup>®</sup>	ProMax <sup>®</sup>	Petrox <sup>®</sup>
Molar Flow	kgmol/h	25.26	24.70	24.43	24.87
Temperature	$^{\circ}\text{C}$	102.0	101.0	101.0	101.0
Benzene Content	ppm	87.10	590.8	130.4	55.95
$C_1$ Content	%	0.07	0.43	0.34	1.66
$C_{2+}$ Content	%	3.55	1.14	0.05	0.67

#### 5.5.4 Discussion of the Results

There are few reliable experimental data available in the literature for the unit studied. For the standard feed current characterized in Table A.1 and the conditions in Tables A.2 to A.5, the dehydrated stream was expected to contain up to 10 ppm of water and 5 ppm of benzene, at a temperature between 15 to 20 $^{\circ}\text{C}$ , based on engineering expertise. Also, the vessel V-03 is expected to be around -25 $^{\circ}\text{C}$  and the difference between the duties of the regenerator reboiler and condenser at roughly 0.5 Gcal/h. There is no detailed data on the real conditions of the VENT stream, but due to environmental restrictions the benzene content ought to be the lowest achievable.

Table 5.44: General results for the the MEG unit equipments. Simulated at: Hysys<sup>®</sup>, Petro-SIM<sup>®</sup>, ProMax<sup>®</sup> and Petrox<sup>®</sup>.

Variable	Unit	Hysys <sup>®</sup>	Petro-SIM <sup>®</sup>	ProMax <sup>®</sup>	Petrox <sup>®</sup>
<b>Vessel V-03</b>					
Temperature	°C	-26.76	-23.24	-24.93	-21.40
Vapour Flow	kgmol/h	167.8	354.3	158.8	370.8
Condensate Flow	kgmol/h	1584	987.1	1441	1059
G21 Flow	kgmol/h	170.5	170.7	170.0	170.1
<b>Duties [Gcal/h]</b>					
Regenerator Condenser (P-01)		0.131	0.065	0.239	0.073
Regenerator Reboiler (P-02)		0.704	0.568	0.742	0.563
Regenerator Reboiler (P-03)		0.348	0.399	0.213	0.314
Pump B-01 Power	HP	22.23	22.11	16.78	26.06

Table 5.45: Dehydrated gas ('HC02') results for the MEG unit. Executed by the Petrox<sup>®</sup> process simulator.

Variable	Unit	SANTOS <i>et al.</i> (2015b)	This Work's Parameters
Molar Flow	kgmol/h	7901	7892
Temperature	°C	18.97	18.84
Water Content	ppm	8.33	9.96
Benzene Content	ppm	4.15	4.11

Table 5.46: Regenerator top outlet conditions ('VENT') results for the MEG unit. Executed by the Petrox<sup>®</sup> process simulator.

Variable	Unit	SANTOS <i>et al.</i> (2015b)	This Work's Parameters
Molar Flow	kgmol/h	24.87	24.93
Temperature	°C	101.0	101.0
Benzene Content	ppm	55.95	98.91
C <sub>1</sub> Content	%	1.66	1.83
C <sub>2+</sub> Content	%	0.67	0.74

According to Tables 5.42 to 5.44, it can be inferred that all process simulators analysed generated similar results, considering the complexity level of the model (high number of recycles, a vessel with vapour-liquid-liquid equilibrium, among others). It is important to inform that each of them used their own calculation methods, then it is natural to expect discrepancies up to a certain level among them.

Nevertheless, all of them attained the expected values for the dehydrated gas stream and the equipments. The only major difference lied on the VENT stream, whose hydrocarbons' contents (including the benzene) varied considerably. For instance, the benzene content in this stream went from 56 ppm (Petrox<sup>®</sup>) to 591

Table 5.47: General results for the the MEG unit equipments. Executed by the Petrox<sup>®</sup> process simulator.

Variable	Unit	SANTOS <i>et al.</i> (2015b)	This Work's Parameters
<b>Vessel V-03</b>			
Temperature	°C	-21.40	-21.53
Vapour Flow	kgmol/h	370.8	373.4
Condensate Flow	kgmol/h	1059	1064
G21 Flow	kgmol/h	170.1	170.1
<b>Duties [Gcal/h]</b>			
Regenerator Condenser (P-01)		0.073	0.055
Regenerator Reboiler (P-02)		0.563	0.534
Regenerator Reboiler (P-03)		0.314	0.327
Pump B-01 Power	HP	26.06	25.98

ppm (Petro-SIM<sup>®</sup>), resuming what was discussed in the Section 2.1.2.

As the Petrox<sup>®</sup> process simulator predicted the lowest benzene content in the VENT, it can be assumed that its simulation is properly modelled, being selected for the comparison with the CPA EoS parameters estimated in this work, presented in the Tables 5.45 to 5.47. In this case, as the entire simulation was set up in the exact same way, except changing the CPA parameters described previously, it is expected that all divergences in the results come from these parameters.

Therefore, when changing the water parameters published by SANTOS *et al.* (2015b) to the 'Set 03' obtained in this work, the only notable difference between the respective results lied on the benzene content of the VENT stream, which rose to almost 100 ppm, but still lower than most of the analysed commercial simulators.

This discrepancy in the benzene composition is one of the major obstacles in modelling an industrial unit that should meet its environmental restrictions. Because of that, it was decided to carry out one more analysis using the Petrox<sup>®</sup> (CPA parameters from this work): the effect of withdrawing the solvation effect of benzene with water and MEG in this simulation. The corresponding binary parameters  $k_{ij}$  were re-estimated:  $k_{benzene-water} = -0.0229$  (ANDERSON and PRAUSNITZ, 1986) and  $k_{benzene-MEG} = 0.0181$  (FOLAS *et al.*, 2006b).

The resulting simulation proved to be practically the same as the original, except of the benzene content in the VENT, which rose from 98.9 ppm to 133.8 ppm. As a consequence, it can be assumed that the solvation effect plays an essential role to lower the contents predicted, approaching the required values. The fact that this solvation effect is supported by the literature (KONTOGEOGRIS *et al.*, 2006a,b) corroborates the results obtained.

In addition to that, one of the issues regarding the lack of experimental data on

benzene content in solutions containing MEG is the high toxicity of this solvent, hindering possible experimental analyses with them. Thus, an alternative solvent with potential dehydrating effects would be preferable. For example, the propylene glycol (PG) isomers are widely used in the food and drug industries and are much more harmless than the former glycol (CSEM, 2007). Therefore, PG was also briefly analysed in this work. Unfortunately, the experimental data for binary mixtures with PG available in the literature is also scarce. The data found for mixtures contain: 1,2-PG with n-heptane and 1,2-PG with water, as shown in Table 5.48.

Table 5.48: Binary parameters obtained (1,2-propylene glycol: component i). All calculations were performed in *ThermOpt*.

Component j	$k_{ij}$	$\beta_{ij}^{cross}$	$\varepsilon_{ij}^{cross} / R$ [K]	Metric
n-Heptane <sup>a</sup>	0.0320	-	-	LLE Compositions (Eq. (3.33))
Water <sup>b</sup>	-0.1806	0.0307	2021.15	Bubble Pressure (Eq. (3.36))

<sup>a</sup>Experimental data: DERAWI *et al.* (2002)

<sup>b</sup>Experimental data: LANCIA *et al.* (1996)

Due to the notorious importance of the benzene effect in the simulation, it was necessary to estimate the parameters of the binary mixture PG-benzene even without available experimental data. To perform such evaluation, two assumptions were made:

- The propylene glycol has a larger structure than the ethylene glycol (MEG) but smaller than the tri-ethylene glycol (TEG). Therefore, the  $k_{ij}$  value of the binary PG + benzene was arbitrated in the mean value of the  $k_{ij}$  of the other glycols + benzene:  $k_{PG-Benzene} \equiv (0.048 + 0.036)/2 = 0.042$ .
- It is expected a solvation effect between PG and benzene. It is assumed, then, that  $\beta_{ij}^{cross} \equiv \beta_{PG} = 0.019$ .

Even though that specific studies should have been carried out to decide the optimal conditions of the new simulations, they were kept the same for this preliminary analysis in order to evaluate the effect of changing the solvents in the dehydration results. Therefore, the main goal of this analysis is to check the dehydration potential of PG, as presented by Table 5.49.

According to the results presented in the Table 5.49, the change of solvents impacted slightly the water content in the simulation output, demonstrating a potential of using this solvent in the industry. Hence, another suggestion for future works is to model a PG dehydration unit as follows:

- Generate experimental data for binary mixtures in LLE with PG and hydrocarbons from  $C_1$  to at least  $C_6$ , specially benzene and toluene.

Table 5.49: Dehydrated gas ('HC02') results for the MEG unit. Executed by the Petrox<sup>®</sup> process simulator using MEG and PG as solvents, respectively. All pure components' parameters were taken from the literature (SANTOS *et al.*, 2015b).

Variable	Unit	MEG Solvent	PG Solvent
<b>HC02</b>			
Molar Flow	kgmol/h	7901	7895
Temperature	°C	18.97	18.92
Water Content	ppm	8.33	8.42
Benzene Content	ppm	4.15	4.07

- Use *ThermOpt* to properly estimate the corresponding binary parameters.
- Analyse the expected behaviour of solutions containing water, PG and hydrocarbons in the possible vent conditions.
- Study thoroughly the optimal conditions using PG, varying particularly the duties of the heat exchangers and the regeneration tower conditions in order to attain similar results to the dehydration unit when using MEG for other streams such as 'VENT'.

# Chapter 6

## Conclusions

The tool developed here, named *ThermOpt*, presents good potential to be a tool for estimating the equation of state (EoS) parameters for several processes, with applications to chemical processes such as the natural gas production and processing. This work succeeded in proposing two new methodologies for parameter estimation in a systematic way: one based on pure (VLE) and LLE properties and the other based on water content in dew point conditions, based on the work of SHIGUEMATSU (2014).

Firstly, in Section 5.1 the calculation speed of the program was evaluated. Considering the complexity of solving the CPA EoS (MICHELSEN, 2006), the results presented were promising, enabling long calculations such as penalization analyses or the VLE-LLE Methodology to be executed in a relatively short time.

Section 5.2 presented an example of penalization analysis using the SRK equation of state, showing that high weights lead to solutions close to the original one, with  $a_0$  and  $b$  calculated using critical properties by Equations (2.4) and (2.5), and  $c_1$  defined by the Kabadi-Danner modification. Thus, it can be considered that *ThermOpt* is well validated, once the results presented by the Table 5.5 tended to the analytical solution to the Equation (2.3) with this EoS. Also, the CPA EoS was used to estimate the parameters of several polar substances by saturation pressure and liquid density, comparing to available literature data.

Thereon, in the Section 5.3 the VLE-LLE Methodology proposed in this work was applied for 4 different glycols, comparing the calculated sets to the literature parameters, showing good agreement using predetermined criteria. After that, the same evaluation was performed for water, selecting among the possible sets one with the parameter  $\varepsilon/R$  relatively close to the hydrogen bond energy for water (KOH *et al.*, 1993).

Section 5.4 applied the proposed methodology for parameter estimation by water content in dew point condition to several aqueous mixtures, from binaries with CO<sub>2</sub>, H<sub>2</sub>S or light alkanes to multicomponent natural gas mixtures. The results

obtained indicated smaller deviations than the ones calculated by the literature parameters reported by TSIVINTZELIS *et al.* (2012)(Tables 5.35, 5.36, 5.39 and 5.40). Consequently, the metric proposed in this work, based on water content calculation, can enable further evaluations at extreme conditions such as high pressures, which is limited in the metric based on bubble or dew pressure.

Finally, Section 5.5 shows an industrial application of all the previous procedures, simulating a part of a dehydration unit using MEG as inhibitor. Comparisons were conducted among various commercial process simulators, pointing out their similarities and limits. Afterwards, the analysis was focused on the Petrox<sup>®</sup> Process Simulator, by testing the effect of the water parameters obtained in this work. It was shown that the only visible difference was in the benzene content of the VENT stream. The new set of parameters reported higher values for this content, but still at the same level of most of the other simulator's results. Moreover, the utilisation of 1,2-propylene glycol instead of MEG was briefly studied and it was found out that its dehydration potential is similar as the ethylene glycol, needing a thorough study to reach more detailed outcomes.

In addition to the conclusions and contributions highlighted in this work, there are numerous possible paths and challenges suggested as future works, such as:

- *Implement parallelism calculations* (MORAES *et al.*, 2015). As the optimizing procedures require a vast quantity of independent calculations of the objective function, this implementation will increase the speed of the thermodynamic calculations inside *ThermOpt*, enabling even more complex analysis.
- *Implement flexible EoS based on the separate Helmholtz energy terms.* Currently the EoS options in *ThermOpt* are considered as independent models. An idea to loosen the limits of the program would be to implement the EoS as Helmholtz energy terms selected by the user in the interface. For example, there would be a term related to a cubic EoS (Peng-Robinson or SRK), an association term (as in the CPA), and other types of terms, such as the Born-Solvation Contribution, the Debye-Huckel expression or the Mean Spherical Approximation (MSA) term. The work of MYERS (2005) shows how these terms can be connected to a single thermodynamic model.
- *Generate detailed PSO histograms in order to select its best internal parameters.* Essentially all of the PSO calculations performed in this work used the same values of internal parameters (cognition parameter  $c_1$ , social parameter  $c_2$ , and the inertial weights  $w_0$  and  $w_f$ ). In thermodynamic calculations, there is a high level of dependency among the manipulated variables, and not all sets of them lead to converged solutions. Therefore,



the right selection of these PSO parameters is important to effectively guide the 'particles' to the global minimum area. Chapter 4 briefly describes the execution of hundreds of PSO calculations in a row in *ThermOpt*, storing each result, generating a histogram-type chart. If the PSO parameters are well chosen, the majority of the solutions attained will be in the region of the global minimum. Thus, the recommended study is to perform this analysis for a multitude of combinations of these parameters, using a specific component and the CPA EoS, until an optimal set is found, which the histogram region would be the narrowest.

- *Execute the penalization analysis using the CPA equation of state for polar compounds.* As explained in Section 5.2, one of the downsides of the CPA equation of state for pure components is its lower accuracy in the critical region, because its association term violate the restrictions imposed in Equation (2.3). On the other hand, the penalization analysis tool may allow the program to find a different set of parameters which results in lower deviations in this region, even at a cost of an increase of the overall deviation, as in a 'short blanket'. The challenge of this study is to find out how far this improvement in the critical region would be worth the global loss of accuracy.
- *Execute the VLE-LLE Methodology with other hydrocarbons as auxiliary compounds.* Section 5.3 studied this approach using the same alkanes as the respective authors used in their works in order to validate this procedure. However, an interesting analysis would be redoing the VLE-LLE Methodology to polar compounds in LLE with other hydrocarbons, including benzene, and drawing for each case an own optimal parameter search space. Eventually, all of these regions would be compared to each other to narrow them until a single set of parameters is found. For example, one would apply this methodology to water + n-pentane, n-heptane, n-octane, n-decane, benzene and toluene. From each case there would be a region of optimal sets, as they are Pareto analyses. The intersection of all these regions would provide a narrower region, facilitating the selection of the optimal parameters.
- *Study the use of propylene glycol isomers as hydrate inhibitors instead of MEG or TEG.* As discussed in Section 5.5, MEG, DEG and TEG are compounds that are toxic to humans, which makes it difficult to carry out experimental analyses of mixtures containing these glycols. On the other hand, the propylene glycol - PG - is practically harmless to the human being (CSEM, 2007), being more appropriate if its dehydration potential would be similar to the previous glycols. In this work it was shown that there is actually such potential, but the process unit was originally modelled to use the MEG as the inhibitor. Besides,

the lack of experimental data for binaries with PG is another obstacle to this current study. Therefore, the last suggestion to future works is to perform this investigation, following the steps detailed in the end of the Section 5.5.

Hence, it can be concluded that there are a variety of research possibilities beyond the contributions described in this dissertation, from the development of *ThermOpt*. With its further implementing and future availability to the academic community, there will be a tool that shows numerous paths, enabling the user to select the equation of state and calculate the best parameter sets for modelling complex mixtures according to specific applications.

# Bibliography

American Institute Of Chemical Engineers, Design Institute for Physical Properties, DIADEM, 2004.

ALBERTON, A. L., 2010, *Estimação de Parâmetros e Planejamento de Experimentos: Estudo de Incertezas e Funções de Informação*. D.Sc. thesis, Universidade Federal do Rio de Janeiro, Rio de Janeiro, Brasil.

ANDERSON, F. E., PRAUSNITZ, J. M., 1986, “Mutual Solubilities and Vapor Pressures for Binary and Ternary Aqueous Systems Containing Benzene, Toluene, m-Xylene, Thiophene and Pyridine in the Region 100-200°C”, *Fluid Phase Equilibria*, v. 32, pp. 63–76.

ANTHONY, R. G., MCKETTA, J. J., 1967, “Phase Equilibrium in the Ethylene-Ethane-Water System”, *Journal of Chemical and Engineering Data*, v. 12, n. 1, pp. 21–28.

ARLT, W., MACEDO, M. E. A., RASMUSSEN, P., SORENSEN, J. M., 1979, *Liquid-Liquid Equilibrium Data Collection. Part 1: Binary Systems*. Frankfurt, Germany, DECHEMA Chemistry Data Series.

ASPEN. Available at: <<https://www.aspentech.com/en/products/engineering/aspen-hysys>>. AspenTech Company Hysys - [Cited 2018 May].

AVLUND, A. S., 2011, *Extension of association models to complex chemicals*. D.Sc. thesis, Center for Energy Resources Engineering, Technical University of Denmark, Denmark.

AVLUND, A. S., ERIKSEN, D. K., KONTOGEORGIS, G. M., MICHELSEN, M. L., 2011, “Application of Association Models to Mixtures Containing Alkanolamines”, *Fluid Phase Equilibria*, v. 306, pp. 31–37.

BELTRÃO, R. L. C., SOMBRA, C. L., LAGE, A. C. V. M., NETTO, J. R. F., HENRIQUES, C. C., 2009, “Challenges and New Technologies for the

Development of the Pre-Salt Cluster, Santos Basin, Brazil”. In: *Offshore Technology Conference*, Houston, Texas, USA.

BRASIL, N. I. D., ARAÚJO, M. A. S., SOUSA, E. C. M., et al., 2011, *Processamento de Petróleo e Gás – Petróleo e Seus Derivados, Processamento Primário, Processo de Refino, Petroquímica e Meio Ambiente*. Rio de Janeiro, Brasil, GEN.

BRE. Available at: <<https://www.bre.com/ProMax-Main.aspx>>. ProMax - [Cited 2018 May].

CHAPMAN, W. G., GUBBINS, K. E., JACKSON, G., 1988, “Phase equilibria of associating fluids: chain molecules with multiple bonding sites”, *Molecular Physics*, v. 65, n. 5, pp. 1057–1079.

CHAPMAN, W. G., GUBBINS, K. E., JACKSON, G., RADOSZ, M., 1989, “SAFT: Equation-of-state solution model for associating fluids”, *Fluid Phase Equilibria*, v. 52, pp. 31–38.

CHAPMAN, W. G., GUBBINS, K. E., JACKSON, G., RADOSZ, M., 1990, “New reference equation of state for associating liquids”, *Ind. Eng. Chem. Res.*, v. 29, n. 8, pp. 1709–1721.

CHAPOY, A., MOHAMMADI, A. H., TOHIDI, B., 2005, “Estimation of Water Content for Methane + Water and Methane + Ethane + n-Butane + Water Systems Using a New Sampling Device”, *J. Chem. Eng. Data*, v. 50, pp. 1157–1161.

CHIAVONE-FILHO, O., PROUST, P., RASMUSSEN, P., 2004, “Vapor-Liquid Equilibria for Glycol Ether + Water Systems”, *J. Chem. Eng. Data*, v. 38, pp. 128–131.

CSEM, 2007, *Ethylene Glycol and Propylene Glycol Toxicity*. Technical report, Agency for Toxic Substances and Disease Registry. Case Studies in Environmental Medicine - CSEM.

DAS, S., KODURU, P., GUI, M., COCHRAN, M., WAREING, A., WELCH, S. M., BABIN, B. R., 2006, “Adding Local search to Particle Swarm Optimization”. In: *IEEE Congress on Evolutionary Computation*, Canada, jul.

DERAWI, S. O., KONTOGEORGIS, G. M., STENBY, E. H., HAUGUM, T., FREDHEIM, A. O., 2002, “Liquid-Liquid Equilibria for Glycols +

- Hydrocarbons: Data and Correlation”, *J. Chem. Eng. Data*, v. 47, pp. 169–173.
- DERAWI, S. O., MICHELSEN, M. L., KONTOGEORGIS, G. M., STENBY, E. H., 2003, “Application of the CPA Equation of State to Glycol/Hydrocarbons Liquid–Liquid Equilibria”, *Fluid Phase Equilibria*, v. 209, pp. 163–184.
- ECONOMOU, I. G., DONOHUE, M. D., 1991, “Chemical, Quasi-Chemical and Perturbation Theories for Associating Fluids”, *AIChE Journal*, v. 37, n. 12, pp. 1875–1894.
- EDOKPOLO, B., YU, Q. J., CONNELL, D., 2015, “Health Risk Assessment for Exposure to Benzene in Petroleum Refinery Environments”, *International Journal of Environmental Research and Public Health*, v. 12, pp. 595–610.
- FOLAS, G. K., KONTOGEORGIS, G. M., MICHELSEN, M. L., STENBY, E. H., 2006a, “Application of the Cubic-Plus-Association (CPA) Equation of State to Complex Mixtures with Aromatic Hydrocarbons”, *Ind. Eng. Chem. Res.*, v. 45, pp. 1527–1538.
- FOLAS, G. K., KONTOGEORGIS, G. M., MICHELSEN, M. L., STENBY, E. H., SOLBRAA, E., 2006b, “Liquid-Liquid Equilibria for Binary and Ternary Systems Containing Glycols, Aromatic Hydrocarbons, and Water: Experimental Measurements and Modeling with the CPA EoS”, *J. Chem. Eng. Data*, v. 51, pp. 977–983.
- FOLAS, G. K., FROYNA, E. W., LOVLAND, J., KONTOGEORGIS, G. M., SOLBRAA, E., 2007, “Data and Prediction of Water Content of High Pressure Nitrogen, Methane and Natural Gas”, *Fluid Phase Equilibria*, v. 252, pp. 162–174.
- GÓRAL, M., MACZYNSKI, A., GOCLOWSKA, B. W., 2004, “Recommended Liquid-liquid Equilibrium Data. Part 3: Alkylbenzene-Water Systems”, *J. Phys. Chem. Ref. Data*, v. 33, n. 2, pp. 579–591.
- GPSA, 1998, *GPSA Engineering Databook*. 11 ed. SI, Oklahoma, USA, GPSA Press.
- HAGHIGHI, H., 2009, *Phase Equilibria Modelling of Petroleum Reservoir Fluids Containing Water, Hydrate Inhibitors and Electrolyte Solutions*. D.Sc. thesis, Petroleum Engineering, Heriot-Watt University.
- HEIDMAN, J. L., TSONOPOULOS, C., 1985, “High-Temperature Mutual Solubilities of Hydrocarbons and Water. Part II: Ethylbenzene,

- Ethylcyclohexane, and n-Octane”, *AIChE Journal*, v. 31, n. 3, pp. 376–384.
- HENDRIKS, E. M., WALSH, J. M., VAN BERGEN, A. R. D., 1997, “A General Approach to Association Using Cluster Partition Function”, *J. Stat. Phys.*, v. 87, pp. 1287–1306.
- HUANG, S. H., RADOSZ, M., 1990, “Equation of state for Small, Large, Polydisperse and Associating Molecules”, *Ind. Eng. Chem. Res.*, v. 29, pp. 2284.
- HUANG, S. S. S., LEU, A. D., NG, H. J., ROBINSON, D. B., 1985, “The phase behavior of two mixtures of methane, carbon dioxide, hydrogen sulfide, and water”, *Fluid Phase Equilibria*, v. 19, pp. 21–32.
- KABADI, V. N., DANNER, R. P., 1985, “A Modified Soave-Redlich-Kwong Equation of State for Water-Hydrocarbon Phase Equilibria”, *Ind. Eng. Chem. Process Des. Dev.*, v. 24, pp. 537–541.
- KBC. Available at: <<https://www.kbc.global/en/software/simulation-and-optimization/process-simulation>>. Petro-SIM - [Cited 2018 May].
- KENNEDY, J., EBERHART, R., 1995, “Particle Swarm Optimization”. In: *Proceedings of IEEE International Conference on Neural Networks*, pp. 1942–1948, Perth, Australia.
- KOBAYASHI, R., KATZ, D. L., 1953, “Vapor-Liquid Equilibria for Binary Hydrocarbon-Water Systems”, *Ind. Eng. Chem.*, v. 45, n. 2, pp. 441–446.
- KOH, C. A., TANAKA, H., WALSH, J. M., CUBBINS, K. E., ZOLLWEG, J. A., 1993, “Thermodynamic and structural properties of methanol-water mixtures: experiment, theory and molecular simulation”, *Fluid Phase Equilibria*, v. 83, pp. 51.
- KONTOGEORGIS, G. M., FOLAS, G., 2010, *Thermodynamic Models for Industrial Applications – From Classical and Advanced Mixing Rules to Association Theories*. Amsterdam, Wiley.
- KONTOGEORGIS, G. M., VOUSAS, E. C., YAKOUMIS, I. V., TASSIOS, D. P., 1996, “An Equation of State for Associating Fluids”, *Ind. Eng. Chem. Res.*, v. 35, pp. 4310–4318.

- KONTOGEORGIS, G. M., YAKOUMIS, I. V., HEIJER, H., HENDRIKS, E., MOORWOOD, T., 1999, "Multicomponent phase equilibrium calculations for water-methanol-alkane mixtures", *Fluid Phase Equilibria*, v. 201, pp. 158–160.
- KONTOGEORGIS, G. M., MICHELSEN, M. L., FOLAS, G. K., DERAWI, S., VON SOLMS, N., STENBY, E. H., 2006a, "Ten Years with the CPA (Cubic-Plus-Association) Equation of State. Part 1. Pure Compounds and Self-Associating Systems", *Ind. Eng. Chem. Res.*, v. 45, n. 14, pp. 4855–4868.
- KONTOGEORGIS, G. M., MICHELSEN, M. L., FOLAS, G. K., DERAWI, S., VON SOLMS, N., STENBY, E. H., 2006b, "Ten Years with the CPA (Cubic-Plus-Association) Equation of State. Part 2. Cross-Associating and Multicomponent Systems", *Ind. Eng. Chem. Res.*, v. 45, n. 14, pp. 4869–4878.
- LANCIA, A., MUSMARRA, D., PEPE, F., 1996, "Vapor-Liquid Equilibria for Mixtures of Ethylene Glycol, Propylene Glycol, and Water between 98° and 122°C", *Journal of Chemical Engineering of Japan*, v. 29, n. 3, pp. 449–455.
- LI, Z., FIROOZABADI, A., 2009, "Cubic-plus-association equation of state for water-containing mixtures: Is cross association necessary?" *AIChE J.*, v. 55, n. 7, pp. 1803–1813.
- LUNDSTRØM, C., 2005, *Modeling of Phase Equilibria for Petroleum Reservoir Fluids Containing Water and Hydrate Inhibitors*. M.Sc. dissertation, Center for Phase Equilibria and Separation Processes (IVC-SEP), Department of Chemical Engineering, Technical University of Denmark, Denmark.
- MACZYNSKI, A., GOCLOWSKA, B. W., GÓORAL, M., 2004, "Recommended Liquid-liquid Equilibrium Data. Part 1: Binary Alkane-Water Systems", *J. Phys. Chem. Ref. Data*, v. 33, n. 2, pp. 549–577.
- MADDOX, R. N., LILLY, L. L., MOSHFEGHIAN, M., ELIZONDO, E., 1988, "Estimating Water Content of Sour Natural Gas Mixtures". In: *Laurence Reid Gas Conditioning Conference*, Norman, OK, USA, mar.
- MATHIAS, P. M., COPEMAN, T. W., 1983, "Extension of the Peng-Robinson EoS to Complex Mixtures: Evaluation of Various Forms of the Local Composition Concept", *Fluid Phase Equilibria*, v. 13, pp. 91–108.

- MICHELSEN, M. L., 2006, "Robust and Efficient Solution Procedures for Association Models", *Ind. Eng. Chem. Res.*, v. 45, pp. 8449–8453.
- MICHELSEN, M. L., HENDRIKS, E. M., 2001, "Physical Properties from Association Models", *Fluid Phase Equilibria*, v. 180, pp. 165–174.
- MOHAMMADI, A. H., CHAPOY, A., RICHON, D., TOHIDI, B., 2004, "Experimental Measurement and Thermodynamic Modeling of Water Content in Methane and Ethane Systems", *Ind. Eng. Chem. Res.*, v. 43, pp. 7148–7162.
- MORAES, A. O. S., MITRE, J. F., LAGE, P. L. C., SECCHI, A. R., 2015, "A Robust Parallel Algorithm of the Particle Swarm Optimization Method for Large Dimensional Engineering Problems", *Applied Mathematical Modelling*, v. 39, pp. 4223–4241.
- MYERS, J. A., 2005, *Thermodynamics of Electrolyte Solutions With a Helmholtz Energy Equation of State*. D.Sc. thesis, University of Delaware, Delaware, USA.
- NELDER, J. A., MEAD, R. A., 1965, "Simplex Method for Function Minimization", *The Computer Journal*, v. 7, pp. 308–312.
- NG, H. J., CHEN, C. J., SCHROEDER, H., 2001, *Water Content of Natural Gas Systems Containing Acid Gas*. GPA Research Report RR-174.
- NIEDERBERGER, J., GAMA, M. S., SANTOS, L. C., et al., 2009, "PETROX – PETROBRAS Technology in Process Simulation", *Comput.-Aided Chem. Eng.*, v. 27, pp. 675–680.
- OLDS, R. H., SAGE, B. H., LACEY, W. N., 1942, "Phase Equilibria in Hydrocarbon Systems. Composition of the Dew-Point Gas of the Methane-Water System", *Ind. Eng. Chem.*, v. 34, n. 10, pp. 1223–1227.
- PENG, D. Y., ROBINSON, D. B., 1976, "A New Two-Constant Equation of State", *Ind. Eng. Chem. Fundam.*, v. 15, pp. 59–64.
- PENG, D. Y., ROBINSON, D. B., CHUNG, S. Y.-K., 1985, "The Development of the Peng-Robinson Equation and its Application to Phase Equilibrium in a System Containing Methanol", *Fluid Phase Equilibria*, v. 24, pp. 25–41.
- PITZER, K. S., 1995, *Thermodynamics*. 3 ed. New York, McGraw-Hill.



- PRAUSNITZ, J. M., LICHTENTHALER, R. M., DE AZEVEDO, E. G., 1999, *Molecular Thermodynamics of Fluid-Phase Equilibria*. 3 ed. Upper Saddle River, New Jersey, USA, Prentice Hall PTR.
- REAMER, H. H., OLDS, R. H., SAGE, B. H., LACEY, W. N., 1943, “Phase Equilibria in Hydrocarbon Systems. Composition of Dew-point Gas in Ethane-Water System”, *Ind. Eng. Chem.*, v. 35, n. 7, pp. 790–793.
- REAMER, H. H., OLDS, R. H., SAGE, B. H., LACEY, W. N., 1944, “Phase Equilibria in Hydrocarbon Systems. Compositions of the Coexisting Phases of n-Butane-Water System in the Three-Phase Region”, *Ind. Eng. Chem.*, v. 36, n. 4, pp. 381–383.
- SANTOS, J. P. L., 2010, *Equilíbrio de Fases de Misturas Polares e Iônicas via Equação de Estado Baseada em Modelo de Rede*. Tese de D.Sc., Universidade Federal do Rio de Janeiro, Rio de Janeiro, Brasil.
- SANTOS, L. C., 2015, *Desenvolvimento de um Modelo de Associação para Cálculo de Equilíbrio de Fases de Misturas Complexas com Ênfase em Sistemas de Interesse no Processamento de Gás Natural*. Tese de D.Sc., COPPE/UFRJ, Rio de Janeiro, Brasil.
- SANTOS, L. C., ABUNAHMAN, S. S., TAVARES, F. W., AHÓN, V. R. R., KONTOGEORGIS, G. M., 2015a, “Modeling Water Saturation Points in Natural Gas Streams Containing CO<sub>2</sub> and H<sub>2</sub>S — Comparisons with Different Equations of State”, *Ind. Eng. Chem. Res.*, v. 54, n. 2, pp. 743–757.
- SANTOS, L. C., ABUNAHMAN, S. S., TAVARES, F. W., AHÓN, V. R. R., KONTOGEORGIS, G. M., 2015b, “Cubic Plus Association Equation of State for Flow Assurance Projects”, *Ind. Eng. Chem. Res.*, v. 54, n. 26, pp. 6812–6824.
- SANTOS, L. C., TAVARES, F. W., AHÓN, V. R. R., KONTOGEORGIS, G. M., 2015c, “Modeling MEA with the CPA equation of state: A parameter estimation study adding local search to PSO algorithm”, *Fluid Phase Equilibria*, v. 400, pp. 76–86.
- SCHWAAB, M., PINTO, J. C., 2007, *Análise de Dados Experimentais I – Fundamentos de Estatística e Estimação de Parâmetros*. Rio de Janeiro, Brasil, e-papers.

- SCHWAAB, M., BISCAIA JR., E. C., MONTEIRO, J. L., PINTO, J. C., 2008, “Nonlinear Parameter Estimation through Particle Swarm Optimization”, *Chemical Engineering Science*, v. 63, pp. 1542–1552.
- SELLECK, F., CARMICHAEL, L., SAGE, B., 1952, “Phase Equilibrium in the Hydrogen Sulfide-Water System”, *Ind. Eng. Chem.*, v. 44, pp. 2219–2226.
- SHI, Y., EBERHART, R., 1998, “A Modified Particle Swarm Optimizer”. In: *Proceedings of the IEEE International Conference on Evolutionary Computation*, Anchorage, Alaska.
- SHIGUEMATSU, F. M., 2014, *Cálculo de Saturação de Água em Gás Natural contendo Gases Ácidos*. M.Sc. dissertation, Universidade Federal do Rio de Janeiro, Rio de Janeiro, Brasil.
- SMITH, J. M., VAN NESS, H. C., ABBOTT, M. M., 2005, *Introduction to Chemical Engineering Thermodynamics*. 7 ed. New York, McGraw-Hill.
- SOAVE, G., 1972, “Equilibrium Constants from a Modified Redlich-Kwong Equation of State”, *Chemical Engineering Science*, v. 27, n. 6, pp. 1197–1203.
- SONG, K. Y., KOBAYASHI, R., 1994, “The Water Content of Ethane, Propane and their Mixtures in Equilibrium with Liquid Water or Hydrates”, *Fluid Phase Equilibria*, v. 95, pp. 281–298.
- TECPETRO. Available at: <<https://tecpetro.com/2015/09/27/hidratos-de-gas-problema-critico-ou-potencial-reserva-energetica/>>. TecPetro - Óleo e Gás - [Cited 2018 May].
- TSIVINTZELIS, I., KONTOGEORGIS, G. M., MICHELSEN, M. L., STENBY, E. H., 2010, “Modeling Phase Equilibria for Acid Gas Mixtures using the CPA Equation of State. Part 1. Mixtures with H<sub>2</sub>S”, *AIChE Journal*, v. 56, pp. 2965–2982.
- TSIVINTZELIS, I., KONTOGEORGIS, G. M., MICHELSEN, M. L., STENBY, E. H., 2011, “Modeling Phase Equilibria for Acid Gas Mixtures using the CPA Equation of State. Part II: Binary Mixtures with CO<sub>2</sub>”, *Fluid Phase Equilibria*, v. 306, pp. 38–56.
- TSIVINTZELIS, I., MARIBO-MOGENSEN, B., FROST, M., et al., 2012, *The Cubic-Plus-Association EoS - Parameters for Pure Compounds and Interaction Parameters*. In: Report, CERRE, Center for Energy Resources - DTU, Copenhagen, Denmark.

- TSONOPOULOS, C., WILSON, G. M., 1983, "High-Temperature Mutual Solubilities of Hydrocarbons and Water. Part I: Benzene, Cyclohexane and n-Hexane", *AIChE Journal*, v. 29, n. 6, pp. 990–999.
- VALDERRAMA, J. O., 2003, "The State of Cubic Equations of State", *Ind. Eng. Chem. Res.*, v. 42, n. 8, pp. 1603–1618.
- VALTZ, A., CHAPOY, A., COQUELET, C., PARICAUD, P., RICHON, D., 2004, "Vapor-liquid equilibria in the CO<sub>2</sub>-H<sub>2</sub>O system, measurement and modeling from 278.2 to 318.2 K", *Fluid Phase Equilibria*, v. 226, pp. 333–344.
- VAN DER WAALS, J. D., 1873, *Over de Continuïteit van den Gas- en Vloeistooftoestand*. Ph.D. thesis, Universiteit Leiden, Leiden, The Netherlands.
- WERTHEIM, M. S., 1984a, "Fluids with Highly Directional Attractive Forces: I. Statistical Thermodynamics", *J. Stat. Phys.*, v. 35, n. 1-2, pp. 19–34.
- WERTHEIM, M. S., 1984b, "Fluids with Highly Directional Attractive Forces: II. Thermodynamic Perturbation Theory and Integral Equations", *J. Stat. Phys.*, v. 35, n. 1-2, pp. 35–47.
- WERTHEIM, M. S., 1986a, "Fluids with Highly Directional Attractive Forces: III. Multiple Attraction Sites", *J. Stat. Phys.*, v. 42, n. 3-4, pp. 459–476.
- WERTHEIM, M. S., 1986b, "Fluids with Highly Directional Attractive Forces: IV. Equilibrium Polymerization", *J. Stat. Phys.*, v. 42, n. 3-4, pp. 477–492.
- WIEBE, R., GADDY, V. L., 1941, "Vapor Phase Composition of Carbon Dioxide-Water Mixtures at Various Temperatures and at Pressures to 700 Atmospheres", *J. Am. Chem. Soc.*, v. 63, pp. 475–477.
- YAKOUMIS, I. V., KONTOGEORGIS, G. M., VOUTSAS, E. C., HENDRIKS, E. M., TASSIOS, D. P., 1998, "Prediction of Phase Equilibria in Binary Aqueous Systems Containing Alkanes, Cycloalkanes, and Alkenes with the Cubic-plus-Association Equation of State", *Ind. Eng. Chem. Res.*, v. 37, pp. 4175–4182.

# Appendix A

## The MEG Dehydration Unit

In this Appendix, the main variables of the MEG dehydration unit studied in this work are summarized.

Table A.1 presents the condition and composition of the feed stream 'HC01'. Tables A.2 to A.5 present the remaining conditions adopted in this system. Also, it is important to inform that the pump efficiency was set to 75%.

Table A.1: Condition of the fictitious feed stream of the MEG unit, labelled as 'HC01'.

Variable	Unit	Value
Molar Flow	kgmol/h	9355
Pressure	kgf/cm <sup>2</sup> g	78
Temperature	°C	37
Molar Composition		
Benzene	ppm	80
H <sub>2</sub> O	%	0.26
CO <sub>2</sub>	%	0.02
N <sub>2</sub>	%	0.59
Methane	%	80.82
Ethane	%	9.25
Propane	%	5.94
i-Butane	%	0.84
n-Butane	%	1.43
i-Pentane	%	0.24
n-Pentane	%	0.30
n-Hexane	%	0.11
n-Heptane	%	0.03
n-Octane	%	0.01

Table A.2: Conditions of the vessels in the MEG unit simulated in this work.

Variable	Unit	Value
Pressure in V-06	kgf/cm <sup>2</sup> g	9
Pressure in V-03	kgf/cm <sup>2</sup> g	55

Table A.3: Conditions of the Regenerator in the MEG unit simulated in this work.

Variable	Unit	Value
Temperature of feed stream G22	°C	72
Top tray pressure	kgf/cm <sup>2</sup> g	0.040
$\Delta P$ in the column	kgf/cm <sup>2</sup>	0.035
Bottom temperature	Celsius	127

Table A.4: Conditions of the glycol injection points in the MEG unit simulated in this work.

Variable	Unit	Value
Flow of G16	kgmol/h	27
Flow of G17	kgmol/h	27
Flow of G18	kgmol/h	27
Flow of G19	kgmol/h	36
Flow of G20	kgmol/h	27

Table A.5: Conditions of the heat exchangers in the MEG unit simulated in this work.

Variable	Unit	Value
Duty of P-04	Gcal/h	2.33
Duty of P-05	Gcal/h	1.77
Duty of P-06	Gcal/h	2.72
Duty of P-07	Gcal/h	3.65
Pressure Drops	kgf/cm <sup>2</sup>	0.30